Identification of the mRNA-associated TOP3β-TDRD3-FMRP (TTF) -complex and its implication for neurological disorders

by

Georg Stoll

from Schweinfurt, Germany

A thesis submitted to the Faculty of Pharmacy and Chemistry of the University of Würzburg, Germany, in fulfillment of the requirement for the degree of

Doctor rerum naturalium (Dr. rer. nat.)

Chair of Biochemistry

Würzburg, Germany, 2015

CC BY NC ND

Date of submission: 19 January 2015

PhD thesis examiners:

1st Examiner: Prof. Dr. Utz Fischer

2nd Examiner: Prof. Dr. Alexander Buchberger

Members of the oral defence commission:

1st Examiner: Prof. Dr. Utz Fischer

2nd Examiner: Prof. Dr. Alexander Buchberger

3rd Examiner: PD Dr. Sibylle Jablonka

Date of oral defence:

Delivery of Dr. rer nat. certificate:

Table of contents

1 Summary

The propagation of the genetic information into proteins is mediated by messenger-RNA (mRNA) intermediates. In eukaryotes mRNAs are synthesized by RNA-Polymerase II and subjected to translation after various processing steps. Earlier it was suspected that the regulation of gene expression occurs primarily on the level of transcription. In the meantime it became evident that the contribution of post-transcriptional events is at least equally important. Apart from non-coding RNAs and metabolites, this process is in particular controlled by RNA-binding proteins, which assemble on mRNAs in various combinations to establish the so-called "mRNP-code".

In this thesis a so far unknown component of the mRNP-code was identified and characterized. It constitutes a hetero-trimeric complex composed of the Tudor domain-containing protein 3 (TDRD3), the fragile X mental retardation protein (FMRP) and the Topoisomerase III beta (TOP3β) and was termed TTF (TOP3β-TDRD3-FMRP) -complex according to its composition.

The presented results also demonstrate that all components of the TTF-complex shuttle between the nucleus and the cytoplasm, but are predominantly located in the latter compartment under steady state conditions. Apart from that, an association of the TTF-complex with fully processed mRNAs, not yet engaged in productive translation, was detected. Hence, the TTF-complex is a component of „early" mRNPs.

The defined recruitment of the TTF-complex to these mRNPs is not based on binding to distinct mRNA sequence-elements in *cis*, but rather on an interaction with the so-called exon junction complex (EJC), which is loaded onto the mRNA during the process of pre-mRNA splicing. In this context TDRD3 functions as an adapter, linking EJC, FMRP and TOP3β on the mRNP. Moreover, preliminary results suggest

that epigenetic marks within gene promoter regions predetermine the transfer of the TTF-complex onto its target mRNAs.

Besides, the observation that TOP3β is able to catalytically convert RNA-substrates disclosed potential activities of the TTF-complex in mRNA metabolism. In combination with the already known functions of FMRP, this finding primarily suggests that the TTF-complex controls the translation of bound mRNAs.

In addition to its role in mRNA metabolism, the TTF-complex is interesting from a human genetics perspective as well. It was demonstrated in collaboration with researchers from Finland and the US that apart from FMRP, which was previously linked to neurocognitive diseases, also TOP3β is associated with neurodevelopmental disorders. Understanding the function of the TTF-complex in mRNA metabolism might hence provide important insight into the etiology of these diseases.

2 Zusammenfassung

Die Umwandlung der genetischen Information in Proteine erfolgt über Boten-RNA (mRNA) -Intermediate. Diese werden in Eukaryonten durch die RNA-Polymerase II gebildet und nach diversen Prozessierungs-Schritten der Translationsmaschinerie zugänglich gemacht. Während man früher davon ausging, dass die Genexpression primär auf der Ebene der Transkription reguliert wird, ist heute klar, dass post-transkriptionelle Prozesse einen ebenso wichtigen Beitrag hierzu leisten. Neben nicht-kodierenden RNAs und Metaboliten tragen insbesondere RNA-Bindungsproteine zur Kontrolle dieses Vorgangs bei. Diese finden sich in unterschiedlichen Kombinationen auf den mRNAs zusammen und bilden dadurch den sog. „mRNP-Code" aus.

Im Rahmen dieser Dissertation wurde eine bislang unbekannte Komponente des mRNP-Codes identifiziert und charakterisiert. Es handelt es sich dabei um einen hetero-trimeren Komplex, welcher aus dem Tudor Domänen Protein 3 (TDRD3) dem Fragilen X Mentalen Retardations-Protein (FMRP) sowie der Topoisomerase III beta (TOP3β) besteht. Aufgrund seiner Zusammensetzung wurde dieser TTF (TOP3β-TDRD3-FMRP) -Komplex genannt.

In der vorliegenden Arbeit konnte der Nachweis geführt werden, dass sämtliche Komponenten des TTF-Komplexes zwischen Zellkern und Cytoplasma pendeln, unter Normalbedingungen jedoch vornehmlich im Cytoplasma lokalisiert sind. Des Weiteren ließ sich eine Assoziation des TTF-Komplexes mit mRNAs nachweisen, die zwar vollständig prozessiert, jedoch noch nicht Teil der produktiven Phase der Translation sind. Der TTF-Komplex ist somit eine Komponente „früher" mRNPs. Die Rekrutierung des TTF-Komplexes an definierte mRNPs wird nicht durch Bindung an spezifische mRNA-Sequenzelemente bedingt, sondern basiert auf einer Interaktion mit dem sog. Exon Junction Complex (EJC), welcher im Kontext des pre-mRNA Spleißens auf die mRNA geladen wird. Hierbei spielt TDRD3 als Adapter zwischen dem EJC, FMRP und TOP3β die entscheidende Rolle. Präliminäre Experimente

legen darüber hinaus den Schluss nahe, dass epigenetische Markierungen im Promotor-Bereich distinkter Gene von entscheidender Bedeutung für den Transfer des TTF-Komplexes auf dessen Ziel-mRNAs sind.

Einen wichtigen ersten Hinweis auf die potentielle Funktion des TTF-Komplexes im Kontext des mRNA Metabolismus erbrachte die Beobachtung, dass TOP3β in der Lage ist RNA katalytisch umzusetzen. Dieser Befund lässt in Verbindung mit den bereits beschriebenen Aktivitäten von FMRP vermuten, dass der TTF-Komplex die Translation gebundener mRNAs kontrolliert.

Zusätzlich zu seiner Rolle im mRNA Metabolismus ist der TTF-Komplex auch aus humangenetischer Sicht hoch interessant. So konnte in Zusammenarbeit mit finnischen und US-amerikanischen Forschern gezeigt werden, dass neben FMRP, einem bekannten Krankheitsfaktor neurokognitiver Syndrome, auch TOP3β mit neurologischen Entwicklungsstörungen assoziiert ist. Das Verständnis der Funktion des TTF-Komplexes im mRNA Metabolismus könnte daher wichtige Einblicke in die Etiologie dieser Krankheiten liefern.

3 Introduction

3.1 Eukaryotic gene expression is a highly regulated process

Gene expression is the key to life in all organisms. It incorporates the flow of the genetic information encrypted in the DNA to a functional gene product (e.g. a protein or a non-coding RNA; Fig. 3.1). Especially in higher eukaryotes this process is tightly controlled and accomplished within a cascade of steps, involving numerous guiding and processing factors. During the past decades lots of scientific effort helped to shed light on the contributing regulatory networks.

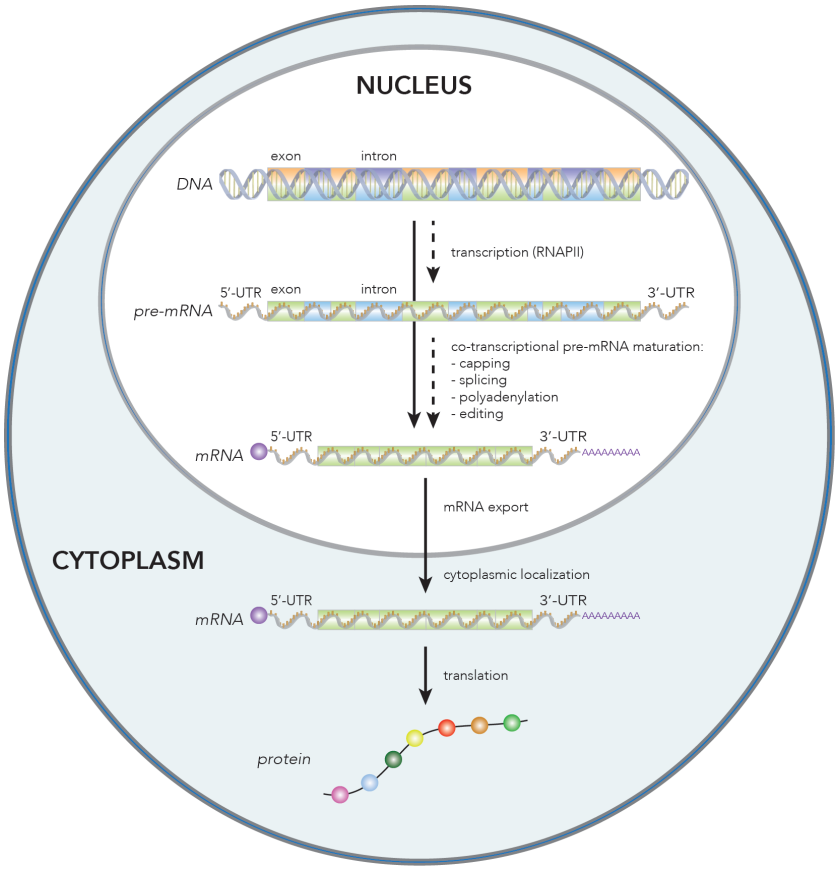

Fig. 3.1 Eukaryotic gene expression. Gene expression is spanning all events transferring the DNA-encoded genetic information to a functional gene product. In the nucleus a protein-coding gene is transcribed into a pre-mRNA by RNAPII, which is modified immediately. Subsequent to intron-excision and end-procession (5′-capping and 3′-polyadenylation) the mature mRNA is exported to the cytoplasm. After transport it is translated into its encoded polypeptide sequence by the ribosome and folding to a functional protein.

Gene expression is initiated in the nuclei of eukaryotic cells. There the DNA, which is typically condensed and packaged into chromatin, is made accessible by

remodeling enzymes. This allows for the binding of RNA-polymerases (RNAPs) and transcription factors. RNAPs catalyze the transcription of DNA into RNA and comprise three types in eukaryotes: RNAP I, II and III. In contrast to RNAP I and III, which account for the synthesis of functional, non-coding ribosomal (rRNAs) or transfer RNAs (tRNAs), respectively, protein-coding genes are transcribed into messenger RNAs (mRNAs) by RNAP II.

Independent from the RNA output, transcription is made up of three major phases: First, the RNAP binds to the DNA, e.g. to a genes promoter region with transcription being initiated after positioning the polymerase at the transcription start site (TSS) sequence. Second, during elongation, the gene is productively transcribed and an RNA complementary to the DNA-template is synthesized. Finally after transcription of a termination signal, the RNA molecule is cleaved and released from the transcription complex. The RNAPs dissociate from the DNA-template downstream of the termination signal. Especially RNAP II and III termination involves a large number of factors and several pathways, which are still not completely understood to date[1].

In most cases transcription produces primary RNA transcripts, which have to be further modified to gain functionality. This is in particular evident for precursor (pre-) mRNAs, which are heavily processed before they can serve as templates for protein production.

Already during RNAPII transcription, the 5'-end of the nascent transcript is modified by the addition of an m7G-cap structure[2]. Moreover, a poly(A)-tail composed of numerous adenosine nucleotides is synthesized at the mRNA's 3'-end[3]. Both structures increase the stability of the transcript and are beneficial for downstream events in the life cycle[4] of an mRNA.

Protein-coding genes constitute themselves not only of coding- (exons), but also of non-coding sequences (introns). Thus, to generate an exon-only template suitable for protein synthesis, the intervening intronic regions need to be removed from the pre-mRNA. Intron excision is accomplished co-transcriptionally by the spliceosome,

a macromolecular machine constituted of six ribonucleoprotein particle (RNP) subunits, all containing a uridine-rich small nuclear RNA (UsnRNA) and distinct sets of proteins[5].

Moreover, mRNA transcripts can be modified by RNA-editing enzymes, which specifically alter single nucleotides. Such variations can manipulate downstream processes, e.g. alternative splicing and thus increase the diversity of the protein-output of a single mRNA[6].

Of note, especially the early steps of gene expression ranging from chromatin remodeling to mRNA maturation are strongly dependent on post-translational protein modifications (PTMs). Amongst other proteins this involves modifications of Histones, the scaffolds of chromatin, but is especially true for RNAP II. RNAP II contains a large carboxyl-terminal-domain (CTD) constituted of a repetitive sequence motif of seven amino acids (YSPTSPS). Several of these amino acids can be modified by phosphorylation of their side chains or by isomerization (proline-*cis/trans*-isomerization)[7]. Due to these PTMs a "code" is established which enables and ensures the timely accurate recruitment of transcription- and mRNA-maturation factors, e.g. 5'- and 3'-end processing enzymes or the spliceosome[8] (Fig. 3.2).

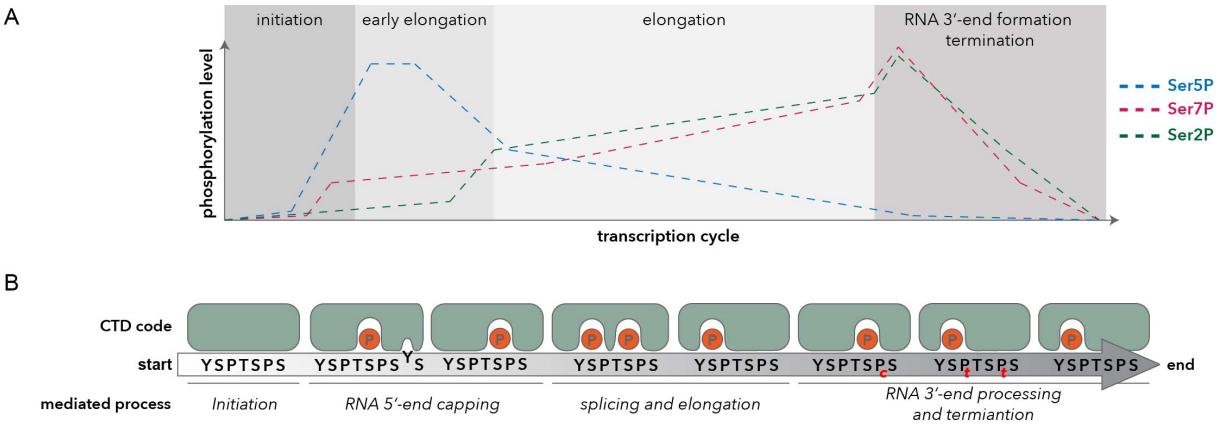

Fig. 3.2 The RNAP II CTD-code. PTMs on the RNAP II CTD create a code responsible for the accurate recruitment of transcription and mRNA processing factors, which guide RNAPII during the transcription cycle or mediate co-transcriptional pre-mRNA processing. **A)** Schematic overview over serine (Ser) phosphorylation variations of Ser2, Ser5 and Ser7 on the RNAPII CTD during the

individual phases of transcription. **B)** Significant CTD modification patterns resulting in the recruitment of mRNA processing factors and the mediated maturation steps. P_c or P_t represents the proline-isomerization state, either *cis* or *trans*, respectively (adapted from[7]).

Once the ends are accurately modified and introns are removed, mRNA maturation is complete. The transcript is subsequently exported from the nucleus to the cytoplasm, where it is translated into its encoded protein sequence by the ribosome. Just like the afore-mentioned spliceosome, the ribosome is built of RNP subunits. Together, the two (40S and 60S) ribosomal subunits contain four rRNAs and 79 ribosomal proteins generating a 3,2 MDa complex, the 80S ribosome. In cooperation with amino acid carrying tRNAs (aminoacly-tRNAs) the ribosome, "reads" the mRNA template and translates its nucleic acid sequence into the corresponding polypeptide, making up the encoded protein[9].

Like transcription, protein synthesis can be divided into initiation, elongation and termination. Initiation spans all processes required for assembly of a catalytically active 80S ribosome at the translation start site. During elongation the actual polypeptide is produced. After the ribosome reaches a termination signal, translation is aborted and the produced protein as well as the ribosome dissociate from the mRNA. Usually several ribosomes translate one mRNA simultaneously, creating ribosome clusters called polysomes. After several rounds of translation, mRNAs are enzymatically degraded, mostly in cytosolic P-bodies where mRNA turnover enzymes are strongly accumulated[10].

3.2 The "mRNP code" regulates post-transcriptional gene expression

The life cycle of an mRNA involves interactions with multiple proteins or RNPs. However, this is not restricted to processing events like maturation or turnover. Quite contrary, all additional steps within mRNA metabolism such as mRNA export, localization or regulation of translation likewise require binding of distinct sets of *trans*-acting proteins, resulting in the formation of messenger RNPs (mRNPs). The constantly changing protein content of mRNPs creates a code ("mRNP-code"),

which is primarily decisive for an mRNA's cellular fate. Thus, mRNPs are today seen as post-transcriptional operons and therefore essential pillars of gene-expression[11]. Recent studies on the mRNA-bound proteome uncovered that the number of mRNP-constituting proteins is by far exceeding previous expectations[12,13]. This finding further emphasizes the importance of the mRNP-code. Notably, the numbers of mRNP-components is certainly even higher, as the studies did only partially cover indirectly mRNA-associated proteins.

In principle the mRNP-code could be established solely by distinct sequence elements on the mRNA that recruit diffusible RNA-binding proteins (RBPs) and their interactors. However, in rare cases RBPs can also be deposited on the transcript without the presence of *cis*-elements. A representative for such a mechanism is the assembly of the exon junction complex (EJC) on spliced mRNAs.

The EJC complex is composed of four proteins (Y14, MAGOH, eIF4AIII and Barentz) and is recruited to mRNAs by the spliceosome[14,15]. It assembles 20-24 nucleotides upstream of splice junctions, irrespective of the mRNA-sequence[16,17]. Once deposited, the EJC was shown to enhance nuclear export[18,19], cytoplasmic localization[20] and translation of mRNAs[21,22]. It further participates in cytoplasmic mRNA quality control, functioning as a marker for the detection of transcripts containing premature translation termination signals[18]. In this context, the EJC represents an essential binding platform for proteins involved in the subsequent degradation of aberrant mRNAs via the nonsense mediated decay (NMD) pathway.

Hence the EJC is a crucial factor for mRNA expression and surveillance. It is stripped off of the mRNA during the first or "pioneer" round of translation (PRT)[23]. This step additionally removes and exchanges multiple proteins specifically associated with "early", but fully processed mRNAs, generating quality-checked mRNPs, suitable for productive translation[24,25]. Thus the remodeling events during the PRT demonstrate how the mRNP-code can influence mRNA-expression (Fig. 3.3).

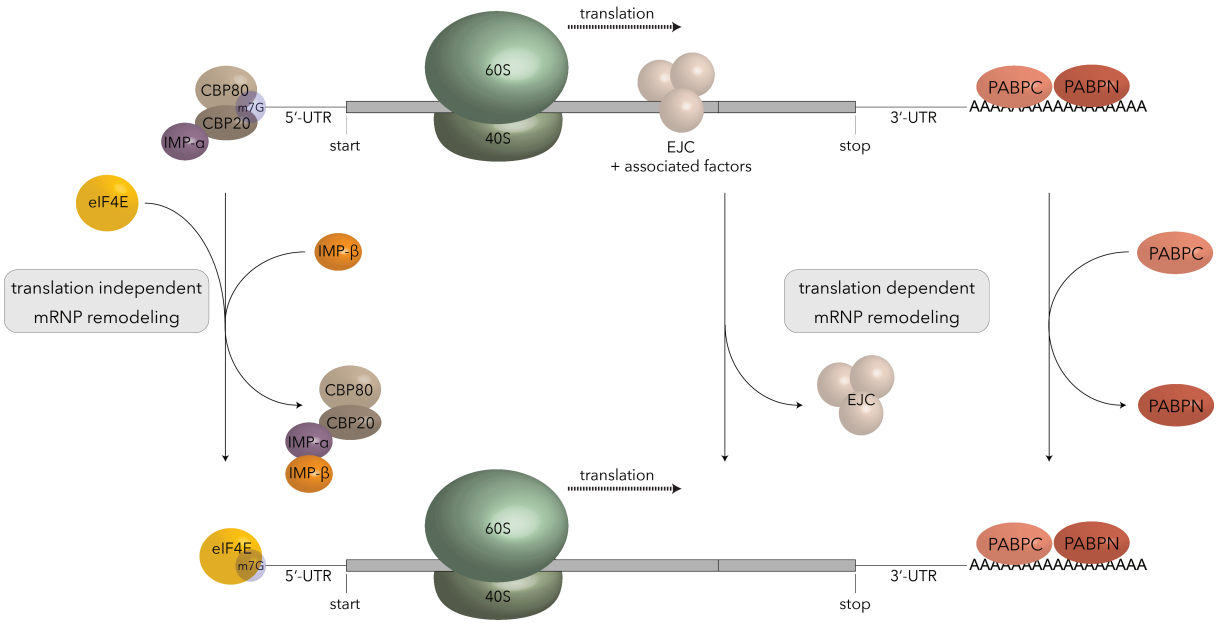

Fig. 3.3 The PRT exemplifies how remodeling of mRNPs determines their cellular fate. The schematics show the specific features of an early, fully processed, exported mRNA (top). It contains a characteristic set of marker proteins, such as the cap binding complex (CBC) consisting of cap binding proteins (CBPs) 20 and 80, which is further associated with importin α (IMPα). Additionally these transcripts carry exon junction complexes (EJCs) upstream of splice junctions and both, the nuclear and the cytoplasmic poly(A)-binding proteins (PABPN and PABPC) on their poly(A)-tail. Whereas the EJC is removed and PABPN is exchanged for PABPC dependent on the first translating ribosome, the CBC is disassembled in a translation independent manner assisted by importin β (IMPβ) and substituted by eIF4E. As part of the mRNA surveillance, these remodeling steps result in a quality checked mRNA suitable for productive translation (bottom) (adapted from[26]).

3.3 The mRNP code is implicated in disease

The continuously increasing importance of the mRNP-code in the regulation of gene expression implicates a potential relevance for the etiology of disease. Indeed, disruptions of the mRNP-code by mutated or deleted RBPs as well as by mRNAs containing aberrant sequences, are causative for a variety of human disorders[27–29].

Apart from unrelated diseases like cancer or muscular atrophies this is especially prominent in neurological disorders. Due to their morphology, neurons are exceedingly dependent on processes like mRNA transport, localization as well as localized translation and rapid degradation[30,31].

Aberrant mRNA metabolism leads to changes in synaptic protein homeostasis, e.g. at the level of receptors. This impairs synaptic plasticity, which is thought to be one of the major contributors to abnormal integration of brain processes[29]. In line with that, altered synaptic plasticity is connected to diseases of the autism spectrum disorder (ASD) range, comprising abnormal behaviors spanning from Autism to Schizophrenia[32]. However, the exact mechanism by which neuronal malfunction translates into neurocognitive phenotypes remains enigmatic and is controversially discussed.

One RBP connected to neurodevelopmental disorders is the fragile X mental retardation protein (FMRP). FMRP is affected in the most common inherited neuropsychiatric disorder fragile X syndrome (FXS; OMIM#300624), but has also been linked to ASD-phenotypes like Schizophrenia[33]. FXS is caused by silencing of the FMRP encoding *FMR1* gene due to a tri-nucleotide (CGG) repeat expansion in its promoter region[34]. However, in rare cases missense mutations affecting the FMRP protein sequence also perturb the FXS phenotype[35].

FMRP is linked to multiple aspects of mRNA metabolism and was shown to bind at least four RNA sequence elements[36–38]. Its most prominent functions in the context of FXS are regulation of mRNA transport and translation[33]. In particular the latter has been extensively studied and represents the accepted basis for deviations in synaptic plasticity[39]. FMRP was shown to inhibit synthesis of neuronal mRNAs during translation elongation by stalling polysomes[40]. This mechanism, lost in FXS patients, contributes to control local protein production in neurons and thus to maintain synaptic plasticity (Fig. 3.4).

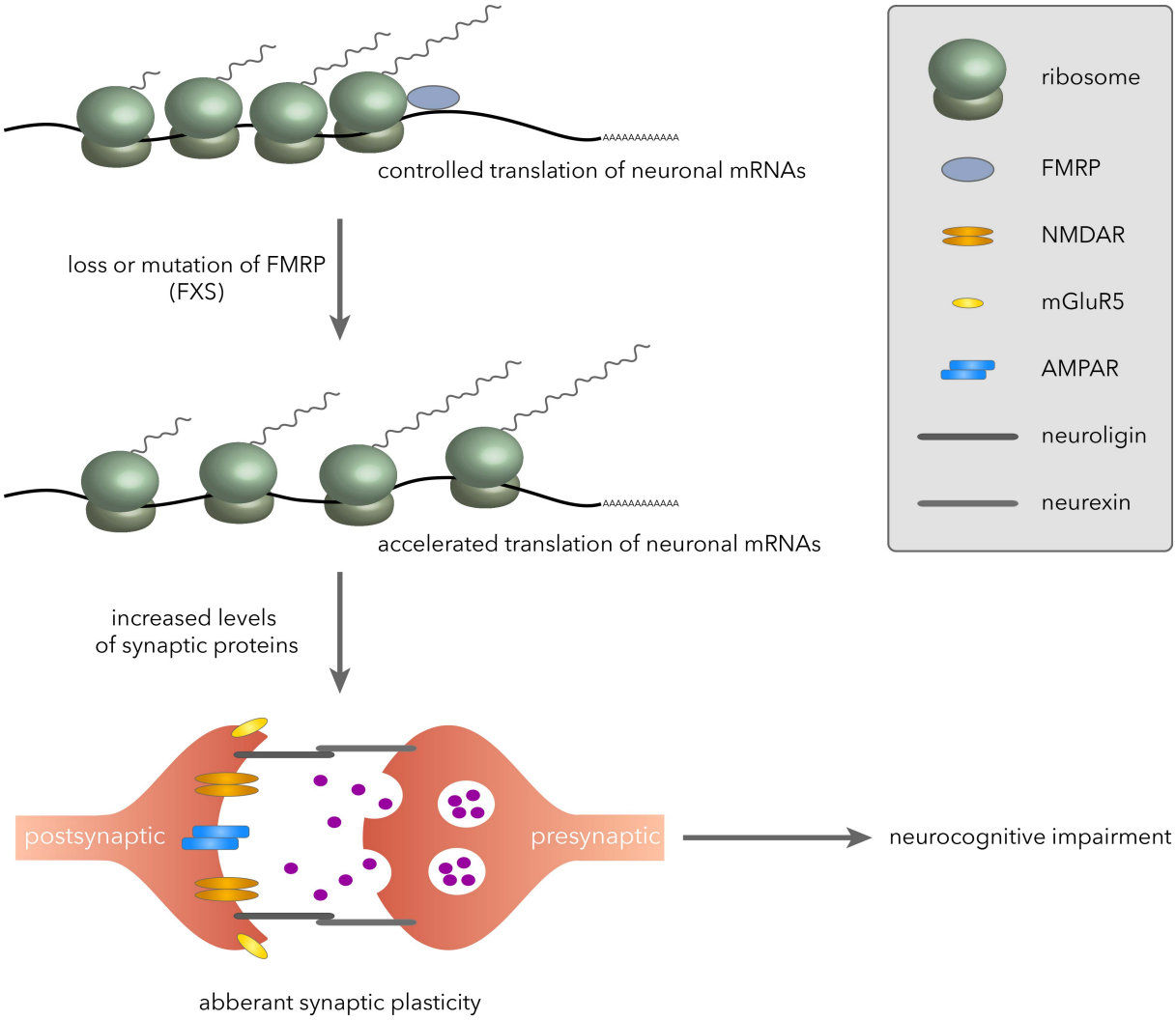

Fig. 3.4 Aberrant neuronal mRNA translation in synapses due to changes in the mRNP code can cause neurological disorders, as exemplified by fragile X syndrome (FXS). The mRNA binding protein FMRP inhibits neuronal mRNA translation by controlling the translocation rate of ribosomes. Loss or mutation of FMRP leads to increased translation of synaptic proteins, e.g. receptors like mGluR or NMDAR. As a final consequence, this alters synaptic plasticity translating to the neurocognitive impairment observed in FXS patients. Abbreviations: FMRP, fragile X mental retardation protein; NMDAR, *N*-methyl-D-aspartate receptor; mGluR, metabotropic glutamate receptor; AMPAR, AMPA (α-amino-3-hydroxy-5-methyl-4-isoxazolepropionic acid)-type glutamate receptor (adapted from[39]).

3.4 RBPs are the major contributors for mRNP-code establishment

As outlined earlier, the establishment of the mRNP-code is primarily mediated by RBPs. This raises the interesting question how their binding to mRNAs is mediated and whether some common features are involved. Indeed, most RBPs share distinct RNA-binding ternary structures. The prevalent RNA binding module amongst RBPs

is the RNA recognition motif (RRM), present in 0,5 - 1 % of human genes[41]. Moreover, other RNA binding folds were identified with the most important being the hnRNP K homology (KH) domain, the double stranded RNA binding domain (DRBD), a variety of zinc finger domains as well as the RGG/RG motif[42,43].

In contrast to other RNA binding domains, the latter motif, alternatively termed glycine-arginine-rich region (GAR) or RGG box, was shown to also mediate protein-protein interactions[42]. It has initially been described in hnRNP U[44] and ever since multiple RGG/RG motifs containing proteins were identified and most were classified as "RNA-binding"[42]. To increase their RNA target diversity or to specifiy protein-protein interactions, GARs are often modified by arginine methylation.

Apart from PTMs, combination of several RNA binding motifs is a common feature amongst RBPs to increase target affinity, diversity and specificity[45]. For instance the afore-mentioned FMRP contains two KH domains and an RGG box, which all contribute to its interaction with distinct RNA sequences and secondary structures[36,46,47].

3.5 RNA associated protein families contribute to the mRNP code

RNPs are not exclusively made up from direct RNA-binding proteins but also from proteins associated via these RBPs. Just like many RBPs share structural elements, indirectly bound RNP components might resemble this characteristic. Exemplified by the Tudor protein family, this assumption is indeed true.

The general feature of this protein family is the name giving Tudor domain[48]. Tudor domains consist of 60 amino acids, forming a barrel-like structure, which contains an aromatic binding pocket. This pocket is selectively accessible for post-translationally methylated arginine side chains. Depending on the precise architecture of the aromatic cage, arginine residues accepted for binding can either be mono-methylated (MMA) or symmetrically- as well as asymmetrically di-methylated (sDMA or aDMA, respectively)[49–52].

The best-studied Tudor domain protein is the survival motor neuron (SMN) protein. SMN is a key factor for the cytoplasmic assembly of spliceosomal UsnRNPs, integrating UsnRNAs and essential spliceosomal proteins[52,53]. Reduced expression of SMN results in altered UsnRNP levels and is the underlying cause for spinal muscular atrophy (SMA), a severe inherited neurodegenerative disease[54].

Besides SMN, multiple Tudor domain-containing proteins (TDRDs) were identified to date[48,55]. In contrast to the SMN Tudor domain, some TDRDs carry additive N- and C-terminal structures flanking the Tudor domain core and were therefore termed extended Tudor domains (eTuds)[51,56]. Importantly, irrespective of such Tudor domain extensions, all so far discovered TDRDs could be functionally linked to RNA metabolism and many of them contain additional RNA-binding folds like KH-domains (TDRD2 and AKAP1), RRMs (TDRD10) or less known Lotus domains (TDRD5) and Staphylococcal nuclease (SN) like domains (SND1)[48].

3.6 TDRD3 is an atypical Tudor domain-containing protein

Most TDRDs are predominantly expressed in the germline. There they govern the P-element induced wimpy testis (PIWI) interacting RNA (piRNA) pathway. This pathway represents a tissue specific variation of the RNA induced silencing pathway and serves to fine-tune gene expression. In this context, TDRDs function by integration of effectors (e.g. arginine methylated PIWI proteins) with substrates and scaffolding factors[57].

An exception is the Tudor domain-containing protein 3 (TDRD3), which represents the focus of this thesis. It is a ubiquitously expressed factor with peak levels in neuronal tissues[58] comprised of 744 amino acids. Apart from the classifying Tudor domain it carries multiple additional folding units (Fig. 3.5).

For instance, TDRD3 contains an N-terminal domain (NTD)[58,59], which is composed of a domain unknown function (DUF) 1767 adjacent to an oligonucleotide/oligosaccharide-binding (OB) fold. Furthermore TDRD3 harbors an ubiquitin associated (UBA) domain, which binds exclusively to lysine 48 (K48) linked

ubiquitin chains, but not to other ubiquitin interlinkages or the small ubiquitin like modifier (SUMO), *in vitro*[58].

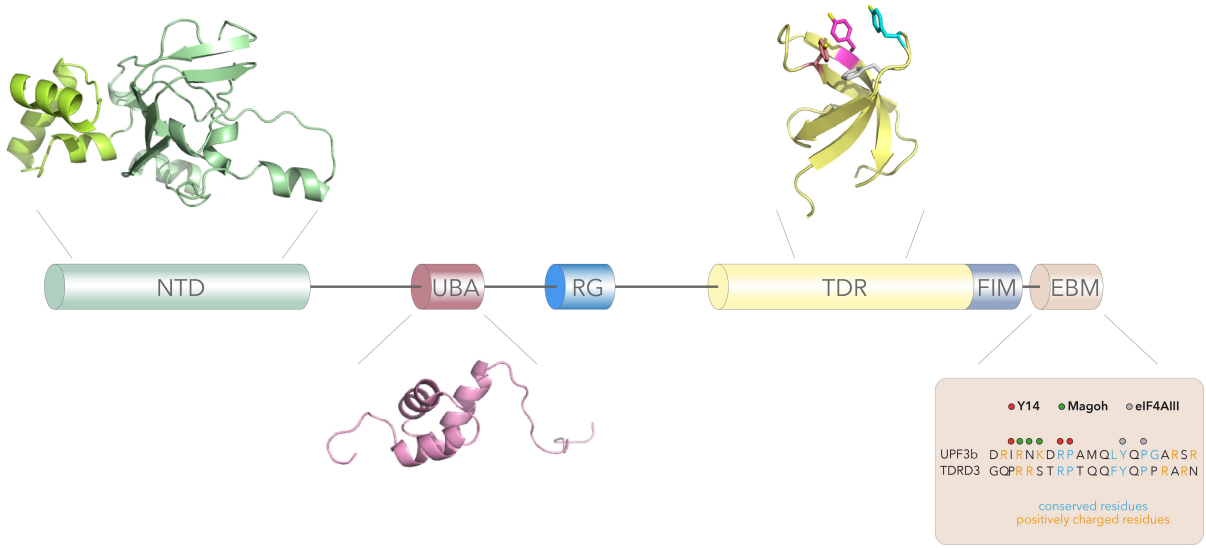

Fig. 3.5 The molecular architecture of TDRD3 comprises several distinct folds and motifs. TDRD3 contains three structural modules: First an N-Terminal domain (NTD, modeled structure based on the homologous NTD of RMI1; pdb3nbi) comprised of a DUF1767 and a β-barrel OB-fold (lime or light green in the structure, respectively), second an ubiquitin associated (UBA) domain with unclear cellular function (pdb1wji) and third, the name-giving Tudor domain (TDR) with its characteristic barrel-like structure formed by 5 β-sheets (pdb3s6w). The residues (YYYF) forming the aromatic aDMA-binding pocket are highlighted in color. The TDRD3 sequence further includes a predicted RGG/RG motif (RG), a FMRP interaction motif (FIM) composed of 20 amino acids C-terminally of the Tudor domain and an exon junction complex binding motif (EBM), whose sequence alignment with the EBM of NMD factor UPF3b is depicted below. Amino acids involved in the binding to the EJC core components MAGOH, Y14 and eIF4AIII are indicated.

When covalently attached to proteins K48 linked ubiquitin chains represent a signal for their proteasomal degradation[60]. Nevertheless the consequences of the NTD and the UBA domain for TDRD3's cellular function remain elusive.

3.7 TDRD3 is implicated in various steps of gene expression

The Tudor domain of TDRD3 shows a high preference of binding to aDMA residues, although it also recognizes sDMA *in vitro*[61–63]. aDMA targets of TDRD3 were recently

found on the tails of Histones H3 (H3R17me2a) and H4 (H4R3me2a)[63], as well as on the afore-mentioned RNAP II CTD (R1810me2a)[64].

With all of these modified proteins involved in the early phase of mRNA expression, TDRD3 was functionally implicated in transcription. It is thought to "read" aDMA PTMs and recruit so far unidentified effectors to the sites of modification, thus acting as a transcriptional co-activator[63].

However, TDRD3 also shows some other features, which indicate a function in later stages of mRNA metabolism. First TDRD3 contains a putative RNA-binding motif (RGG/RG), so far lacking further characterization. Second, its far C-terminus forms a functional exon junction complex binding motif (EBM)[65]. As mentioned earlier, the EJC is associated with spliced, post-transcriptional mRNAs. Third, TDRD3 is a predominantly cytoplasmic protein localizing to stress granules (SGs)[58,59]. SGs are cytoplasmic foci where translationally silenced mRNAs are temporarily stored upon environmental stress (e.g. UV-irradiation, oxidative stress or amino acid starvation)[66,67]. Apart from mRNAs many translation associated RBPs and small ribosomal subunits accumulate in these highly dynamic aggregates[68]. Fourth, TDRD3 interacts directly with the prototype RBP FMRP via a stretch of 20 amino acids in the C-terminal proximity of the Tudor domain termed FMRP interaction motif (FIM)[58]. This binding is of outstanding interest as it is disrupted by a highly pathogenic point mutation of FMRP (I304N)[58], which excludes FMRP from polysomes[69] and hence prevents its function as a translational regulator[40].

Taken together, these characteristics strongly point to a role of TDRD3 in cytoplasmic regulation of mRNA metabolism and thus gene expression. Moreover they raise the question for a potential role of TDRD3 in in the context of neurodevelopmental disorders.

4 Results

Most Tudor domain-containing proteins orchestrate the assembly of larger, often RNA-containing, complexes by acting as molecular adaptors. Moreover, some TDRDs are connected to disease. Hence, the finding of an interaction between TDRD3 and FMRP gave reason to believe in a potential involvement of TDRD3 in the etiology of FXS[58]. This assumption was further supported, as the highly pathogenic FMRP missense mutant I304N failed to bind to TDRD3[58]. This represents the only protein interaction altered by this mutation so far. Consequently, a closer inspection of TDRD3's cellular properties and interactions could be highly beneficial for our understanding of the molecular basis of FXS.

4.1 TDRD3 forms a complex with FMRP and TOP3β

To shed light onto the TDRD3 interaction network, classical yeast two-hybrid screening as well as mass spectrometry-coupled immunoprecipitation approaches were initially employed[70].

Apart from the binding to FMRP, the latter approach revealed an association of TDRD3 with the human DNA topoisomerase IIIβ (TOP3β). This was confirmed by *in vitro* binding assays using purified, recombinant proteins (Fig. 4.1A). GST-TOP3β-6xHis or GST-6xHis alone were immobilized on Glutathione Sepharose (Fig. 4.1A, lanes 2 and 3) and incubated with His-tagged TDRD3 (Fig. 4.1A, lane 1). TDRD3 stoichiometrically bound to GST-TOP3β-6xHis but failed to interact with GST alone (Fig. 4.1A; compare lanes 4 and 5), illustrating the direct interaction.

Consistent with this result *in vivo* immunoprecipitations from mouse brain lysates with antibodies directed against endogenous TOP3β or TDRD3 efficiently captured both proteins and additionally FMRP (Fig. 4.1B, lanes 3 and 4). Moreover, precipitation of this heterotrimer was insensitive to RNase-treatment, demonstrated by RNase A-containing anti-FLAG immunoprecipitations from inducible Flp-In T-Rex

cell lines, stably expressing either N-terminally FLAG/HA-tagged TDRD3 or TOP3β (Fig. 4.1C and D; lanes 5 and 6 in each case).

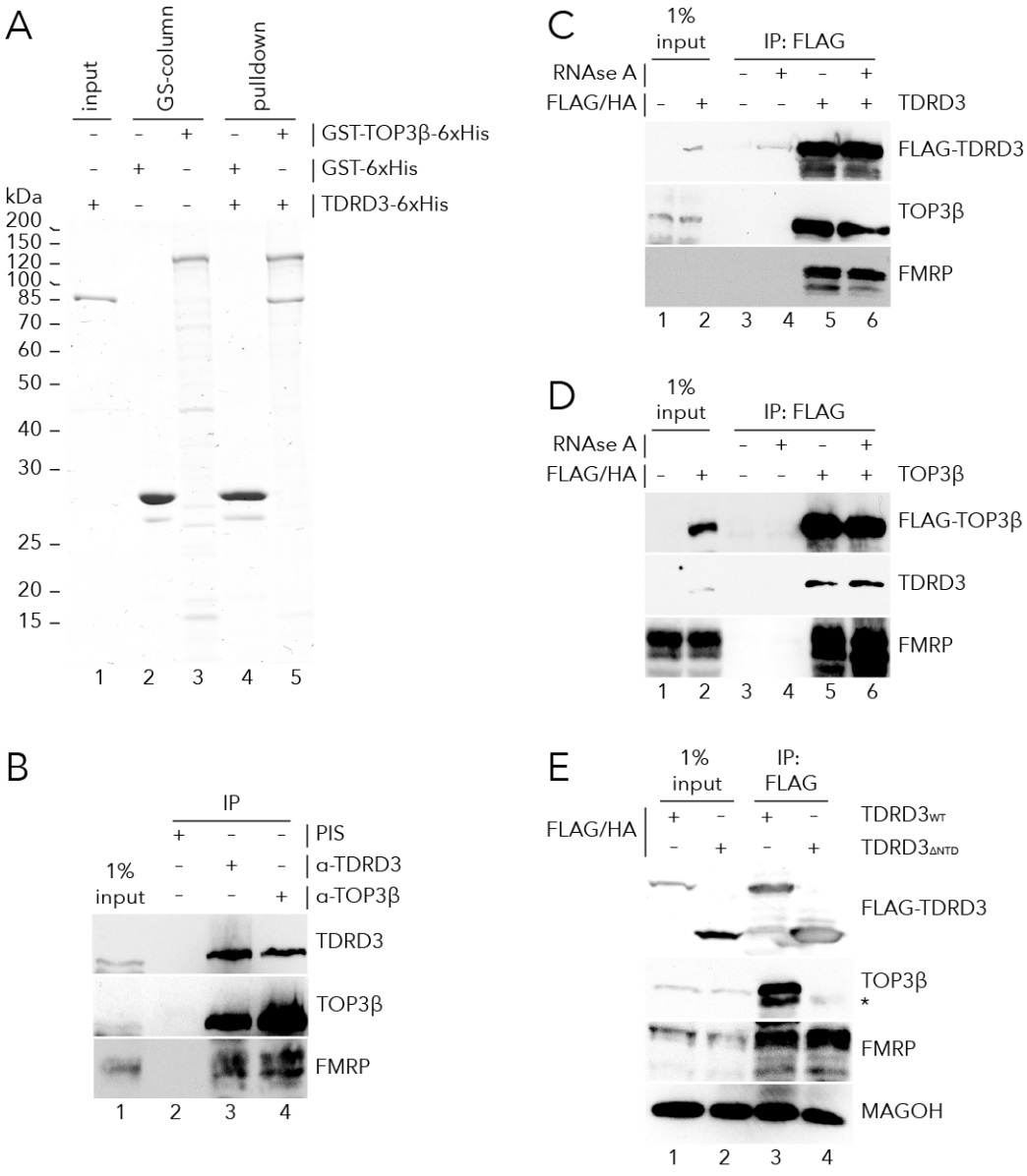

Fig. 4.1 TDRD3 forms a complex with TOP3β and FMRP. **A)** TDRD3 binds directly to TOP3β *in vitro*. Recombinant 6xHis-tagged TDRD3 (lane 1) was incubated either with immobilized recombinant GST-TOP3β-6xHis or GST-6xHis control, (lanes 2 and 3). TDRD3 was only captured by TOP3β (lane 5) but not by GST-6xHis (lane 4). **B)** In contrast to a pre-immune serum (PIS) control (lane 2), antibodies against either TDRD3 or TOP3β co-precipitate the corresponding antigen and interactor as well as FMRP from mouse brain lysates (lanes 3 and 4). **C)** Lysates of non-induced (lane 1) or induced (lane 2) stably FLAG/HA-TDRD3 expressing Flp-In T-Rex cells were either left untreated (lanes 3 and 5) or incubated with RNase A (lanes 4 and 6). Anti-FLAG affinity purification (lanes 3-6) shows an RNase-insensitive binding of TDRD3 to TOP3β and FMRP. **D)** Same as C) but using TOP3β

expressing Flp-In T-Rex cells. **E)** TOP3β binding is mediated by TDRD3's N-terminal domain (NTD). Flp-In T-Rex cell lysates stably expressing either FLAG/HA-tagged $TDRD3_{WT}$ (wildtype, lane 1) or $TDRD3_{\Delta NTD}$ (lane2) were subjected to anti-FLAG immunoprecipitation (lanes 3 and 4) and proteins of interest were immunodetected. $TDRD3_{WT}$ but not $TDRD3_{\Delta NTD}$ efficiently co-purifies TOP3β. Interactions of TDRD3 with FMRP or the EJC (represented by MAGOH) are not affected. Asterisk indicates an unspecific cross-reactivity of the TOP3β antibody.

Binding of TOP3β was attributed to the N-terminal domain (NTD) of TDRD3 by incubation of *in vitro* translated TDRD3 truncations with immobilized recombinant TOP3β[70]. This was validated *in vivo*, again by anti-FLAG-immunoprecipitations from lysates of stable Flp-In T-Rex cells expressing N-terminally FLAG/HA-tagged $TDRD3_{WT}$ (wildtype) or a truncation lacking the NTD ($TDRD3_{\Delta NTD}$). TOP3β only bound to $TDRD3_{WT}$ but not to $TDRD3_{\Delta NTD}$ (Fig. 4.1E; lanes 3 and 4). In contrast, interactions with FMRP or the EJC (exemplified by detection of MAGOH) via their C-terminally located binding motifs, were unaffected in both cases pointing to the functionality of the overexpressed TDRD3 variants. These results showed that TOP3β, TDRD3 and FMRP form a heterotrimeric (TTF) -complex, in which TDRD3 acts as a scaffold, indirectly linking the other complex components.

4.2 TOP3β is a type IA topoisomerase

TOP3β is a 95kD (862 amino acids) protein composed of a N-terminal catalytic Toprim domain and a large unstructured C-terminal region. The latter contains four putative zinc finger motifs potentially involved in nucleic acid binding.

Topoisomerases are particularly involved in DNA metabolism. These enzymes modify the topological state of their substrate by catalyzing temporary cleavage of the DNA, to allow for strand-passage through the breaking gap. Topoisomerases play significant roles in processes like DNA replication, DNA recombination, chromosome segregation, chromosome condensation but also DNA transcription[71]. Two major classes of topoisomerases are known, differing mainly in their way of substrate-procession. Unlike type I topoisomerases, which cleave only a single DNA-

strand without the necessity of additional energy, type II topoisomerases catalyze cleavage of both DNA-strands in an ATP-consuming reaction[71].

Despite this difference, the underlying catalytic mechanism of both topoisomerase subfamilies is comparable. First, the nucleic acid strand backbone is attacked by the hydroxyl-group of the enzymes active site tyrosine, resulting in a covalent, transient phosphodiester bond. During the lifetime of this covalent intermediate, substrate topology can be altered by facilitation of strand passages. Finally, the enzyme is released from its substrate after the phosphotyrosine intermediate is attacked by the free hydroxyl-group of the non-covalently bound nucleic acid strand, leading to re-ligation.

Each of the topoisomerase subfamilies can be further subdivided into group A or B, based on whether they form covalent linkages with the 5′- or 3′-phosphate at the substrate cleavage site (Fig. 4.2). Due to this classification, TOP3β has been attributed to the type IA topoisomerase family.

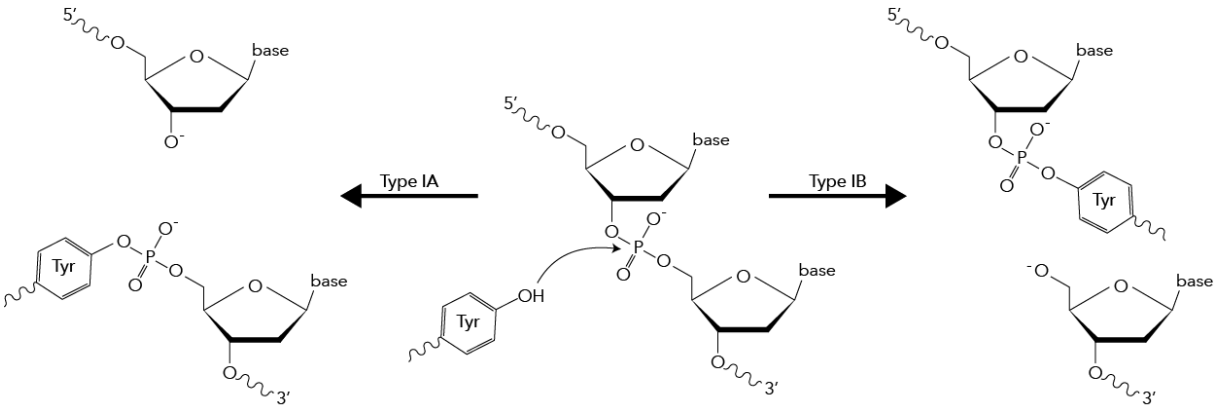

Fig. 4.2 Reaction mechanisms of type I topoisomerases. Catalysis of strand passage by topoisomerases requires formation of a reversible covalent enzyme-substrate adduct, through their active site tyrosine (Tyr). Type I topoisomerases differ in whether adducts are formed with the 3′- (Type IA; left) or the 5′- (Type IB; right) end of the substrate.

4.3 TOP3β is associated with neurocognitive disorders

Apart from early reports providing some evidence for the involvement of TOP3β in DNA metabolism[72–74], hardly anything is known about its cellular function.

However, copy number variants (CNVs) of the *TOP3B* gene could be connected to neurocognitive impairment in human genetic studies that were performed at the Sanger Institute (UK) in a collaborative manner. The group of Aarno Palotie has a high expertise for the implication of particular genes in the generation of complex brain and behavioral disorders. Due to an extreme genetic drift, as a consequence of bottleneck events during Finnish settlement, some rare Mendelian diseases are more frequent in some regions of Finland then elsewhere in the world. The prevalence of neurodevelopmental phenotypes in population isolates is almost threefold higher in the country's Northeast than in Finland overall, which is exemplified by the autism spectrum disorder Schizophrenia[75].

By using genome-wide single nucleotide polymorphism (SNP) arrays, the geneticists were able to significantly (P = 0,007) connect a CNV on chromosome 22 (240 kb deletion at position q11.22) enriched in a Northern Finnish cohort to Schizophrenia and cognitive impairment (Fig. 4.3A).

How this CNV translates to the associated neurodevelopmental phenotype, is illustrated by four homozygous deletion carriers, all displaying cognitive impairment and two of them being diagnosed with Schizophrenia (Fig. 4.3B). Apart from a pseudogene (IGLV2-14), the deleted chromosomal region exclusively encompasses the *TOP3B* gene and is flanked by two low copy repeats, presumably facilitating the deletion (Fig 4.3A). Of note, comparative microarray analysis showed that the deletion had no significant effect on global mRNA levels in peripheral blood cells of patient versus control samples[75]. This suggests, that the observed phenotype is most likely not related to a general role of TOP3β in transcriptional regulation, as aberrant transcription should yield an altered cellular mRNA output.

In summary, the genetic association of TOP3β with neurocognitive impairment further emphasizes the significance of the TTF-complex for the development of ASD phenotypes.

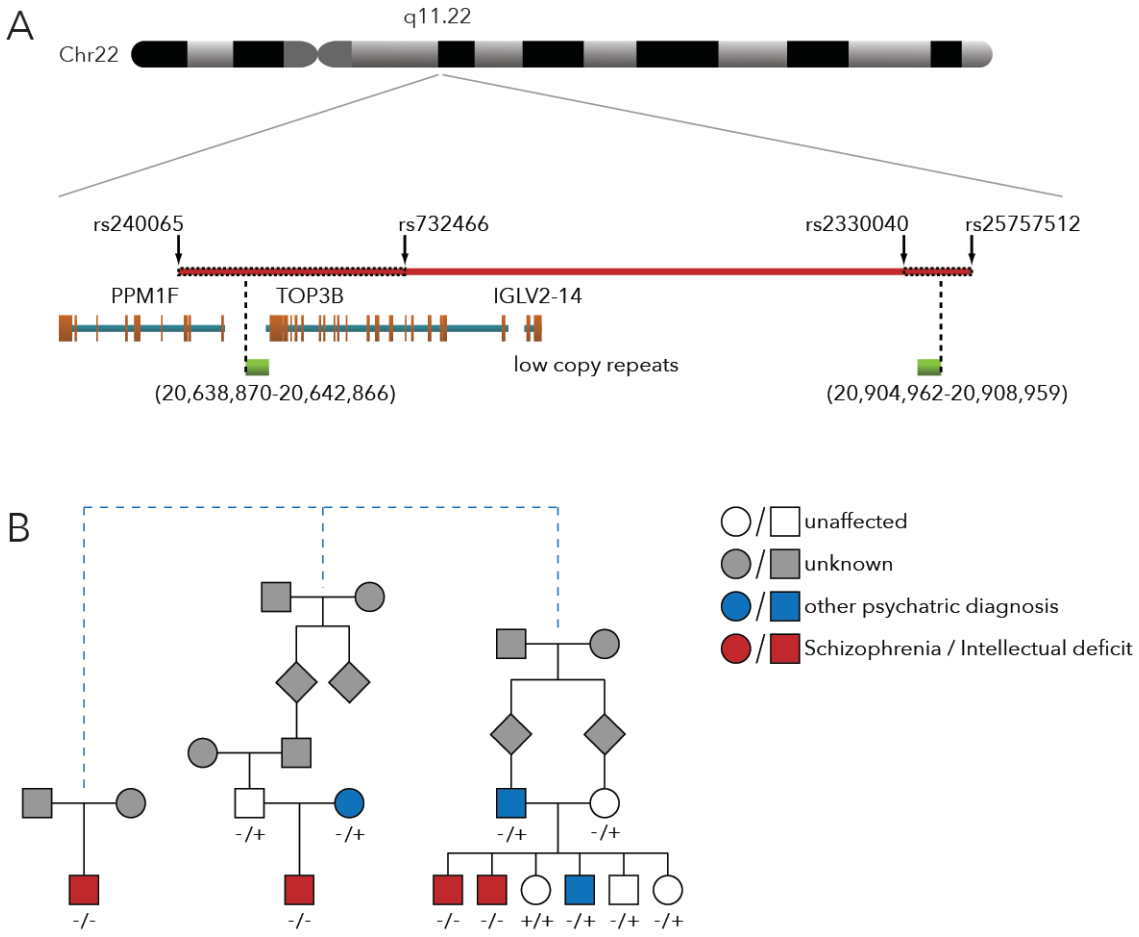

Fig 4.3 Deletion of the TOP3β-encoding chromosomal region is connected to Schizophrenia and neurocognitive impairment. **A)** The rare 22q11.22 240 kb deletion, enriched in a Finnish population isolate encompasses only one protein coding gene (*TOP3B*) and is flanked by two low copy repeats (green) potentially facilitating the deletion. The SNPs defining the breakpoint region are indicated by arrows, the deletion itself is marked by dashed lines. **B)** The connection of *TOP3B* deletions and neurocognitive phenotypes is represented by four (homozygous) individuals (red), all of whom displaying Schizophrenia or other intellectual impairment. The pedigrees, including two documented consanguineous matings, were presumed to descend from a common ancestor (dashed lines) based on the common haplotype observed among all of the homozygous deletion carriers.

4.4 TOP3β is a predominantly cytoplasmic protein

At steady state, TDRD3 and FMRP are localized predominantly in the cytosol, rather than in the nucleus[58]. Hence, the interaction with TOP3β, an enzyme thought to act exclusively in the latter compartment, was quite unexpected.

To elucidate where the proteins interact within the cell, the cellular distribution of TOP3β was monitored. Surprisingly, indirect immunofluorescence studies performed in HeLa cells with antibodies directed against endogenous TOP3β revealed a prevailing cytoplasmic localization, reminiscent of the intracellular distribution of TDRD3 and FMRP (Fig. 4.4A, upper panel). The same finding was obtained when HeLa cells were transfected with recombinant GFP-tagged TOP3β (Fig. 4.4A, lower panel).

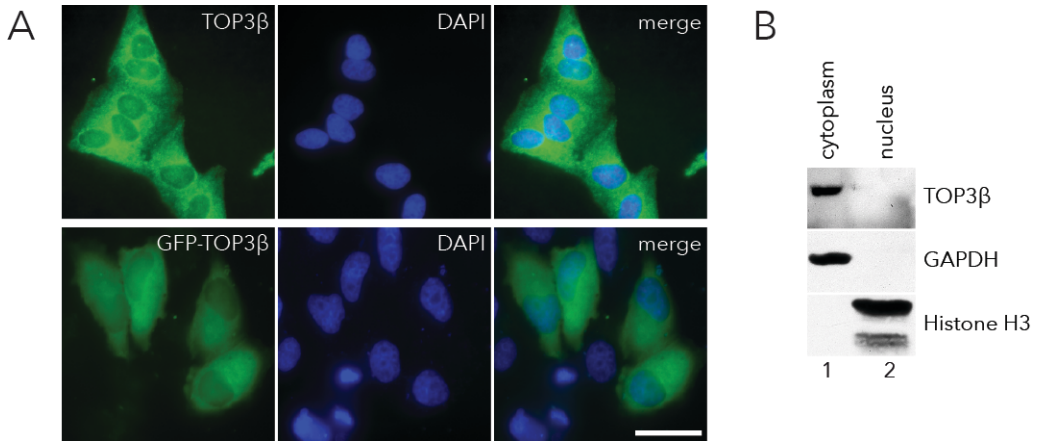

Fig. 4.4 TOP3β is a predominantly cytoplasmic protein. **A)** Fluorescence microscopy of HeLa cells using either an indirectly stained TOP3β specific monoclonal antibody (upper panel) or transfected GFP-tagged recombinant TOP3β (lower panel) revealed a cytoplasmic localization of the TOP3β protein. DAPI staining was used as a nuclear marker, scale bar represents 50 µm. **B)** The cytoplasmic pattern of TOP3β could be further confirmed by immunodetection of endogenous TOP3β after nulceo-cytoplasmic fractionation of HeLa cells. TOP3β was predominantly present in the cytoplasmic (lane1) but not in the nuclear fraction (lane 2).

To further strengthen this result, nuclear and cytoplasmic extracts were prepared from HeLa cells and the presence of endogenous TOP3β was detected by Western blotting. The purity of the respective fractions was confirmed by a nuclear and a cytosolic marker protein, histone H3 and GAPDH, respectively. TOP3β was found to be strongly enriched in the GAPDH-containing, cytoplasmic fraction, matching the microscopic observations (Figure 4.4B, compare lane 1 and 2).

In summary, the localization of TOP3β was perfectly consistent with the distribution of the other TTF-complex components and supportive of a cohesive function in the cytoplasm.

4.5 TDRD3 and TOP3β are exported from the nucleus in a CRM1 dependent manner

FMRP is actively exported from the nucleus[76–78]. This is accomplished by either an export signal included in its protein sequence[76,78] or by indirect export of the protein along with mRNAs[77]. Which of the two pathways prevails for FMRP and where they intersect is not yet determined.

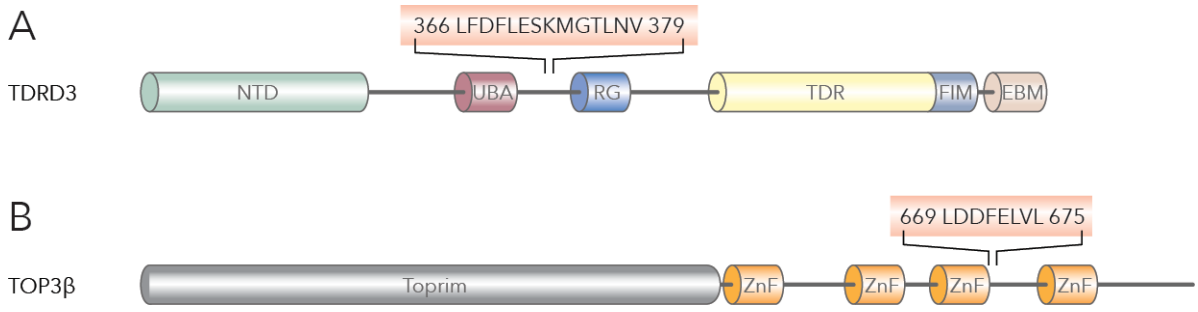

Fig 4.5 TDRD3 and TOP3β contain putative NESs (prediction by NetNES 1.1; http://www.cbs.dtu.dk/services/NetNES/). Depiction of the NES localization in **A)** TDRD3 and **B)** TOP3β. NES amino acid sequence and position are indicated and highlighted in light red.

The dynamics underlying FMRP's cellular distribution gave rise to the notion that the localization of TDRD3 and TOP3β might follow the same principles. Hence, the sequences of TOP3β and TDRD3 were analyzed for putative cellular localization signals. This prediction detected classical nuclear export signals (NES) in both proteins which access the chromosome region maintenance 1 (CRM1) / exportin1 (XPO1) mediated export pathway. In TDRD3 the potential NES is located in the unstructured region between UBA and Tudor domain (amino acids 366-379; Fig. 4.5A), whereas it resides in the unstructured C-terminus of TOP3β (amino acids 669-675; Fig. 4.5B).

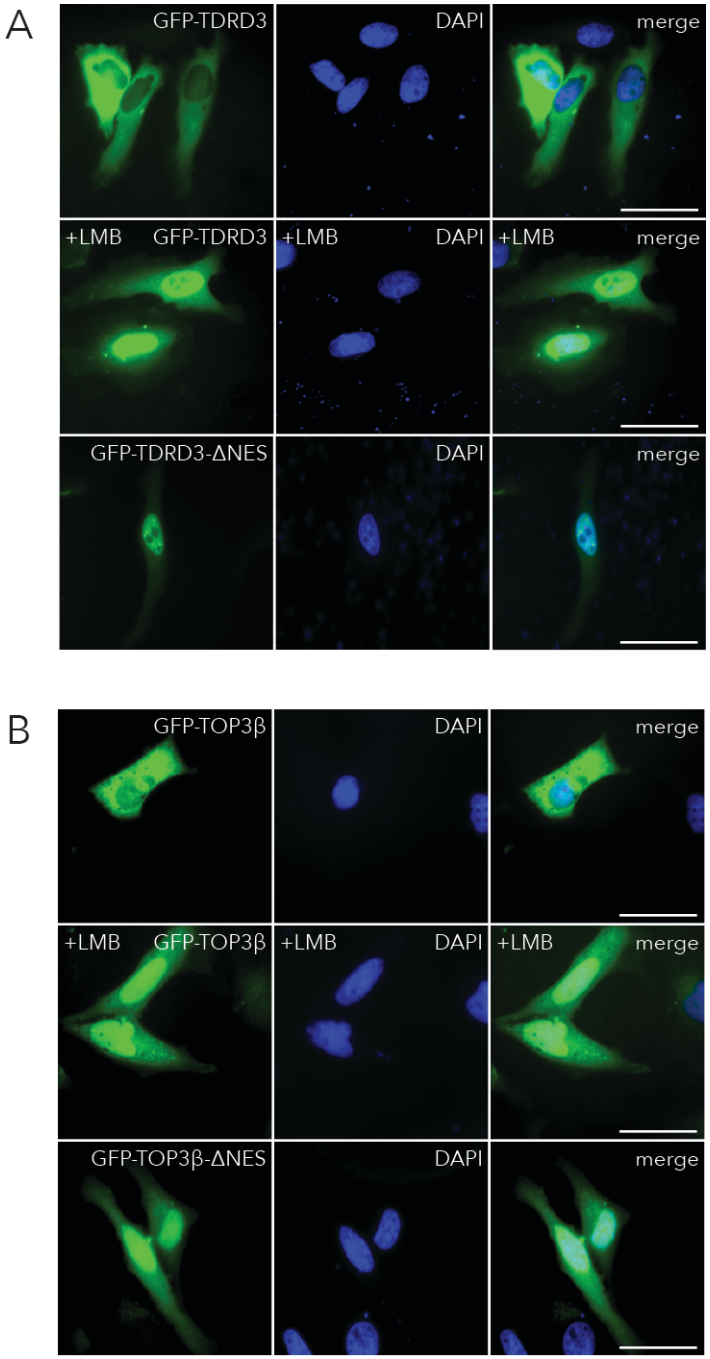

Fig. 4.6 TOP3β and TDRD3 are shuttling between nucleus and cytoplasm in a CRM1 dependent manner. **A)** Detection of recombinant GFP-tagged TDRD3 in HeLa cells by fluorescence microscopy. Compared to control conditions (upper panel), GFP-TDRD3 is retained in the nucleus upon Leptomycin B (+LMB) treatment (middle panel). This nuclear retention was also observed upon transfection of a GFP-TDRD3 variant lacking the putative NES (GFP-TDRD3$_{\Delta NES}$; see fig. 5.5 for details). Nuclei were visualized via DAPI staining; scale bars represent 50 µm.
B) Same experimental setup as in A) but here recombinant GFP-tagged TOP3β was analyzed instead of TDRD3.

The functional relevance of the potential NESs was addressed by two sets of experiments. First, after transfection with plasmids encoding for GFP-tagged TDRD3 or TOP3β, HeLa cells were treated with LeptomycinB (LMB) and the distribution of the recombinant proteins was monitored via fluorescence microscopy. LMB blocks the CRM1-dependent nuclear export pathway by covalent binding to a specific cysteine residue on CRM1 interfering with NES recognition[79]. Second GFP-tagged,

NES-lacking mutants of TDRD3 and TOP3β (ΔNES) were generated and tested for alterations in their cellular localization. Both, LMB treatment and deletion of the NES led to nuclear translocation of GFP-TDRD3 and TOP3β (Fig. 4.6A and B).

This demonstrates that the identified NESs were functional and necessary to perpetuate the predominant cytoplasmic localization of the two proteins. In conclusion and in respect to the reported dynamics leading to FMRP localization, all TTF-components share the same molecular basics determining their cellular distribution.

4.6 TOP3β is catalytically active on RNA substrates *in vitro*

The active nuclear export of TOP3β points to a functional role for this enzyme in the cytoplasm. However, given the lack of DNA in this compartment, the only available nucleic acid substrate is RNA. Although it is known that the presence of RNA can alter topoisomerase activity on DNA substrates[80,81], catalytic conversion of RNA was so far only reported for *E. coli* TOPOIII *in vitro*[82,83], but still lacks functional relevance *in vivo*. It was reasonable to assume that RNA-topoisomerase activity might also be a property of TOP3β, as this enzyme shares large homologies with *E. coli* TOPOIII and both proteins belong to the Type IA topoisomerase subfamily[73].

To investigate this, cleavage assays with radioactively labeled oligonucleotides that were demonstrated to be processed by TOPOIII[82] were applied. The assay is based on the formation of covalent enzyme-substrate intermediates between topoisomerase and substrate nucleic acid strands as previously described (Fig. 4.2). After incubation, formed catalytic intermediates are disrupted by denaturation of the enzymes tertiary structure by the addition of SDS. This results in the release of the loosely associated 5'-part of the cleaved substrate and the covalently bound enzyme-3'-segment (Fig. 4.7A). Both molecules can be specifically visualized dependent on the location of the radioactive label on the substrate, at either the 5'- or 3'-end.

First the general catalytic activity of the Baculovirus-expressed TOP3β or a catalytically dead mutant thereof (Fig. 4.7B) was tested on a 5′-radiolabeled 30-nucleotide DNA substrate (Fig. 4.7C). Released 5′-fragments were separated from full-length oligomers by denaturing urea polyacrylamide gel electrophoresis (urea-PAGE). Due to an amino acid substitution at the active center (Y336F), the mutant lacks its active site hydroxyl group that is essential for the nucleophilic attack on the substrates' phosphodiester backbone.

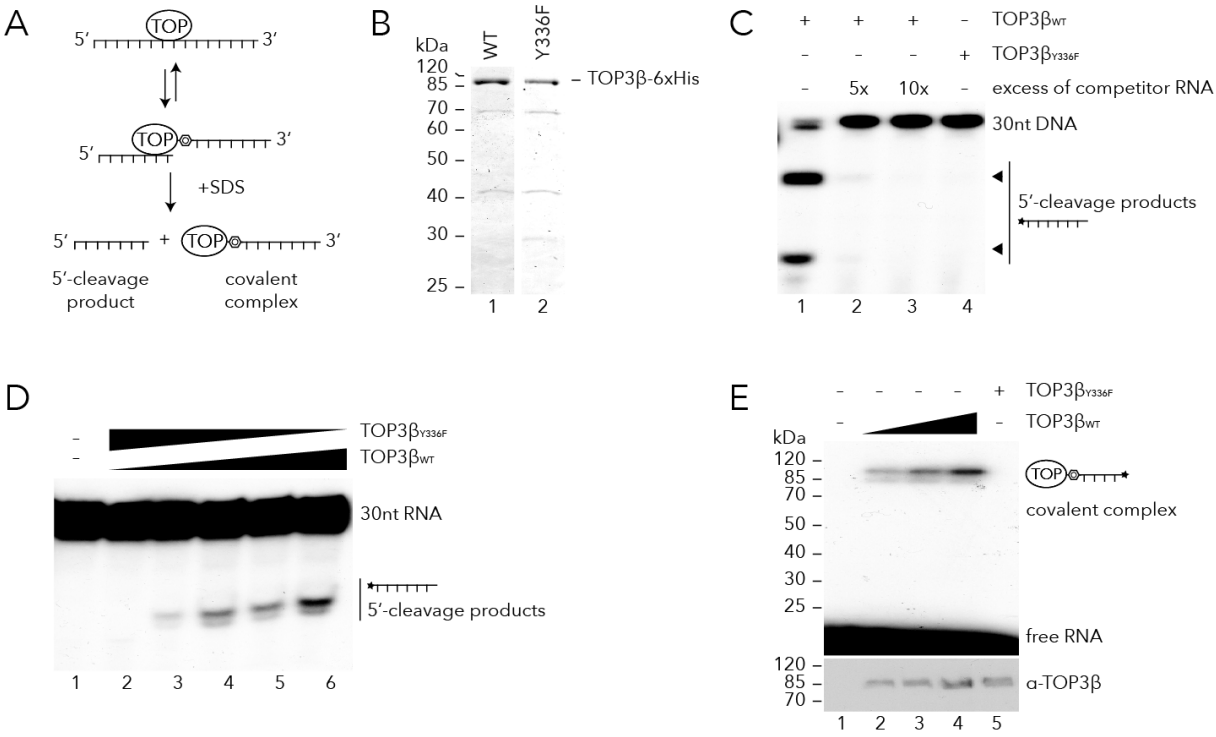

Fig. 4.7 TOP3β possesses RNA-topoisomerase activity *in vitro*. **A)** Schematic representing the mechanism underlying a cleavage assay. Type IA topoisomerases interconvert nucleic acid single strands upon formation of a covalent enzyme-5′-phosphodiester intermediate followed by re-ligation. To visualize this intermediate, the enzyme needs to be denatured during its catalytic cycle, e.g. by SDS addition. **B)** Coomassie stain of recombinant TOP3β variants expressed in the Baculovirus system, as they were used in C-E (catalytically active $TOP3\beta_{WT}$ (wildtype; lane 1) or an active site point mutant (Y336F; lane 2)). **C)** The DNA-topoisomerase activity of TOP3β (lane1) on a 5′-radiolabeled 30mer DNA was inhibited by addition of a 5- or 10-fold excess of a DNA-identical RNA oligonucleotide (lanes 2 and 3, respectively). The Y336F-mutant generally failed to cleave the DNA (lane 4). Cleavage products were resolved by denaturing PAGE and visualized by autoradiography. **D)** Cleavage of a 5′-radiolabeled 30mer RNA-substrate by TOP3β (lane 6). Titration of the active site

mutant from 0-1 pmol (0.25 pmol steps) revealed cleavage-specificity of the WT-enzyme (lanes 2-6). Cleavage products were analyzed like described in D. **E)** TOP3β formed covalent intermediates with a 3'-radiolabeled RNA substrate. Cleavage reactions using increasing amounts (0.5, 1 or 1.5 pmol) of $TOP3\beta_{WT}$ (lanes 2-4) or 1.5 pmol of Y336F-mutant (lane 5) were subjected to SDS-PAGE after denaturation. The autoradiography (upper panel) shows a specific signal at the molecular weight of TOP3β only for the WT but not for the mutant enzyme. TOP3β presence was controlled by Western blot detection using antibodies directed against TOP3β (lower panel).

$TOP3\beta_{WT}$ displayed catalytic activity as indicated by the appearance of cleavage products (Fig. 4.7C; lane 1). As expected, such products were not detectable in the mutant reaction (Fig. 4.7C; lane 4). Interestingly, the titration of a competitor RNA, identical to the DNA oligomer sequence, strongly altered the enzymatic reaction (Fig. 4.7C; lanes 2 and 3). Consequently, the RNA oligonucleotide itself was radiolabeled either at its 5'- or 3'-end and analyzed for either cleavage products or covalent intermediates by urea- or SDS-PAGE, respectively. Cleavage assays with the 5'-labeled RNA oligonucleotide clearly demonstrated catalytic activity of TOP3β on this substrate (Fig. 4.7D; lane 6).

Additionally cleavage assays on the 3'-labeled RNA resulted in the formation of covalent, SDS resistant enzyme-substrate complexes (Fig. 4.7E; lanes 2-4). In both cases the reaction was specifically mediated by TOP3β, as its active site mutant failed to produce any cleavage products or catalytic intermediates (Fig. 4.7D and E; lanes 2 and 5, respectively).

In summary, these results clearly showed that TOP3β does possess transesterification activity on RNA substrates making the enzyme a bona fide RNA-topoisomerase *in vitro*.

4.7 TOP3β is associated with mRNPs *in vivo*

The enzymatic activity of TOP3β on RNA *in vitro*, its cytoplasmic localization and its interaction with FMRP and TDRD3 all argue for an association with mRNAs *in vivo*.

Accordingly, several experiments were carried out to test this hypothesis. In a first approach, stably expressed FLAG-tagged TOP3β was immunopurified from Flp-In T-

Rex cells and mRNP components were detected by Western blotting (Fig. 4.8A). Indeed, PABPC1 as well as the EJC-component MAGOH were co-precipitated in an RNase-sensitive manner, demonstrating that these interactions are indirectly bridged by mRNA (Fig. 4.8A; lanes 5 and 6).

Thus, TOP3β behaves like its interactor TDRD3, which exhibits the same precipitation pattern when subjected to the identical experimental setup (Fig. 4.8B). In a vice versa experiment, mRNAs from lysates of stably FLAG/HA-TOP3β-expressing cells were captured by oligo(dT)-chromatography via their poly(A)-tails. Subsequently, bound proteins were analyzed by Western blotting. Consistent with its previous RBP co-precipitation, TOP3β co-purified with cellular mRNAs sensitive to RNase-treatment along with FMRP and PABPC1 (Fig. 4.8C; lanes 2 and 3).

The oligo(dT)-approach proceeds under very stringent conditions, therefore primarily precipitating proteins closely connected to mRNAs. Consequently, a potential direct interaction of TOP3β with mRNA was elucidated.

Therefore, stable Flp-In T-Rex cells stably expressing FLAG-tagged TOP3β were irradiated with UV-light (254nm) prior to lysis. This procedure induces covalent crosslinks between amino acids of RBPs and bound RNA-nucleotides. Importantly, UV-crosslinking only affects proteins in direct proximity to RNA[84]. After anti-FLAG immunoprecipitation, the purified TOP3β-complexes were treated with different concentrations of RNase T1 to partially digest potentially co-precipitated RNAs. Next, these RNAs were 5'- radiolabeled, resolved via SDS-PAGE and finally subjected to Western blotting.

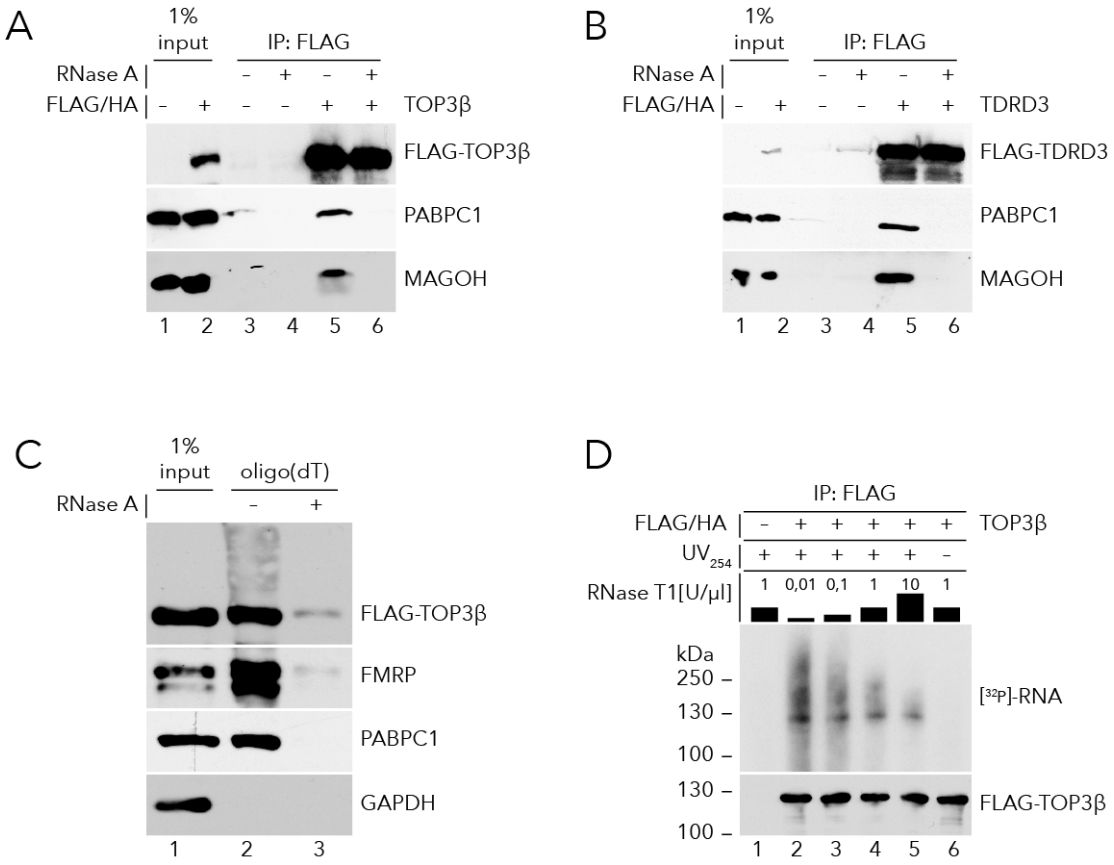

Fig. 4.8 TOP3β is a novel RBP associated with mRNAs. **A)** Western blot analysis of an immunoprecipitation of FLAG/HA-TOP3β from stable Flp-In T-Rex cellular lysates via anti-FLAG antibodies showed co-precipitation of mRNP-marker proteins (PABPC1 and MAGOH) in an RNase-sensitive manner (lanes 5 and 6). Anti-FLAG immunoprecipitations from non-induced Flp-In T-Rex cells served as a negative control (lanes 3 and 4). **B)** The pattern of RNA-marker proteins precipitated by TOP3β was reminiscent to TDRD3 when subjected to an identical experimental setup. **C)** Western blot of an oligo(dT)-pulldown from lysates of stable FLAG/HA-TOP3β expressing cells in presence or absence of RNase A. TOP3β co-purifies with polyadenylated mRNAs in an RNase-sensitive manner (compare lanes 2 and 3). The mRNA-binding proteins FMRP and PABC1 served as positive, GAPDH as a negative control. **D)** CLIP experiment from either non-induced (lane 1) or induced (lanes 2-6) FLAG/HA-TOP3β expressing Flp-In T-Rex cells. Cells were UV-irradiated (254 nm; lanes 1-5) or left untreated (lane 6) prior to lysis. Anti-FLAG immunopurified complexes were treated with the indicated amounts of RNase T1 and trimmed co-precipitated RNAs were 5'-radiolabeled prior to SDS-PAGE and Western blotting. Autoradiography of the blot membrane shows an RNase T1-sensitive signal at ≥120 kDa (upper panel) corresponding to TOP3β as detected by anti-FLAG antibodies (lower panel).

Autoradiography of the membrane showed radiolabeled nucleic acid species migrating at the molecular weight of TOP3β (Fig. 4.8D; upper panel; lanes 2-5), validated by probing with anti-FLAG antibodies (Fig. 4.8D; lower panel). This was specific, as the labeled TOP3β-nucleic acid complexes were only visible when the cells expressed TOP3β and were UV-irradiated (Fig. 4.8D; lanes 2-5). Moreover, the labeled nucleic acids are highly responsive to RNase T1-treatment, depicting that indeed RNA and not DNA was purified along with TOP3β.

In conclusion, these results show that TOP3β is a novel mRNA-associated RNA binding protein *in vivo*.

4.8 The TTF-complex participates in cytoplasmic mRNA metabolism

Both, TDRD3 and FMRP localize to accumulations of translationally repressed mRNAs when cells are exposed to environmental stress[58,59,85]. Therefore, it was reasonable to assume that TOP3β might resemble this SG-association. To investigate this notion, HeLa cells were treated with Arsenite to induce oxidative stress and endogenous TOP3β was visualized by indirect immunofluorescence. Just like the positive controls TDRD3 and FMRP, oxidative stress caused a shift of TOP3β to distinct cytoplasmic foci (Fig. 4.9A, B and C; lower panels), further expanding the cellular commonalities amongst all TTF-complex components.

Apart from scaffolding proteins (e.g. TIA1 and TIAR), SGs are especially rich in translation initiation factors and mRNP-components involved in translational regulation. Hence it is not surprising that mRNAs stored in SGs are thought to be re-integrated into productive translation after stress is abrogated[67]. Consequently, a role of the TTF-complex in the context of translation was conceivable, especially given that FMRP is a major inhibitor of protein synthesis. To test this assumption HeLa cellular extracts were fractionated via density gradient centrifugation to resolve the translational machinery. Sedimentation of all TTF-components was subsequently analyzed by Western blotting and controlled by rRNA profiling as well as detection of PABPC1 (Fig. 4.10A).

Like FMRP, TDRD3 and TOP3β were present in fractions containing 40- and 60S ribosomal subunits as well as in 80S and polysomal fractions (Fig. 4.10A; middle panel). Importantly, disruption of polysomes by RNase A-treatment prior to centrifugation shifted TDRD3 and TOP3β to lighter gradient fractions, showing that their co-sedimentation was mRNA-dependent (Fig. 4.10A; lower panel).

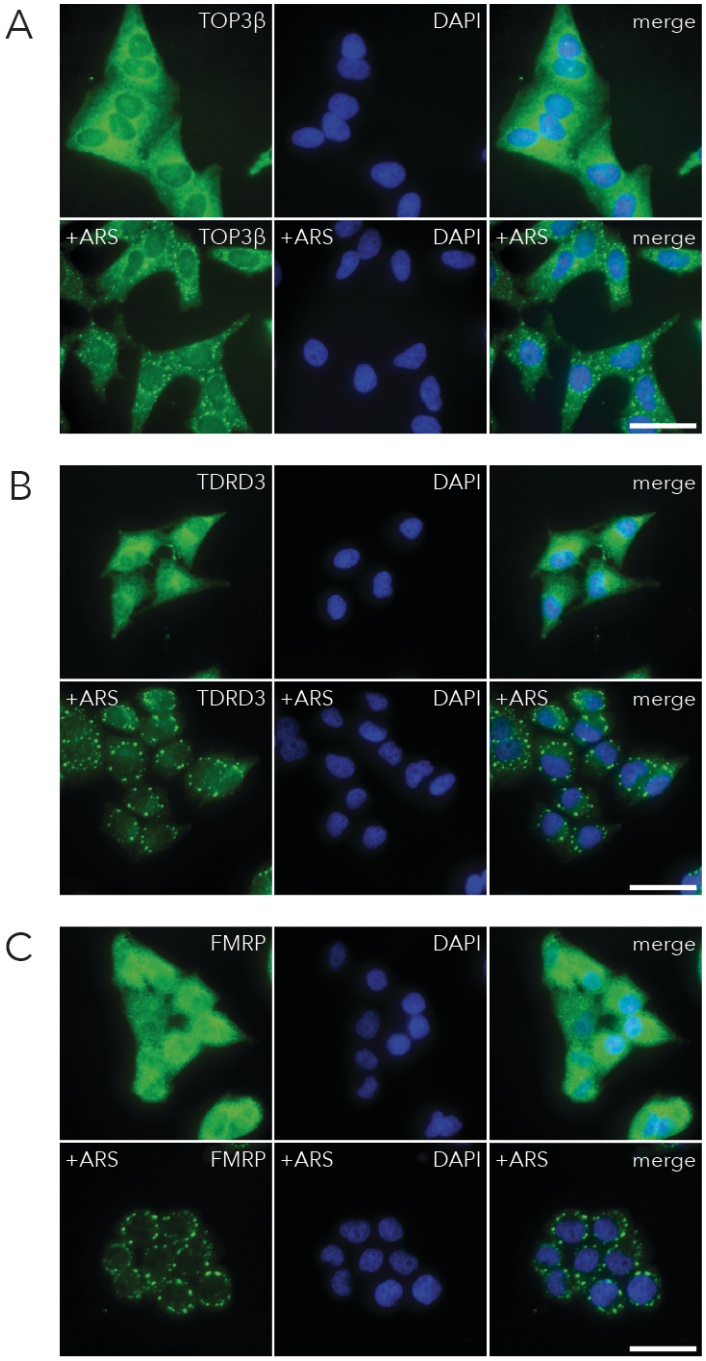

Fig. 4.9 The TTF-complex proteins are components of cytoplasmic stress granules. **A)** Immunofluorescence detection of endogenous TOP3β in HeLa cells using specific antibodies. Cells were either left untreated (upper panel) or were exposed to Arsenite for 45 min to induce oxidative stress (lower panel). Arsenite treatment led to an accumulation of TOP3β in SGs. Nuclei were stained with DAPI, scale bars represent 50 µm. **B)** and **C)** analogous to A) but with detection of the two other TTF-complex components TDRD3 (B) and FMRP (C), which are known SG-proteins [58,86].

The association of TDRD3 and TOP3β with translating mRNPs was additionally validated by ribosome salt wash (RSW) assays, a more stringent experimental approach (Fig. 4.10B). In brief, crude mRNPs are pelleted from cytoplasmic extracts by centrifugation. Loosely associated factors are released by re-suspension of the mRNP-fraction in high-salt buffer and separated from integral ribosomal components by further centrifugation.

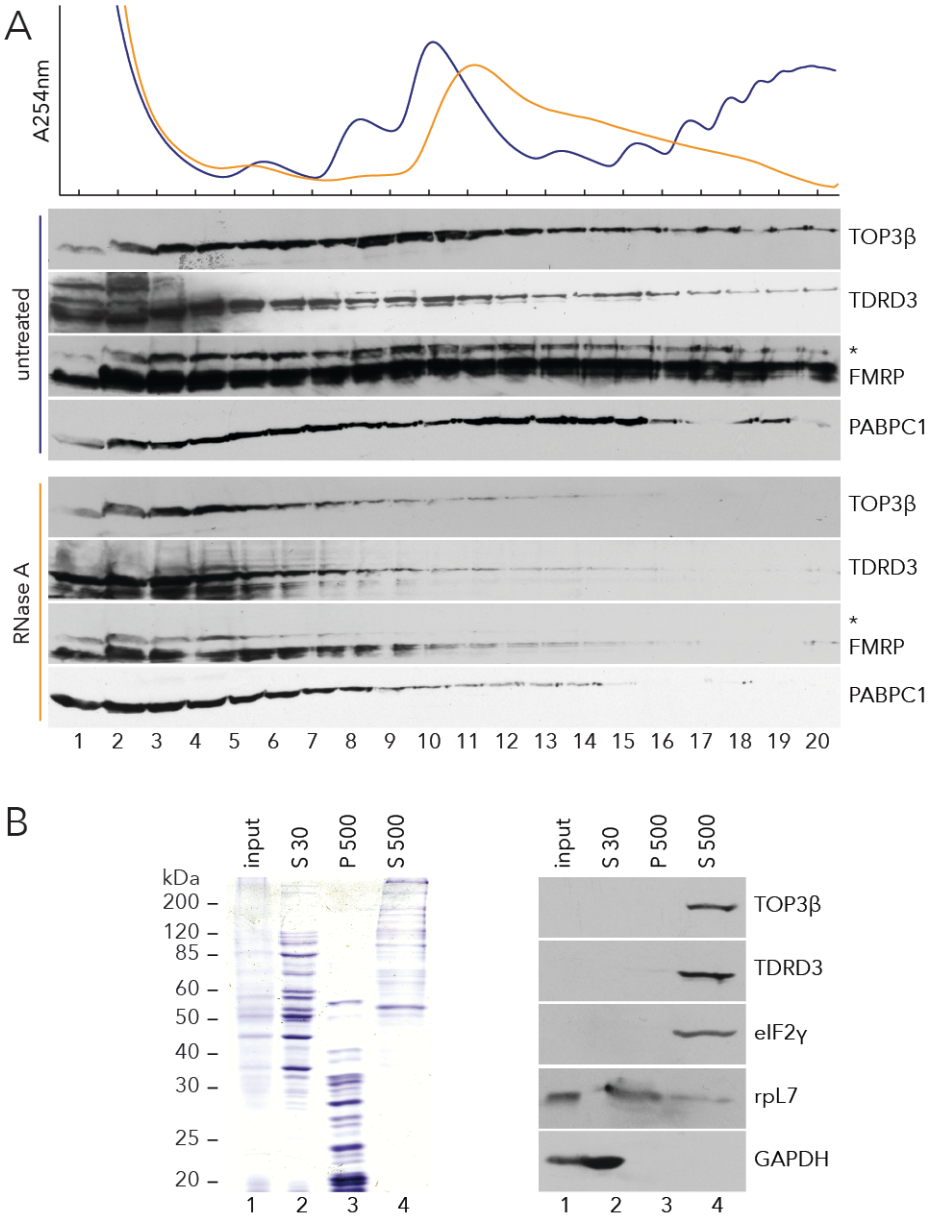

Fig. 4.10 The TTF-complex is associated with the translational machinery. **A)** Western blotting of HeLa cellular extracts separated via sucrose density gradient centrifugation (5-45%) shows the co-sedimentation of all TTF-complex components with the translational machinery (untreated (blue)

panel). This co-migration is dependent on the presence of mRNA, as RNase-treatment shifts the complex components (RNase A (orange) panel). Centrifugation was controlled by measuring rRNA absorbance (A256 nm; upper panel) and by detection of the mRNP marker PABPC1. Asterisk indicates residual TOP3β signal. **B)** High salt purification of ribosomes showing that TDRD3 and TOP3β co-fractionate with translation factors. Coomassie stained SDS-gel of the purification (left panel) with the hypotonic HeLa cellular lysate (lane 1), separated into free proteins (lane 2, S30) and translating mRNPs (lanes 3 and 4) by centrifugation. Loosely associated factors were released from the purified mRNPs by high salt treatment and again fractionated by centrifugation into a pure ribosomal pellet (lane 3, P500) and a translation factor containing supernatant (lane 4, S500). Proteins of interest were detected by Western blotting of the individual fractions (right panel). GAPDH, rpL7 and eIF2γ were used as markers for soluble cytoplasmic-, ribosomal- or translating mRNP-proteins, respectively.

A Coomassie stained SDS-gel of the individual purification steps is depicted in Figure 4.10B (left panel). Western blotting showed the presence of TOP3β and TDRD3 in the high salt supernatant (Fig. 4.10B; right panel; lane 4). This fraction contains translation factors like eIF2γ (Fig. 4.10B; right panel; lane 4) and reportedly FMRP[87]. On the other hand, no integral ribosomal components such as rpL7 were present, which are instead found in the pure ribosomal pellet (Fig. 4.10B; right panel; lane 3).

Together, these findings show an association of all TTF-complex components with translating as well as temporarily silenced mRNPs, unequivocally connecting the TTF-complex to mRNA metabolism at the level of translation.

4.9 The TTF-complex is associated with mRNPs during the PRT

The protein repertoire of mRNPs is constantly remodeled, depending on their expression level. Hence, it was investigated at which stage of translation the TTF-complex associates with mRNPs.

For this purpose, TTF-containing mRNPs were affinity-purified via the TTF-scaffold TDRD3 and tested for the presence of RBPs specific for certain functional mRNP states. Anti-FLAG immunoprecipitations from stable, FLAG/HA-TDRD3 expressing

Flp-In T-Rex cells were carried out in presence or absence of RNase A to discriminate between direct and RNA-mediated interactions.

First, the efficient precipitation of the TTF core components was monitored by Western blot probing with antibodies directed against TOP3β and FMRP. Both proteins are co-purified independent of RNase A-treatment, consistent with their direct interaction (Fig. 4.11; compare lanes 5 and 6). Second, the co-precipitation of early mRNP components was tested. This appeared obvious, given that all TTF components are nucleo-cytoplasmic shuttling proteins, and TDRD3 interacts directly with the EJC[65], a distinguishing feature of newly synthesized but fully processed mRNAs[24,25]. Interestingly, RNase-sensitive co-purification of the cap-binding complex (consisting of CBP20 and 80) was observed (Fig. 4.11). Like the EJC, this protein assembly is removed when an mRNA is translated for the first time[24,25].

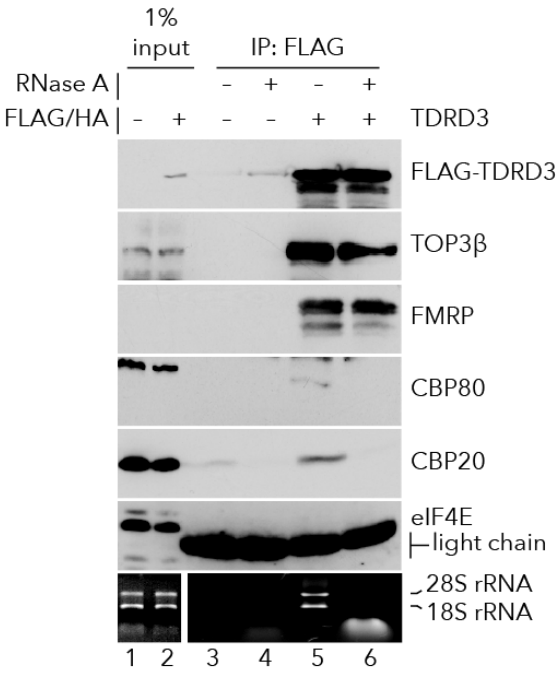

Fig. 4.11 The TTF-complex co-purifies with mRNPs engaged in the pioneer round of translation. An immunoprecipitation of the TTF-complex via FLAG/HA-TDRD3 with anti-FLAG antibodies showed an RNase A-sensitive, mRNA-mediated binding of the cap-binding complex (CBP80 and CBP20; compare lanes 5 and 6), which is removed from the mRNA prior to productive translation. In contrast, the translation initiation factor eIF4E, a marker for steady state protein synthesis was not co-purified (lanes 5 and 6). General translation-activity is indicated by co-precipitation of 28S and 18S rRNA

In contrast, eIF4E was not found in mRNPs purified along with the TTF-complex. eIF4E is the factor substituting for the CBC on mRNAs undergoing productive translation[24,25]. In line with the polysomal association of the TTF-components (Fig.

4.10A), these findings were complemented by co-purification of rRNA (Fig. 4.11; lane 5).

Thus, the TTF-complex binds to mature mRNPs prior and during the PRT, which represents a key step in the regulation of mRNA expression.

4.10 TDRD3 and TOP3β do not influence mRNA stability

One of the major functions of the PRT is the detection and subsequent degradation of transcripts containing so-called pre-mature termination codons (PTCs).

Such translation termination signals within the open reading frame (ORF) can be introduced to mRNAs upon transcriptional errors or mutation of the template DNA-sequence. Translation of these mRNAs would result in the production of truncated, potentially non-functional proteins, necessitating a mechanism for their degradation. The responsible quality control pathway is the so-called nonsense-mediated decay (NMD)[88].

NMD is based on a network of proteins detecting EJCs downstream of translation termination codons, marking them as premature, given that EJCs are typically not present outside the ORF[17]. This triggers a factor-recruiting cascade, finally resulting in the degradation of the mRNA upon binding of endonucleases. The pathway depends on the EJC's property to act as a binding platform for numerous proteins. Several NMD-factors interact with the EJC via an exon junction complex binding motif (EBM)[65].

TDRD3 contains such a conserved sequence motif in its far C-terminal region and it was thus conceivable that TDRD3 and coherently TOP3β might participate in the NMD-pathway. This was tested by so-called tethering assays, an experimental setup artificially "tethering" a protein of interest to a β-globin reporter mRNA, allowing to monitor reporter-stability in dependency of the bound protein [89]. The protein-mRNA interaction is based on tagging the protein of interest with a viral MS2-coat protein combined with the introduction of MS2-stem-loops sequences in the 3'-UTR of the

β-globin reporter, which are specifically recognized by the MS2-coat protein (Fig. 4.12A).

HeLa cells were co-transfected with the β-globin reporter and plasmids encoding for either MS2/V5-tagged TDRD3 or TOP3β. Co-transfection of a reporter lacking the MS2-stem-loops (β-globin wildtype (WT)) was used as an internal control. Furthermore MS2/V5 alone or a MS2/V5-fusion of the known NMD-factor SMG5 served as negative and positive controls, respectively. Expression of the MS2/V5-fusion proteins was monitored by Western blotting with anti-V5 antibodies (Fig. 4.12B; upper panel). Northern blot transfer of the cellular RNA content was controlled by Ethidium-bromide staining of the blot membrane (Fig. 4.12B; middle panel). As expected, probing the β-globin reporters with a α-UTP-labeled antisense transcript showed that presence of SMG5 resulted in the degradation of the MS2-reporter but not of the WT-transcript (Fig. 4.12; lower panel; lane 4). Likewise to the MS2/V5-control, expression of MS2/V5-TOP3β did not decrease stability of either one of the reporters (Fig. 4.12B; lower panel; compare lanes 1 and 3). In contrast, MS2/V5-TDRD3 led to a clear reduction of reporter levels, comparable to SMG5 (Fig. 4.12B; lower panel; compare lanes 1 and 2). This finding was highly reproducible and quantification of two biological replicates (including four technical replicates) showed a TDRD3-dependent reduction of the MS2-reporter to 28% (SD: ± 4%) compared to β-globin WT-reporter levels, whereas TOP3β even increased reporter abundance to 120% (SD: ± 5,5%; Fig. 4.12C).

Nonetheless, the decrease in reporter-stability caused by TDRD3 was relatively mild compared to SMG5 (4%; SD: 1,5%), an effect sometimes observed for EBM-containing proteins not directly involved in NMD-mediated mRNA degradation (Niels Gehring; personal communication). This is attributed to an indirect recruitment of EJCs to the reporter 3'-UTR via the EBM of the tethered protein, thereby converting the natural translation termination signal into a PTC. Thus, a TDRD3-EBM point mutant (EBMmut) deficient in EJC-binding[65] was tested in the identical experimental setup. A TDRD3 Tudor domain point-mutant (TDRmut)

exhibiting impaired aDMA-binding[64] was tested as well, as such PTMs might also contribute to the EJC interaction (for details on the mutations of EBM and Tudor domain see Fig. 4.14). Indeed, TDRD3's effect on the reporter-transcript stability was lost with the EBM-mutant (Fig. 4.12D; compare lanes 1 and 2), whereas the Tudor domain mutant still caused efficient reporter degradation, comparable to $TDRD3_{WT}$ (Fig. 4.12D;

lower panel; lanes 1 and 3). Again MS2/V5 and SMG5 were used as controls (Fig. 4.12D; compare lanes 4 and 5).

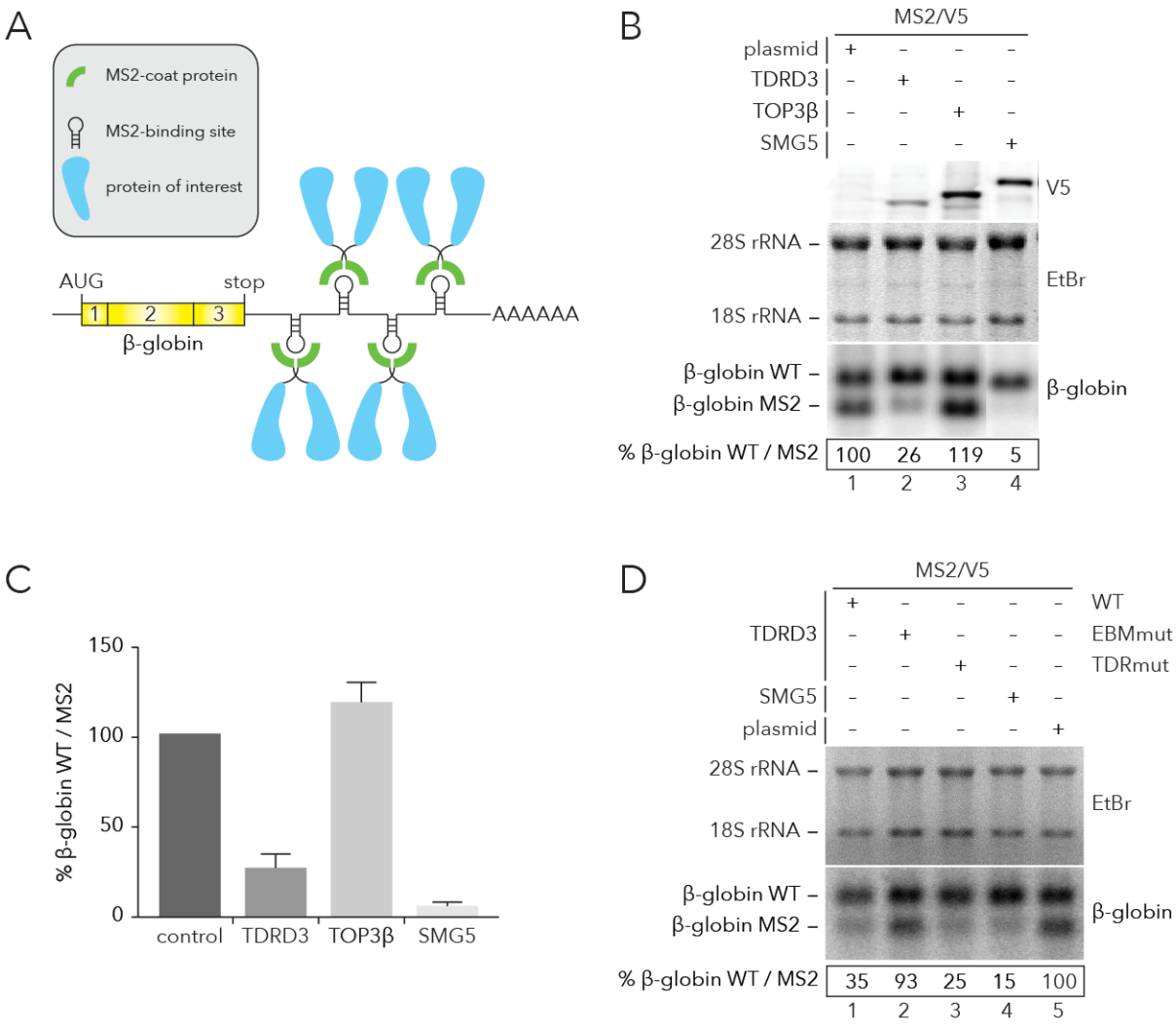

Fig. 4.12 TDRD3 and TOP3β do not alter mRNA-stability. **A)** Schematic depiction of the principles underlying tethering assays (see text for details). **B)** Tethering assay using MS2/V5-tagged TDRD3 and TOP3β (lanes 2 and 3; respectively). MS2/V5 alone (lane 1) or MS2/V5-SMG5 (lane 4) were used as positive and negative controls, respectively. Fusion-protein expression was monitored by Western

blotting using anti-V5 antibodies (upper panel), RNA quality and Northern blot transfer was checked by Ethidium bromide (EtBr) staining of the blot membrane (middle panel).
In contrast to TOP3β, TDRD3 reduced reporter-stability (compare lanes 2 and 3). Framed numbers below represent quantifications of MS2-reporter RNA vs. β-globin wildtype (WT) RNA, used as internal control. **C)** Quantification of a series of tethering experiments analogous to B), (n=4; error bars represent SD). **D)** The effect of TDRD3 on reporter-stability was based on indirect NMD-activation due to recruitment of the EJC, as a mutation of the EBM (EBMmut) did not result in reporter destabilization (compare lanes 1 and 2). In contrast, interfering with aDMA-binding by mutating the Tudor domain (TDRmut) did not influence the ability of TDRD3 to enforce reporter degradation (compare lanes 1 and 3), indicating that PTMs are not involved in the TDRD3/EJC-interaction. Controls are analogous to B) (lanes 4 and 5).

These experiments clearly showed that neither TDRD3, although containing an EBM, nor TOP3β are direct NMD-factors and do not influence mRNA stability as demonstrated in tethering assays. Furthermore, it was revealed that aDMA-modifications are not involved in the binding of TDRD3 to the EJC.

4.11 The assembly of TTF-mRNPs is orchestrated by TDRD3

Two proteins of the TTF-complex, TOP3β and FMRP, possess an intrinsic RNA-binding capacity. Notably, the central complex component TDRD3 only interacts indirectly with mRNPs, primarily via its association with the EJC. This of course raised the question for TTF-complex related functions of TDRD3, apart from this scaffolding capacity. To analyze a potentially expanded role of TDRD3 a commercially available TDRD3-deficient cell line[90] (ΔTDRD3) was utilized. This allowed for monitoring the cellular characteristics of FMRP and TOP3β against a TDRD3-devoid background.

First, polysome gradient centrifugation was applied to test integration of the fragmentary TTF-complex into translating mRNPs. Polysomal amounts of TOP3β and FMRP were quantified by Western blot (Fig. 4.13A). Strikingly, TOP3β was no longer co-sedimenting with polysomes in the absence of TDRD3, a defect, which was rescued upon transfection of $TDRD3_{WT}$. This was specifically linked to the ability of

TDRD3 to bind to mRNPs, as transfection of the $TDRD3_{EBMmut}$ failed to restore the polysomal association of TOP3β.

In contrast, FMRP did not show significant TDRD3-dependency in its sedimentation pattern, clearly demonstrating that TDRD3 is not *per se* necessary for FMRP's overall association with mRNAs.

Accordingly, the presence of FMRP exclusively on TTF-containing mRNPs was monitored. Therefore ΔTDRD3 cells were co-transfected with GFP-TOP3β and either FLAG/HA-$TDRD3_{WT}$, a TDRD3 mutant lacking the FMRP interaction motif (FLAG/HA-$TDRD3_{\Delta FIM}$) or FLAG/HA alone. Subsequently, an anti-GFP column was used to purify TTF-mRNPs via GFP-TOP3β immunoprecipitation (Fig. 4.13B). Again, TOP3β failed to bind to FMRP and mRNPs (represented by MAGOH and PABPC1) in the absence of TDRD3 (Fig. 4.13B; lane 6) but the defect was completely restored upon co-transfection of $TDRD3_{WT}$ (Fig. 4.13B; lane 8). Importantly, co-transfection of $TDRD3_{\Delta FIM}$ only rescued the interaction of TOP3β with mRNPs but still did not result in a co-precipitation of FMRP (Fig. 4.13B; lane 7).

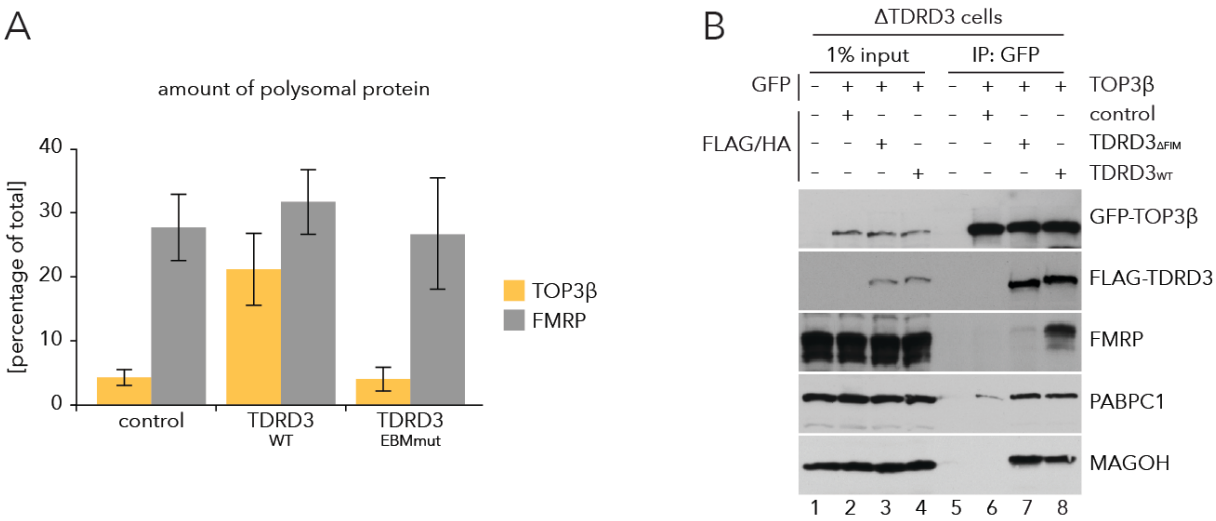

Fig. 4.13 TDRD3 orchestrates TTF-mRNP assembly. **A)** Quantifications (n=3, error bars represent SD) of polysomal Western blot signals of TOP3β (orange) and FMRP (gray) in TDRD3 deficient cells (ΔTDRD3). Polysomal protein amounts were either measured in absence of TDRD3 (control) or upon transfection of FLAG/HA-$TDRD3_{WT}$ ($TDRD3_{WT}$). Specificity was controlled by transfection of the non-mRNP-binding FLAG/HA-tagged $TDRD3_{EBMmut}$. In contrast to FMRP, TOP3β only associates with

translating mRNPs when TDRD3 is available. . **B)** Anti-GFP immunoprecipitations from ΔTDRD3 cells upon co-transfection of GFP-TOP3β and either FLAG/HA alone (lane 6), FLAG/HA-TDRD3$_{\Delta FIM}$ (lane 7) or FLAG/HA-TDRD3$_{WT}$ (lane 8). Western blotting of FMRP shows that it is only a component of TTF-mRNPs in presence of wildtype TDRD3. mRNP-integration was controlled by immunodetection of PABPC1 and MAGOH. An anti-GFP immunoprecipitation without transfected GFP-TOP3β served as an additional negative control (lane 5).

In conclusion, alike TOP3β, the incorporation of FMRP into TTF-mRNPs is strictly dependent on the availability of TDRD3, which tethers the assembled TTF-complex to EJCs on spliced mRNAs.

4.12 The Tudor domain of TDRD3 is required for proper mRNP-integration and TTF-complex assembly

The finding that TDRD3 is an essential adapter for the mRNP integration of the TTF-complex necessitated a deeper understanding for the molecular basics of TDRD3's mRNA-association. To accurately analyze the underlying principles, a series of stable cell lines expressing various TDRD3 mutants was generated (Fig. 4.14). This comprised a point mutant defective in EJC-binding[65] (TDRD3$_{EBMmut}$), a FIM deletion mutant (TDRD3$_{\Delta FIM}$) deficient for the FMRP interaction and lastly a point mutant of the Tudor domain (TDRD3$_{TDRmut}$), which interferes with the binding of TDRD3 to aDMA residues on histones and RNAPII-CTD[64].

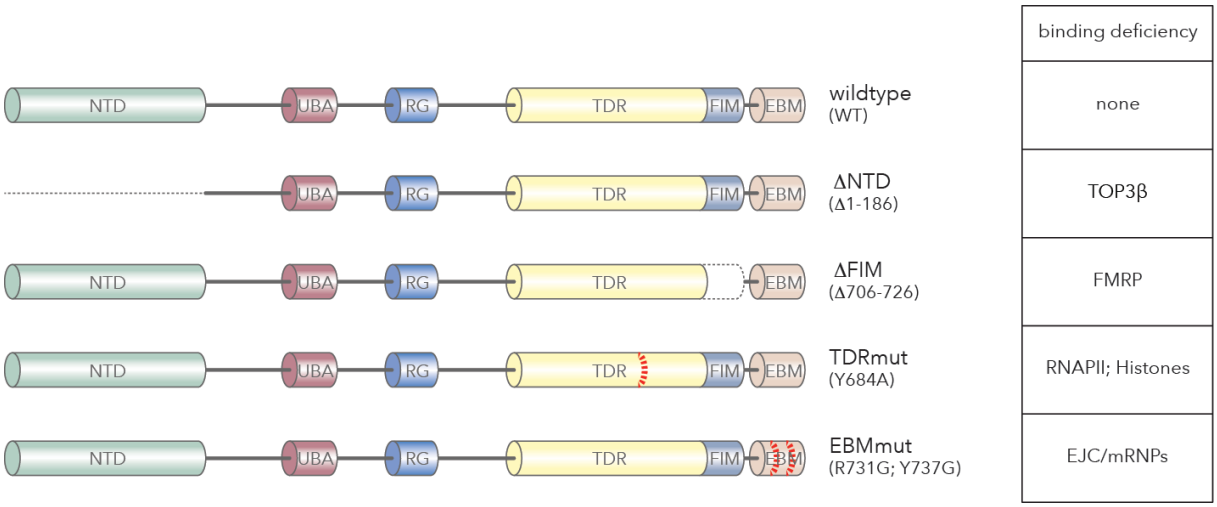

Fig. 4.14 Schematic depiction of the TDRD3 mutants used for TTF-assembly and mRNP-integration

studies. Apart from the wildtype protein ($TDRD3_{WT}$), a TOP3β-binding mutant ($TDRD3_{\Delta NTD}$), an FMRP-binding mutant ($TDRD3_{\Delta FIM}$), an EJC-interaction mutant ($TDRD3_{EBMmut}$) and a Tudor domain mutant ($TDRD3_{TDRmut}$) impairing binding to aDMA residues present on RNAPII-CTD and histones H3 and H4 were generated. Point mutations and deletion are indicated.

First, these mutants and an additional truncation lacking the TOP3β interaction surface (termed ΔNTD) were tested for their association with polyribosomes by gradient centrifugation with extracts derived from the individual mutant-expressing cell lines (Fig. 4.15). Interfering with the ability of TDRD3 to interact with the EJC by EBM-mutation impeded its polysomal co-sedimentation. In contrast, neither binding to TOP3β nor to FMRP turned out to be required for TDRD3 to associate with translating mRNPs, demonstrated by the ΔNTD and ΔFIM mutants, respectively. Thus, the interactions with the TTF-RBPs were negligible in this context. Notably, $TDRD3_{TDRmut}$ also failed to bind to polysomes, resembling the sedimentation pattern of $TDRD3_{EBMmut}$. This result was surprising, as the Tudor domain has so far only been implicated in potential nuclear functions of TDRD3[63,64].

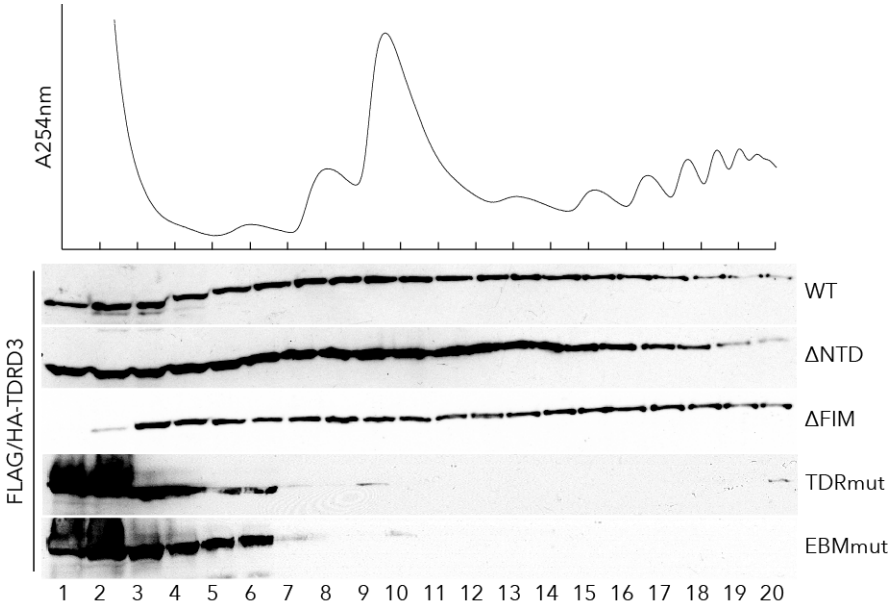

Fig. 4.15 Mutation of the EBM and Tudor domain preclude co-sedimentation of TDRD3 with translating mRNPs. Western blot of the migration of the TDRD3 mutants described in Fig. 4.14, plus a truncation lacking the TOP3β interacting NTD (ΔNTD) in polysome gradients. Interfering with the TTF-complex interactions (ΔFIM and ΔNTD) did not alter TDRD3's polysomal co-sedimentation. In contrast, disruptions of the EBM as well as the Tudor domain dismissed TDRD3 from ribosome-containing gradient fractions.

Consequently, the impact of the interaction of TDRD3 domains on mRNP integration as well as on TTF-integrity was analyzed in more detail. The individual mutants were purified from cellular extracts by FLAG-immunoprecipitation and co-precipitation of the TTF-complex components as well as mRNP-marker proteins was monitored by Western blot (Fig. 4.16A).

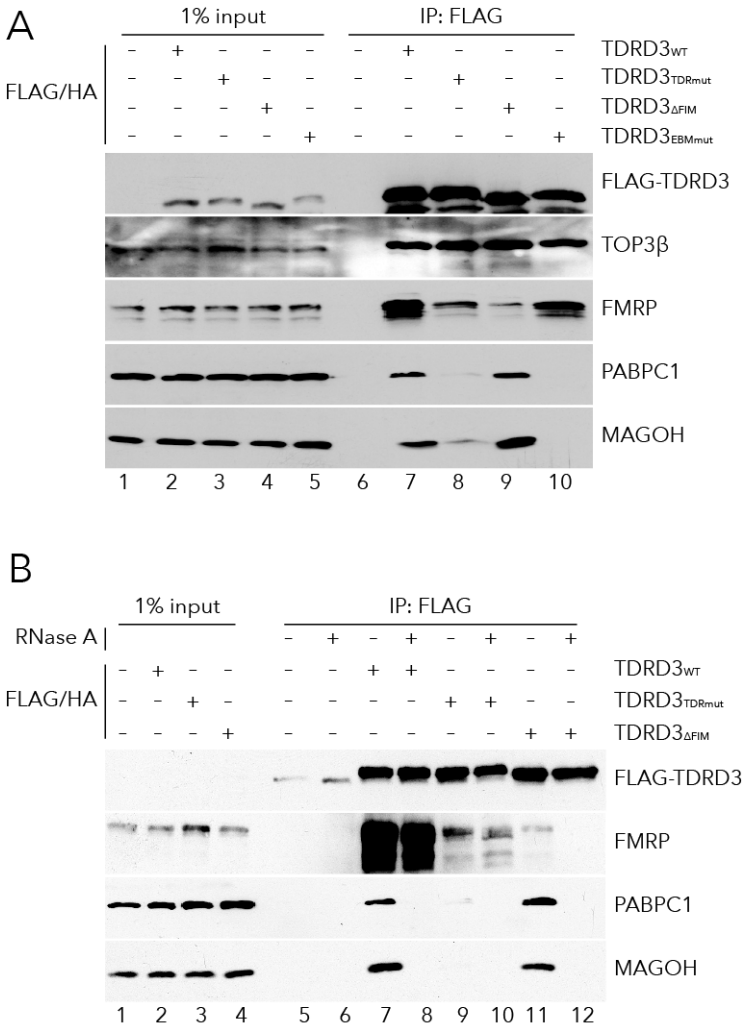

Fig. 4.16 The Tudor domain of TDRD3 is involved in TTF-complex assembly. **A)** Anti-FLAG immunoprecipitations of the TDRD3 mutants described in Fig. 4.14. Mutation of the Tudor domain did not only alter the mRNP association of TDRD3, indicated by co-precipitation of PABPC1 and MAGOH, but also led to reduced binding of FMRP (lane 8). $TDRD3_{\Delta FIM}$ failed to bind to FMRP but was efficiently integrated into mRNPs (lane 9), whereas the $TDRD3_{EBMmut}$ left TTF-integrity untouched but was no longer associated with mRNPs (lane 10). Non-induced cells were used as negative control (lane 6). **B)** Comparative anti-FLAG immunoprecipitations with untreated or RNase A-digested extracts from $TDRD3_{\Delta FIM}$ or $TDRD3_{TDRmut}$ expressing Flp-In T-Rex cellular extracts (lanes 9-12). In contrast to $TDRD3_{\Delta FIM}$, residual FMRP-binding by $TDRD3_{TDRmut}$ results form a specific TTF-assembly deficit and not from mRNA-mediated co-precipitation of FMRP. IPs from non-induced or $TDRD3_{WT}$ expressing cells served as controls (lanes 5-8).

Consistent with the result obtained by gradient centrifugation, deletion of the FIM only resulted in a loss of FMRP but did not affect the mRNP-integration of TDRD3 depicted by the co-precipitated TOP3β, PABPC1 and MAGOH (Fig. 4.16A; lane 9). The $TDRD3_{EBMmut}$ again behaved as expected. It was deficient in mRNP-binding, without additional consequences for TTF-complex integrity as it only failed to co-purify MAGOH and PABPC1 and thus mRNPs (Fig. 4.16A; lane 10).

Importantly, precipitation of the $TDRD3_{TDRmut}$ reproduced the outcome of the polysome gradient centrifugation analysis, showing impaired binding to mRNPs by dramatically reduced levels of co-precipitated MAGOH and PABPC1 compared to $TDRD3_{WT}$ (Fig. 4.16A; compare lanes 7 and 8).

Moreover, mutation of the Tudor domain also altered the TTF-complex composition by impeding the efficient co-purification of FMRP (Fig. 4.16A; lane 8). Note that in contrast to $TDRD3_{\Delta FIM}$, residual FMRP purified along with $TDRD3_{TDRmut}$ was not sensitive to RNase-treatment, indicating that in the latter case the TTF-complex was functionally formed, albeit with an efficiency lower to that of $TDRD3_{WT}$ (Fig. 4.16B; compare lanes 10 and 12). This was surprising, as previous data generated in our group clearly demonstrated that even the deletion of the whole Tudor domain did not affect FMRP-binding *in vitro*[70].

In summary, this showed that apart from the EBM, the Tudor domain contributed significantly to the mRNP-association of TDRD3. Coevally these findings suggest the existence of a Tudor-domain-dependent mechanism for TTF-complex assembly on mRNPs *in vivo*.

4.13 The recruitment of TDRD3 to mRNPs is potentially predetermined by epigenetics

The Tudor-domain mediates the aDMA-dependent interaction of TDRD3 with histones at transcriptional start sites (TSS) of certain genes as well as binding to RNAPII-CTD[63,64]. Given the alterations in FMRP-binding and mRNP-integration,

caused by the TDRD3$_{TDRmut}$ *in vivo*, a co-transcriptional assembly of the TTF-complex on newly synthesized mRNAs was well conceivable.

If this assumption was true, two requirements should be met: First there should be no difference per se between the affinities of the TDRD3$_{TDRmut}$ and TDRD3$_{WT}$ for binding to FMRP and the EJC. Second TDRD3 should be associated with mRNAs originating from its TSS-/gene-targets.

To compare the affinities of TDRD3$_{WT}$ and TDRD3$_{TDRmut}$ for FMRP and MAGOH, GST-fusions of both TDRD3 variants were expressed and purified from *E. coli* (Fig. 4.17A; lanes 2 and 3). Additionally, TDRD3$_{EBMmut}$ served as a non-mRNP-associating control and GST-6xHis as a general background control (Fig. 4.17A; lane 4 and 5). After immobilization on Glutathione Sepharose, the proteins were incubated with HeLa total extracts and subsequent to stringent washing, binding of FMRP and MAGOH was analyzed by Western blot.

TDRD3$_{WT}$ efficiently pulled down both, FMRP and MAGOH (Fig. 4.17A lane 2). As expected, the TDRD3$_{EBMmut}$ did only show binding to FMRP but not to MAGOH (Fig. 4.17A lane 4). In contrast to the previously described *in vivo* results, TDRD3$_{TDRmut}$ completely resembled the interactions of the wildtype protein, without any sign of altered affinities for either FMRP or MAGOH (Fig. 4.17A lane 3).

In a second approach stably expressed, FLAG/HA-tagged TDRD3$_{WT}$, TDRD3$_{TDRmut}$ and TDRD3$_{EBMmut}$ were immunoprecipitated from Flp-In T-Rex-cells. Co-purified mRNAs were isolated and reversely transcribed into cDNA. Next, the cDNA was analyzed for the presence of chromatin immunoprecipitation (ChIP) targets of TDRD3, identified by Yang et al., 2010 (Fig. 4.17B; for PCR-quantifications see Fig 4.17C). Actually, unlike the non-target negative control (GAPDH), all tested ChIP-target-corresponding mRNAs (DDX5, NRAS, DNAJC9 and TRIM37) were enriched by TDRD3$_{WT}$ (Fig. 4.17B; lane 2). In line with the previous findings, co-purification of these mRNAs was strongly decreased in immunoprecipitations of TDRD3$_{TDRmut}$ and TDRD3$_{EBMmut}$ (Fig. 4.16B; lanes 3 and 4).

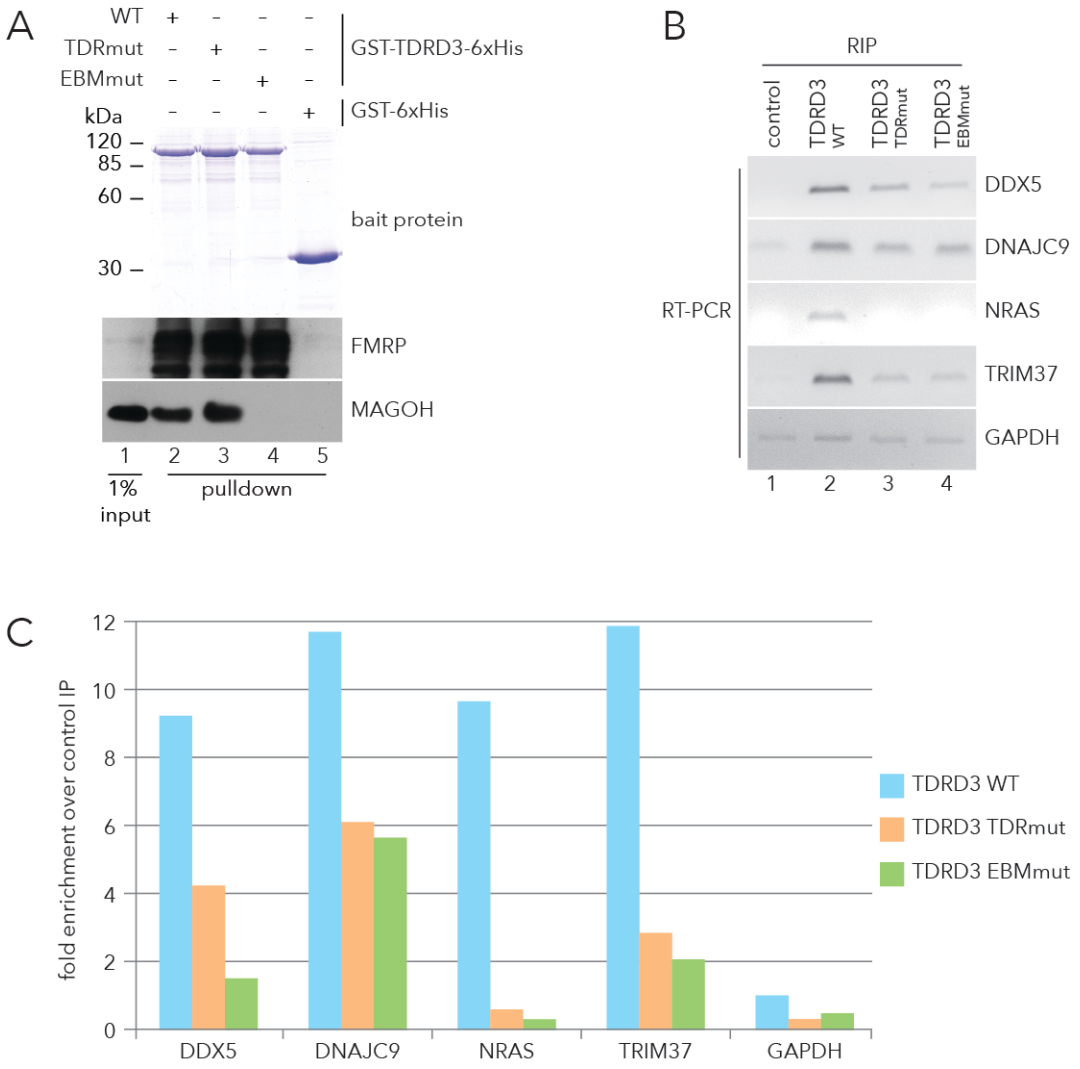

Fig. 4.17 TDRD3-mediated TTF-complex assembly and mRNP-integration depend on aDMA-binding by the Tudor domain. **A)** Coomassie stained SDS-gel of GST-TDRD3-6xHis variants or GST-6xHis alone, expressed in *E. coli* and immobilized on Glutathione Sepharose (upper panel). After incubation with HeLa cellular extracts, binding of FMRP and mRNPs (represented by MAGOH) was analyzed by SDS-PAGE and Western blot. In contrast to the results obtained *in vivo* (Fig. 4.16), no FMRP- or mRNP-binding deficits were observed for recombinant $TDRD3_{TDRmut}$ (lane 3) compared to $TDRD3_{WT}$ (lane 2). General specificity of the interactions was controlled by GST-6xHis (lane 5) or GST-$TDRD3_{EBMmut}$-6xHis (mRNP-binding control, lane 4). **B)** RT-PCRs on mRNAs derived from TDRD3-chromatin-targets (Yang et al., 2010) co-precipitated with FLAG/HA-TDRD3 variants (for quantifications see **C)**). PCR-products were separated by Agarose-GE and stained with Ethidium bromide. All probed target cDNAs (DDX5, DNAJC9, NRAS and TRIM37) were, unlike a non-target control (GAPDH), enriched in the $TDRD3_{WT}$ IP over control IP (lanes 1 and 2). Consistent with the findings in Fig. 4.16 co-purification of these targets was not only reduced in $TDRD3_{EBMmut}$, but also in $TDRD3_{TDRmut}$ IPs (lanes 3 and 4).

Together, although lacking final validation, these findings strongly substantiate a co-transcriptional, TDRD3-dependent, recruitment mechanism for the TTF-complex to mRNPs.

5 Discussion

Any living cell continuously produces a multitude of different mRNAs. To ensure their adequate spatio-temporal expression specific regulatory networks are required. mRNA regulation is mostly accomplished by transcript-associated proteins but also by small RNAs and even metabolites. mRNA-bound factors are not only responsible for transcript-maturation, but decisively connect and mediate all steps in mRNA metabolism from synthesis to decay.

The diversity of mRNA-containing particles is reflected by the very large number of associated proteins, many of which have only been identified recently[12,13]. Coevally, this implicates the existence of a multitude of control pathways respective to individual mRNP-compositions. Especially the recent connection of many, so far unrelated enzymes with mRNPs shows that our current knowledge on the mRNA-bound proteome only scratches the surface of its potential functionalities[13].

In this thesis a novel mRNA-associated protein complex of unexpected composition was identified. It comprises the Tudor domain-containing protein 3 (TDRD3), the DNA-topoisomerase III β (TOP3β) and the fragile X mental retardation protein (FMRP) and was hence termed TTF-complex. The TTF-complex is likely to be of major importance for the understanding of neurodevelopmental disorders as it unites FMRP and TOP3β, two factors implicated in autism spectrum disorders. Furthermore the discovery of TOP3β in this complex was remarkable from a biochemical point of view, as this finding provides the first connection of a topoisomerase with mRNA metabolism.

Through TDRD3's interaction with the exon junction complex, the TTF-complex specifically associates with early but fully processed transcripts. How the TTF-complex is loaded onto mRNAs and what function it may have is currently unclear. However, the findings presented in this thesis and elsewhere suggest, that the TTF-complex is transferred to specific sets of mRNAs to regulate their activity,

presumably already at the level of transcription, involving post-translational chromatin modifications.

5.1 The molecular architecture of the TOP3β-TDRD3-FRMP (TTF)-complex

In vitro binding experiments with recombinant proteins, complemented by immunoprecipitations from cellular extracts (Fig. 4.1), demonstrated the existence of the heterotrimeric TTF-complex consisting of TDRD3, TOP3β and FMRP, termed TTF-complex. Moreover, the mode of interaction of its individual components within the TTF-complex was established. Results of this thesis indicate that TDRD3 functions as the molecular scaffold of this protein assembly by connecting TOP3β and FMRP (Fig. 5.1). Both proteins fail to form a stable complex in absence of TDRD3 (Fig. 4.13).

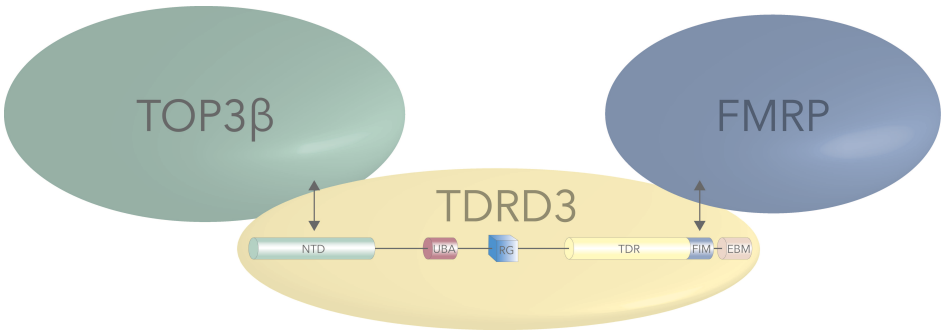

Fig. 5.1 Schematic representation of the TOP3β-TDRD3-FMRP (TTF)-complex. TDRD3 binds to TOP3β via its N-terminal domain (NTD). FMRP is connected to TDRD3 by a stretch of 20 amino acids adjacent to the Tudor domain of TDRD3, termed FMRP interaction motif (FIM). Thus TDRD3 represents the molecular backbone of the TTF-complex by offering distinct binding-modules for the other complex-components.

The association of TDRD3 with FMRP, an RNA binding protein functioning in translational regulation was previously studied in detail by yeast-two hybrid and *in vitro* binding studies[58]. The interaction was assigned to a specific stretch of 20 amino acids in C-terminal proximity of the Tudor domain, which was confirmed in this thesis by anti-TDRD3 immunoprecipitations from cellular extracts and termed FMRP interaction motif (FIM; Figs. 4.1, 4.13 and 4.16).

While the C-terminus provides the binding site for FMRP, TOP3β is associated with the N-terminal part of TDRD3. This protein-segment is composed of two distinct motifs, an oligonucleotide/oligosaccharide binding (OB)-fold adjacent to a domain of unknown function (DUF) 1767 (Fig. 5.2A). A homologous tandem-motif exists in the N-terminal domain of BLAP75 (Bloom associated protein of 75 kDa) and its yeast ortholog RMI1 (RecQ mediated genome instability 1)[91].

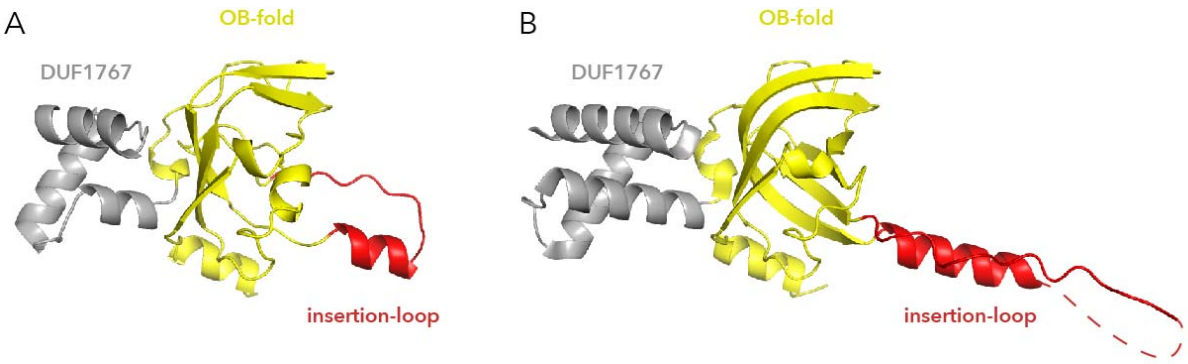

Fig. 5.2 Tandem DUF1767/OB-fold motifs might represent a general type IA topoisomerase interaction platform. **A)** Predicted structure of TDRD3's N-terminal domain. The DUF1767 forms a triple-helix bundle (gray) followed by an OB-fold β-barrel (yellow). A homologous structure exists in BLAP75/RMI1 (pdb3nbi) on which the modeling of the TDRD3-NTD was based **B)**. Binding of either TOP3β (by TDRD3) or TOP3α (by BLAP75/RMI1) is defined by a loop inserted in the OB-fold β-barrel (red).

Notably, both proteins also interact with eukaryotic type IA topoisomerases (mammalian TOP3α and yeast TOP3, respectively) via their NTDs. These findings hence indicate, that the common domain found in TDRD3, BLAP75 and RMI1 creates a general type IA topoisomerase interaction surface. This notion is supported by a recently published study, showing that the differential binding of TOP3β and TOP3α by either TDRD3 or BLAP75/RMI1 is determined by a flexible loop region of the OB-fold[92] (compare Fig. 5.2A and B).

In summary the biochemical investigation of the TTF-complex provided valuable information regarding its architecture and set the stage for crystallographic approaches.

5.2 TOP3β is associated with mRNPs in the cytoplasm

TOP3β is part of an enzyme-family functionally connected to DNA metabolism. Members of this family typically localize in DNA-containing organelles such as the nucleus or mitochondria. Hence, the incorporation of TOP3β into a complex, made up of predominantly cytosolic proteins was puzzling.

FMRP and TDRD3 shuttle between nucleus and cytoplasm involving the transport factor CRM1 ([76,78] and Fig. 4.6, respectively). Hence, it was reasonable that the TTF-complex exists only in the nuclear compartment. Several lines of evidence, including immunofluorescence studies and cellular fractionation however showed that TOP3β was just like TDRD3 and FMRP primarily found in the cytosol (Fig. 4.4). This localization also adapted from CRM1-dependent export dynamics, demonstrated by Leptomycin B treatment and a TOP3β$_{\Delta NES}$ deletion mutant (Fig. 4.6.). Moreover, reminiscent to TDRD3 and FMRP, TOP3β accumulated in cytoplasmic stress granules (SGs) upon oxidative stress treatment (Fig. 4.9).

As outlined earlier, SGs represent storage-sites for mRNAs temporarily repressed in translation. Thus, in addition to its interaction with TDRD3, the incorporation into SGs provided another connection between TOP3β and mRNA metabolism. Consistent with that, comparative immunoprecipitations from lysates of stable cell lines, expressing either TDRD3 or TOP3β resulted in the identical RNase A-sensitive co-precipitation of mRNP marker proteins (Fig. 4.8). Moreover, polysomal co-sedimentation in gradient centrifugations further substantiated a role for TOP3β in mRNA metabolism (Fig. 4.10), especially as TOP3β also co-purified with cellular mRNAs when those were captured via oligo(dT)-cellulose (Fig. 4.8C).

Thus, the studies presented in this thesis demonstrated the existence of a cytoplasmic TTF-complex that could be linked to mRNA metabolism.

5.3 TOP3β is a RNA-topoisomerase

The association of the TTF-complex with cellular mRNAs raised the possibility that TOP3β may enzymatically act on the bound transcripts. In line with this view, CLIP-

experiments revealed that TOP3β could be crosslinked to nucleic acids by UV-light (Fig. 4.8D). The fact that the co-purified nucleic acid species were highly sensitive to RNase T1-treatment demonstrated that TOP3β was indeed directly associated with RNA but not DNA in this experimental setup. This is consistent with recent studies on the mRNA-interactome in which TOP3β emerged as a putative RNA-binding protein[12,13].

Several lines of evidence supported the notion that TOP3β is catalytically active on its bound mRNAs. First, the DNA-topoisomerase activity of recombinant TOP3β was strongly inhibited upon addition of RNA (Fig. 4.7C). Second, TOP3β_{WT}, but not an active site mutant, produced cleavage products when subjected to cleavage assays with RNA-oligonucleotides *in vitro* (Fig. 4.7D). At the same time covalent enzyme-RNA intermediates were formed under these experimental conditions (Fig. 4.7E). Thus, TOP3β was capable to catalyze transesterification reactions on RNA-substrates.

To date, the only topoisomerase known to catalyze strand passage on RNA was bacterial TOPO3[82,83]. Unlike TOP3β, however, this enzyme has so far not been shown to associate with RNAs *in vivo*. Therefore, the identification of TOP3β as a genuine cytoplasmic RNA-topoisomerase is striking, as it introduces a novel enzymatic activity to mRNA metabolism, simultaneously disclosing numerous potential functions.

5.4 The TTF-complex acts in the PRT

It is widely accepted, that the protein content of any given mRNP is highly dynamic and changes according to its cellular needs. As a consequence, each step in the life of an mRNA is defined by distinct sets of associated proteins. This is particularly evident at early stages of translation, which are accompanied by heavy remodeling events, where many proteins are removed or exchanged (see also Fig. 3.3 for details). For instance, the cap-binding complex (CBC) consisting of CBP20 and CBP80 is replaced by the eukaryotic translation initiation factor 4E (eIF4E) after the

PRT. Additionally the exon junction complexes (EJCs) deposited during mRNA-maturation are removed by the translating ribosome.

The PRT is a crucial step in mRNA metabolism. It represents a quality checkpoint for any mRNA exported to the cytoplasm[26]. The EJC plays a central role in the integration of almost any regulatory pathway coupled to this stage of gene expression. It is involved in the detection of premature termination codons (PTCs) and coordinates degradation of such defective transcripts by acting as a general binding platform for nonsense-mediated decay (NMD)-factors[93]. Moreover, the activated ribosomal protein S6 kinase beta-1 (S6K1), is tethered to the EJC by the adaptor protein SKAR and modulates a splicing dependent increase in translational efficiency[94].

Based on TDRD3's interaction with the EJC, an association of the TTF-complex with mRNAs in the PRT was likely. In agreement, immunoprecipitations of TTF-complex-containing mRNPs via TDRD3 resulted in the co-purification of CBP20, CBP80 and the EJC-component MAGOH (Fig. 4.11). In contrast, eIF4E, the marker for steady state translation, was not present in the purifications of TTF-mRNPs. Combined with the polysomal co-sedimentation of all TTF-complex components (Fig. 4.10) the repertoire of co-purified mRNP-markers clearly demonstrates a connection of the TTF-complex with mRNAs engaged in the PRT. This indicated that the TTF-complex acts in decisive, PRT-linked cellular pathways. The scope of potential TTF-functions during the PRT was experimentally constricted, as neither TDRD3 nor TOP3β reduced the half-life of reporter transcripts in tethering assays (Fig. 4.12). This demonstrated that the TTF-complex is not involved in mRNA-destabilization resulting from NMD. At the same time, the finding rather suggested a role in translational regulation during the PRT.

5.5 Potential functions of the TTF-complex during translation

Discussing functions of the TTF-complex in the context of translation presupposes a closer look at potential mRNA-related roles of its unusual component TOP3β.

At a first glance, topological issues appear to be dispensable in the context of mRNA metabolism. However, it is noteworthy that the bulk of mRNAs undergoing translation do not exist as linear molecules[95]. Rather they are circularized upon protein-protein interactions between eIF4G, the scaffolding component of the 5'-cap-associated eIF4F-complex and PABPC1 bound to the 3'-poly(A)-tail[96]. It is hence conceivable that interlaces are being introduced during the circularization process. Upon translation, such "knotty" transcripts might cause severe topological problems, when ribosome occupancy lessens the flexibility of the circular template[97]. An mRNA-associated topoisomerase could potentially manage such topological obstacles and thereby increase translation rates. Alternatively, and not mutually exclusive with this scenario, TOP3β might alter mRNA-topology to slow down translation to control protein synthesis. Recently published HITS-CLIP data depicted a predominant association of TOP3β with exceptionally long mRNAs[92]. Since longer transcripts bear a higher statistical risk for interlace-formation during mRNA-circularization, this finding supports a scenario proposed above.

Of note, the PRT appears to represent an ideal stage of action for an mRNA-remodeling enzyme to ensure that only templates with adequate topology are sequestered to productive protein synthesis.

The TTF-EJC axis also offers an interesting new perspective for the regulation of post-transcriptional gene expression mediated by FMRP. A critical pathway in the pathogenesis of Fragile X Syndrome is the mTOR signaling cascade which controls the translation of dendritic mRNAs upon synaptic activation[98,99]. Interestingly, the EJC-bound S6K1 is, apart from the above-mentioned function in translation, also an effector kinase of the mTOR pathway and additionally the major FMRP-phosphorylating kinase[100]. Thus, upon binding to the EJC the TTF-complex might integrate the actions of two key players that control localized translation of neuronal transcripts, namely FMRP and mTOR.

Taken together, the components of the TTF-complex may regulate the PRT by various means, but a potential mechanism awaits further investigation.

5.6 The TTF-complex contributes to neurodevelopmental disorders

mRNA metabolism is often closely connected to neurological diseases. Consistent with that, genetic studies carried out in Finnish population isolates linked copy number variants of the *TOP3B* gene to neurocognitive impairment and Schizophrenia (Fig. 4.3). Hence, the mRNA-associated TTF-complex comprises two proteins causative for autism spectrum disorders, TOP3β and FMRP. In this context it is again important to note, that the best studied FXS-causing missense mutant FMRP I304N is no longer bound by TDRD3[58] and therefore also lost from the TTF-complex. Concordantly, TOP3β was shown to bind to several mRNAs derived from Schizophrenia risk genes and generally showed a significant overlap with FMRP mRNA-targets[92]. For instance, this includes the mRNA encoding for protein tyrosine kinase 2 (PTK2). FMRP and TOP3β co-regulate PTK2 expression in *Drosophila* neurons[92]. PTK2 influences axonal growth and synapse formation[101,102] and is a reported Schizophrenia risk factor[103]. However, whether this regulation provided by TOP3β and FMRP solely occurs at the level of translation and if it can be generalized for all TTF-associated mRNAs remains to be determined.

Studies of this thesis and from other laboratories hence raise the possibility, that the TTF-complex is involved in the translational regulation of mRNAs important to maintain neuronal integrity. Disease causing mutations in *FMRP* and *TOP3B* may lead to alterations in the metabolism of these transcripts and result in ASD-phenotypes. However, due to the lack of knowledge about the precise function of the TTF-complex, this scenario is at present speculative and awaits further experimental support.

5.7 TDRD3 orchestrates the mRNP-integration of the TTF-complex

Apart from the identification of the first eukaryotic RNA-topoisomerase and its importance for neurocognitive impairment, this work also led to the discovery of an unusual mechanism by which TTF-mRNPs are assembled.

Mutagenesis studies showed that TDRD3 is specifically recruited to mRNPs without the necessity for the direct RNA-interactions mediated by TOP3β and FMRP. However, the ability of TDRD3 to bind to the EJC turned out to be essential for the association with translating mRNAs (Fig. 4.15).

Moreover, TDRD3 emerged as the key factor for the integration of the whole TTF-complex into mRNPs. TOP3β was no longer associated with polyribosomes in a TDRD3-depleted system and consistently also failed to co-precipitate mRNP-marker proteins (Fig. 4.13). In contrast, the polysomal sedimentation pattern of FMRP was generally not altered, when TDRD3 was missing. However, when TTF-mRNPs were immunopurified via TOP3β, the ability of TDRD3 to interact with FMRP was required to recruit FMRP to these particles (Fig. 4.13B).

This suggested that TTF-mRNPs only represent a small subset of FMRP-containing mRNAs and that also other routes for the mRNA-association of FMRP must exist. However, TDRD3 is absolutely essential for FMRP's binding to this particular mRNA-pool. It was already speculated about a protein-dependent mRNA-recruitment of FMRP[40] and the TDRD3-mediated association of FMRP with TTF-mRNPs represents the first validation of this hypothesis so far.

For the etiology of the above-mentioned neurodevelopmental disorders the TDRD3-mediated co-integration of the ASD-disease factors FMRP and TOP3β into mRNPs is of outstanding interest. In case of FMRP mutation (I304N) or loss, a dimer of TDRD3 and TOP3β associates with target mRNAs while TOP3β deficiency results in mRNPs carrying only TDRD3 and FMRP. Thus potential dysregulation of mRNA-activity due to impaired TTF-complex composition is the likely cause for the observed disease-phenotypes.

5.8 mRNP-integration of TDRD3 might be coordinated by epigenetics

Tudor domains are often involved in orchestrating assembly pathways, as shown for the Tudor domain of SMN during UsnRNP-assembly[104]. In this thesis the importance of TDRD3's Tudor domain in the context of the TTF-mRNP-assembly was analyzed.

Immunoprecipitations revealed that $TDRD3_{TDRmut}$ with impaired aDMA-recognition[64] no longer bound to the EJC and FMRP (Figs. 4.15 and 4.16). Consistent with the impaired EJC-interaction, the mutant also failed to co-sediment with translating mRNPs in polysome gradient centrifugations.

These findings were surprising, as both interactions were shown to occur *in vitro* independent of a functional Tudor domain ([70] and C. Brosi, PhD-thesis). In addition, upon incubation of recombinant $TDRD3_{WT}$ and $TDRD3_{TDRmut}$ with cellular extracts containing post-translationally modified proteins, both TDRD3 variants captured the EJC and FMRP with identical efficiencies (Fig. 4.17A).

This implicated that the observed alterations in TTF-mRNP-assembly were potentially caused by impaired Tudor domain mediated interactions upstream to the integration of TDRD3 into mRNPs. So far, the only reported cellular role for TDRD3's Tudor domain is its binding to aDMA-modified histones (H3 and H4) and RNAP II-CTD. Given that all TTF-complex components shuttle between nucleus and cytoplasm it was thus reasonable that the nuclear, aDMA-dependent function of TDRD3 during transcription is a prerequisite for TTF-mRNP-assembly.

Consistent with that notion, $TDRD3_{WT}$ associated with mRNAs derived from its ChIP-target genes[63] (Fig. 4.17B and C). This association was in contrast not recapitulated by $TDRD3_{TDRmut}$ and $TDRD3_{EBMmut}$. Furthermore, genes carrying TDRD3 at their TSSs[63] were compared to FMRP-target mRNAs derived from HITS-CLIP and RIP-chip experiments[40]. These datasets showed a small but significant overlap ($P < 0{,}0001$; Fig. 5.3), which is also consistent with the above discussed idea that TTF-mRNPs define only a small subset of the total of FMRP-target mRNAs. Together, both findings were in agreement with a Tudor domain-dependent, co-transcriptional mRNA-recruitment of the TTF-complex.

Of course, additional evidence is needed to finally prove this hypothesis. Nevertheless, such a mechanism would be truly remarkable, arguing that the protein content of mRNPs and coherently their expression can be predetermined by epigenetic marks.

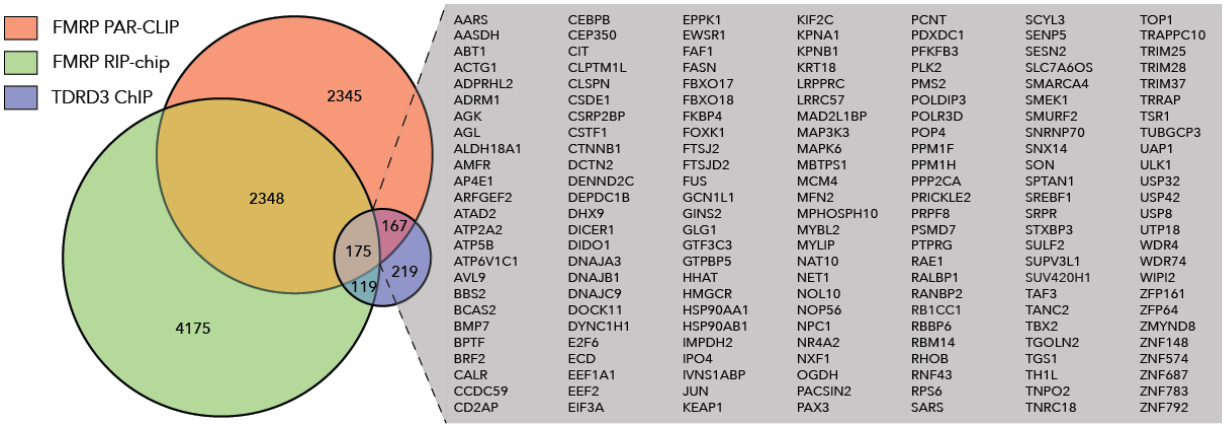

Fig. 5.3 Venn diagram depicting the overlap between genes with TDRD3 bound to their TSS and FMRP target mRNAs. Datasets were derived from TDRD3 ChIP-seq (blue)[63] and FMRP HITS-CLIP (orange) and RIP-chip (green) analyses[40], respectively.

5.9 Potential DNA-linked functions of the TTF-complex

Previous reports from the Bedford lab proposed that binding of TDRD3 to post-translationally aDMA-modified histones, co-activates transcription by recruiting additional effectors[63]. A recent study from the same group unveiled a potential mechanism for this transcriptional co-activation by TDRD3, showing that the TDRD3-mediated binding of TOP3β promotes transcription of target genes[105]. The authors provided evidence that the observed effect was due to reduced R-loop accumulation during transcription. R-loops are formed when the nascent mRNA loops back and base pairs with its complementary template DNA region prior to re-annealing of the DNA-strands. The presence and stability of R-loops contributes to negative supercoiling of the region just transcribed by RNAP II, which impedes polymerase progression.

Recently also FMRP was found to associate with chromatin upon histone H2A.X phosphorylation, to participate in the DNA damage response[106] (DDR). Its binding to chromatin is based on the N-terminal tandem Agent domains of FMRP, a region irrelevant for its interaction with TDRD3.

Given their proven predominant cytoplasmic localization a sole function of the TTF-complex components in the context of transcription or DDR is unlikely. Hence, the

here presented results are not contradictory to putative nuclear functions of the TTF-complex components, but rather denote that their nuclear and cytoplasmic activities might be closely connected at very early stages of gene expression.

5.10 Assembly of TTF-mRNPs: a model

Combining all data generated in this thesis with the current state of research, a model for the TTF-complex assembly on mRNAs can be proposed (Fig. 5.4).

First, a TTF-core consisting of TDRD3 and TOP3β is recruited to transcription start sites harboring aDMA-modifications where it might support transcription of the associated gene ①. This recruitment is facilitated by TDRD3's Tudor domain.

Second, after associating with chromatin, the TDRD3/TOP3β dimer is complemented by FMRP making up the heterotrimeric TTF-complex ②.

Again mediated by TDRD3, the protein assembly is subsequently transferred to EJCs on the nascent mRNA, potentially necessitating a transient interaction with the aDMA-modified RNAP II-CTD ③.

After nuclear export ④, the complex contributes to translational regulation during the PRT ⑤.

At this stage, many factors are specifically detached from the mRNA. For example the EJC itself is removed by the ribosome bound factor PYM[23]. In contrast, the fate of the TTF-complex after this step is not yet fully resolved.

One possibility is that the complex stays intact and is removed as a unit by the translating ribosome along with the EJC. This is however unlikely, given the slight but reproducible variations in the polysomal co-sedimentation pattern of all complex-components (Fig. 4.10). Whereas FMRP and TOP3β are comparably distributed over the gradient, TDRD3 shows a "fading" presence towards larger polysomes. With TDRD3 being less abundant in those fractions compared to the other TTF-components, this indicates that the complex is disassembled during the PRT and TOP3β and FMRP stay associated with the mRNP for an extended time.

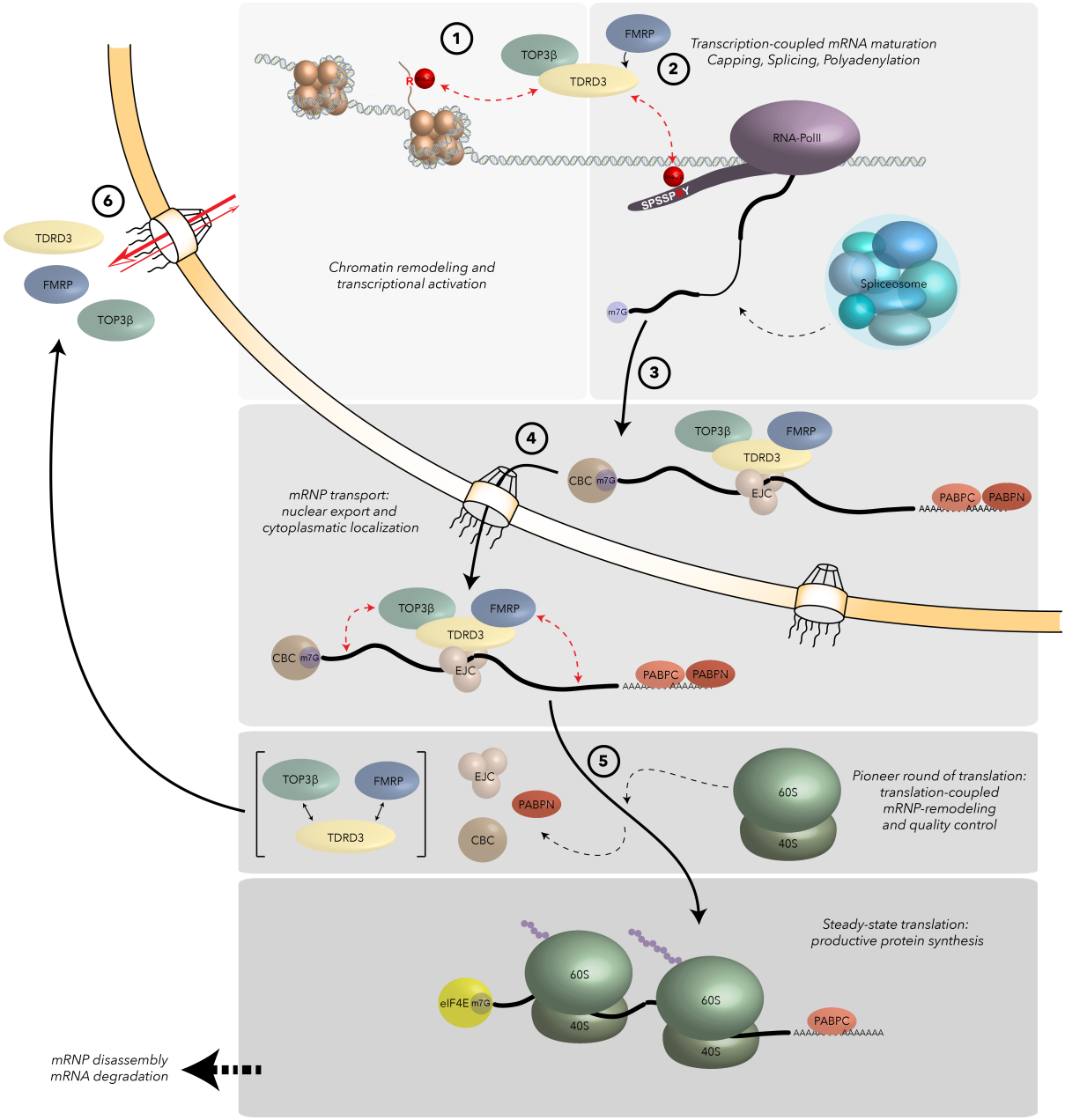

Fig. 5.4 Model depicting the co-transcriptional integration of the TTF-complex into mRNPs. The assembly is highly dependent on the adaptor TDRD3 and the interactions mediated by its distinct domains and motifs, as well as PTMs at the TSS or on initiating RNAP II. See text for details.

After release of all three proteins, they are reimported into the nucleus to start the cycle all over again ⑥.

6 Material & methods

6.1 Materials

All used chemicals were purchased from BD Biosciences, Merck, Serva, Sigma-Aldrich, Boehringer Ingelheim, Riedel-de Haen and Roth. Radiochemicals were purchased from Hartmann Analytic. Laboratory consumables were obtained from Hartenstein, Macherey-Nagel, Eppendorf, Sarstedt, Satorius stedim, Dispomed and Geiner.

6.1.1 Nucleotide and Protein Ladders

GeneRuler™ DNA Ladder Mix	Thermo Fisher Scientific
GeneRuler™ 100bp Plus DNA Ladder	Thermo Fisher Scientific
PageRuler™ Prestained Protein Ladder	Thermo Fisher Scientific
PageRuler™ Plus Prestained Protein Ladder	Thermo Fisher Scientific
PageRuler™ Unstained Protein Ladder	Thermo Fisher Scientific

6.1.2 Standard buffers

5x Tris/EDTA/borate (TBE)	445 mM Tris-HCl, pH 8.3 445 mM boric acid 10 mM Na_2EDTA
10x Phosphate buffered saline (PBS)	1.4 M NaCl 27 mM KCl 100 mM Na_2HPO_4 18 mM KH_2PO_4
6x Protein sample buffer	300 mM Tris-HCl, pH 6.8 12% (w/v) SDS 30% (v/v) Glycerol

	600 mM DTT
	0.04% (w/v) Bromphenol blue
DNA-sample buffer	50 % (v/v) Glycerol
	5 mM Tris HCl pH 8.0
	0.05 mM EDTA
	0.04 % (w/v) Bromphenol blue
	0.04 % (w/v) Xylene cyanol
2x RNA-sample buffer	8 M Urea
	10 mM EDTA
	0.04 % (w/v) Bromphenol blue
	0.04 % (w/v) Xylene cyanol
2x BBS	for 50 ml (store at -20 °C)
0.533g	BES (cell culture tested)
2.8 ml	5M NaCl
500 µl	0.15 M Na_2HPO_4 (cell culture tested)

mix with 30 ml of ddH_2O and adjust pH to exactly 6.96 (use a freshly calibrated pH-meter) then adjust volume to 50 ml with ddH_2O

6.1.3 Cell culture

6.1.3.1 Bacterial cells

Strain	*Chromosomal genotype*	*Supplier*
E. coli DH5α	F^-Φ80*lacZ*ΔM15 Δ(*lacZ*YA-*arg*F) U169 *rec*A1 *end*A1 *hsd*R17 (r_k^-, m_k^+) *pho*A *sup*E44λ^- *thi*-1 *gyr*A96 *rel*A1 λ^-	Invitrogen
E. coli XL1 Blue	F' ::Tn10 $proA^+B^+$ $lacI^q$ Δ(*lacZ*)M15/*rec*A1 *end*A1 *gyr*A96 (Nal^r)	Stratagene

	*thi hsd*R17 (r_K^- m_K^+) *gln*V44 *rel*A1 lac	
E. coli BL-21-Rosetta	F^- *ompT hsd*S_B($r_B^-m_B^-$) *gal dcm* pRARE (Cam^R)	GE Healthcare

6.1.3.2 Bacterial cell culture media

Luria broth (LB)	1.0 % (w/v) Bacto™ Tryptone (BD Biosciences) 1.0 % (w/v) NaCl 0.5 % (w/v) Bacto™ Yeast Extract (BD Biosciences)
Super broth (SB)	3.5 % (w/v) Bacto™ Tryptone (BD Biosciences) 0.5 % (w/v) NaCl 2.0 % (w/v) Bacto™ Yeast Extract (BD Biosciences) set pH to 7.5 using NaOH
Terrific broth (TB)	1,2 % (w/v) Bacto™ Tryptone (BD Biosciences) 2,4 % (w/v) Bacto™ Yeast Extract (BD Biosciences) 0,4 % (v/v) Glycerol 17 mM KH_2PO_4 72 mM K_2HPO_4

For generation of selection media desired combinations of 100 µg/ml Ampicillin (Roth), 50 µg/ml Kanamycin plus 50 µg/ml Chloramphenicol (Sigma-Aldrich) were added to the medium. Agar plates were generated by addition of 2 % (w/v) Bacto™ Agar (BD Biosciences).

6.1.3.3 Mammalian cell lines

Cell type	*Description*	*Supplier*
HeLa S3	Human cervix carcinoma cell line	ECACC
HEK293	Human embryonic kidney	DSMZ (ACC 035)

	cell line	
"ΔTDRD3" JCRB0814 [VMRC-LCD]	Human lung adenocarcinoma cell line	JCRB Cell Bank (National Institute of Biomedical Innovation)
Flip-In™ T-REx™ 293	Human embryonic kidney cell line	Invitrogen (R780-07)
Flip-In™ T-REx™ 293 $TDRD3_{WT}$		This work
Flip-In™ T-REx™ 293 $TDRD3_{TDRmut}$		This work
Flip-In™ T-REx™ 293 $TDRD3_{EBMmut}$		This work
Flip-In™ T-REx™ 293 $TDRD3_{\Delta FIM}$		This work
Flip-In™ T-REx™ 293 $TDRD3_{\Delta NTD}$		This work
Flip-In™ T-REx™ 293 TOP3β		This work
Flip-In™ T-REx™ 293 $TOP3\beta_{Y336F}$		This work

6.1.3.4 Mammalian cell culture media

If not noted otherwise, media for mammalian cells were purchased from Life Technologies. Antibiotics were purchased from InvivoGen, Serva, Sigma-Aldrich and Life Technologies. Sterile cell culture consumables were obtained from Becton Dickinson, Sarstedt, Greiner and TPP.

Medium for HeLa, 293 and JCRB0814 [VMRC-LCD]	DMEM 10 % (v/v) FBS

	1 % (v/v) Pen Strep
Medium for Flip-In™ T-REx™ 293 cells	DMEM
	10 % (v/v) FBS
	10 µg/ml Blasticidin
	100 µg/ml Zeocin
Medium for stable Flip-In™ T-REx™ 293 cells	DMEM
	10 % (v/v) FBS
	10 µg/ml Blasticidin
	100 µg/ml Hygromycin B
Cryo-medium	70 % (v/v) culture medium
	20 % FBS
	10 % DMSO

6.1.4 Antibodies

6.1.4.1 Primary antibodies

Antibody	*Supplier*	*Dilution (Western blot)*
FLAG	Sigma (A2220)	1:1000
HA	HISS (MMS-101R)	1:1000
GFP	Roche (11814460001)	1:1000
TDRD3	Bethyl (A310-983A)	1:500
TOP3β	Abcam (ab56445)	1:500
FMRP	Linder et al., 2008	1:500-1000
PABPC1	Abcam (ab21060)	1:750
GAPDH	Abcam (ab9485)	1:1000
rpL7	Abcam (ab72550)	1:1000
MAGOH	Santa Cruz (sc-271405)	1:500

CBP80	Santa Cruz (sc-271304)	1:200
CBP20	Santa Cruz (sc-48793)	1:500
eIF2γ	Proteintech (11162-1-AP)	1:500
eIF4E	Abcam (ab1126)	1:200
β-Actin	Sigma-Aldrich	1:1000

6.1.4.2 Secondary antibodies

All secondary antibodies were used at a dilution of 1:5000 for Western blotting or 1:500 for immunofluorescence.

Antibody	*Supplier*
Alexa Fluor^{R} 488 F(ab')2 fragment α-mouse IgG	Invitrogen (A11017)
Alexa Fluor^{R} 594 F(ab')2 fragment α-rabbit IgG	Invitrogen (A11072)
α-mouse gIgG (whole molecule) peroxidase conjugate	Sigma-Aldrich (A4416)
α-rabbit gIgG (whole molecule) peroxidase conjugate	Sigma-Aldrich (A6154)

6.1.5 Plasmid vectors

Plasmid	*Description*	*Cloning*	*Reference/Supplier*
pEGFP-C1 *Mammalian expression vector*			Clonetech
pEGFP-C1::TOP3β	TOP3β-ORF insertion		Plöttner, 2001
pEGFP-C1::TOP3β$_{\Delta NES}$	NES-deletion (669-675)	Mutagenesis	This work
pEGFP-C1::TDRD3	TDRD3-ORF insertion		Plöttner, 2001
pEGFP-C1::TDRD3$_{\Delta NES}$	NES-deletion (366-379)	Mutagenesis	This work

pHA *Mammalian expression vector*	5'- HA-tag-insertion into pcDNA3.1		Plöttner, 2001
pFRT/TO/MCS *Mammalian expression vector*	5'-FLAG/HA-tag -insertion into pcDNA5/FRT/TO		Küspert, 2014
pFRT/TO/MCS::TOP3β$_{WT}$	TOP3β-ORF insertion	BamHI/XhoI	This work
pFRT/TO/MCS::TOP3β$_{Y336F}$	Y336F	Mutagenesis	This work
pFRT/TO/MCS::TDRD3$_{WT}$	TDRD3-ORF insertion	BamHI/XhoI	This work
pFRT/TO/MCS::TDRD3$_{TDRmut}$	Y684A	Mutagenesis	This work
pFRT/TO/MCS::TDRD3$_{EBMmut}$	R731G/Y737G	BamHI/XhoI	Insert supplied by Elisa Izaurralde MPI Tübingen
pFRT/TO/MCS::TDRD3$_{\Delta FIM}$	FIM-deletion (703-723)	Mutagenesis	This work
pFRT/TO/MCS::TDRD3$_{\Delta NTD}$	Truncation lacking amino acids 1-186	BamHI/XhoI	This work
pGEX-6P-1 *Bacterial expression vector*			GE-Healthcare
pGEX-6P-1 dTag *Bacterial expression vector*	3'-insertion of a 6xHis-tag into pGEX-6P-1	XhoI	This work
pGEX-6P-1::TOP3β	TOP3β-ORF$_{\Delta stop}$ insertion	BamHI/XhoI	This work

pGEX-6P-1::TDRD3	TDRD3-ORF$_{\Delta stop}$ insertion	BamHI/XhoI	This work
pACEBac1 *Insect cell expression vector*			Geneva Biotech
pACEBac1::TOP3β$_{WT}$	TOP3β-ORF insertion		This work (Cornelia Brosi)
pACEBac1::TOP3β$_{Y336F}$	Y336F	Mutagenesis	This work (Cornelia Brosi)
pVenus *Mammalian expression vector*			Niels Gehring
WT300+e3 *Mammalian expression vector*	β-globin		Niels Gehring
215 delta C4 MS2 *Mammalian expression vector*	β-globin-MS2		Niels Gehring
pCI-MS2-V5 *Mammalian expression vector*			Niels Gehring
pCI-MS2-V5::SMG5			Niels Gehring
pCI-MS2-V5::TOP3β	TOP3β-ORF insertion	XhoI/NotI	This work
pCI-MS2-V5:: TDRD3$_{WT}$	TDRD3-ORF insertion	XhoI/NotI	This work
pCI-MS2-V5:: TDRD3$_{TDRmut}$	TDRD3 Y684A - ORF insertion	XhoI/NotI	This work

pCI-MS2-V5:: TDRD3$_{EBMmut}$	TDRD3 R731G/ Y737G -ORF insertion	XhoI/NotI	This work

6.1.6 DNA and RNA oligonucleotides

6.1.6.1 DNA oligonucleotides (cloning)

Primer name	*Sequence (5'-3')*
TDRD3 (BamHI) forward	aataggatccatggcccaggtggccg
TDRD3 (XhoI) reverse	tatgatcagctcgagttagttccgagcccggggtg
TDRD3 (XhoI) reverse Δstop	ttatctcgaggttccgagcccggggt
TDRD3 (XhoI) forward	aatactcgagatggcccaggtggccg
TDRD3 (NotI) reverse	aatagcggccgcttagttccgagcccggggtg
TDRD3 ΔNTD (BamHI) forward	aataggatccccttttggacagaagtg
TOP3β (BamHI) forward	aataggatccatgaagactgtgctcatggttgc
TOP3β (XhoI) reverse	aatactcgagtcatacaaagtaggcggccagg
TOP3β (XhoI) reverse Δstop	aatactcgagtacaaagtaggcggccagggct
TOP3β (XhoI) forward	aatactcgagatgaagactgtgctcatggttgc
TOP3β (NotI) reverse	aatagcggccgctcatacaaagtaggcggccagg

6.1.6.2 DNA oligonucleotides (mutagenesis)

Primer name	*Sequence (5'-3')*
TDRD3 ΔFIM sense	ggtgctactgagcaatatcaagcccggaggtgatggccagccaagacg
TDRD3 ΔFIM antisense	cgtcttggctggccatcacctccgggcttgatattgctcagtagcacc
TDRD3 ΔNES sense	gccatcagcaccaagcacaaatgtggaagaacctaaat
TDRD3 ΔNES antisense	atttaggttcttccacatttgtgcttggtgctgatggc
TDRD3 Y684A sense	gcactttattgggaagacaacaagtttgcccgggcagaagttg
TDRD3 Y684A antisense	caacttctgcccgggcaaacttgttgtcttcccaataaagtgc
TOP3β Y336F sense	cgcaaggctacatcagcttcccacggaca
TOP3β Y336F antisense	tgtccgtgggaagctgatgtagccttgcg

TOP3β ΔNES sense	tccgctgccctctgctgtggtcatcagg
TOP3β ΔNES antisense	cctgatgaccacagcagagggcagcgga

6.1.6.3 DNA oligonucleotides (tag-insertion)

Primer name	*Sequence (5'-3')*
6xHis-linker-stop sense	tcgagggaggaggatcacatcatcatcatcatcatggatcataatgag
6xHis-linker-stop antisense	tcgactcattatgatccatgatgatgatgatgatgtgatcctcctccc

6.1.6.4 DNA oligonucleotides (expression analysis)

Primer name	*Sequence (5'-3')*
DDX5 (1-428) sense	taggaggcggtccagactataaaa
DDX5 (1-428) antisense	aggtgcaccaaaccctcggt
NRAS (30-339) sense	ctgccgcatgactcgtggtt
NRAS (30-339) antisense	tcccaacaccacctgctcca
TRIM37 (181-542) sense	tgagccgggagaaaggagct
TRIM37 (181-542) antisense	atccattgcctccggctctc
DNAJC9 (161-391) sense	aggtccgacgaggctaccacaa
DNAJC9 (161-391) antisense	agtcctcgtccactgttccctg
DIDO1 sense	tcgcagcatcatgttcaacc
DIDO1 antisense	gactccatcacagatctcgct
GCN1L1 sense	agtatgtgcgtgaggctgc
GCN1L1 antisense	acagctgcttaggagcacag
PTK2 sense	ggtccgagcagaactggg
PTK2 antisense	ttggggtcaaggtaagcagc
TNRC18 sense	cttctctgaggacgagcacc
TNRC18 antisense	gcggtatatgtctggcgagt
NHP2 sense	ggtgaaagaggttcagaaatttg
NHP2 antisense	ctccaggcactcatcgtaag
SNRBP sense	gagggactccaatgggcatg
SNRBP antisense	cagacaatcccatgagactcc

MALAT1 sense	tgggggagtttcgtactgag
MALAT1 antisense	tctccaggacttggcagtct
HISTONE H2 sense	ggaatgacgaagagctcaacaag
HISTONE H2 antisense	gaatgagtatggtgtcaagcctc

6.1.6.5 DNA oligonucleotides (topoisomerase substrates)

Primer name	*Sequence (5'-3')*
D3+	gggattattgaactgttgttcaagcgtggt

6.1.6.6 RNA oligonucleotides (topoisomerase substrates)

Primer name	*Sequence (5'-3')*
R3+	gggauuauugaacuguuguucaagcguggu

6.2 Methods

6.2.1 Molecular biological methods

6.2.1.1 Polymerase chain reaction (PCR)

PCR was utilized to enzymatically produce DNA-amplicons for cloning purposes. Therefore 50 ng of an adequate DNA-template (plasmid-vector or cDNA library) was mixed with forward and reverse primers (10 µM each) and of 10x Phusion High Fidelity PCR master mix (Thermo Scientific) was added to a final concentration of 1x. The mixtures were transferred to a thermo cycler were it was first denatured at 98°C for 90 sec. After this 25-30 cycles (denaturation (98°C for 30 sec), annealing (°C according to primer melting temperatures +3°C for 30 sec) and then elongation (72°C for 15-30 sec/kb amplicon) were carried out for amplification, followed by a final elongation (72°C for 7 min). The amplified PCR reactions were stored at 4°C until further processing. 1 µl of the PCR reactions was mixed with 6x DNA sample buffer and checked by Agarose gel electrophoresis

6.2.1.2 Agarose gel electrophoresis

To separate longer nucleic acids (DNA: plasmid vectors, inserts, PCR products or RNAs: ribosomal RNA, *in vitro* transcripts) by size, Agarose gel electrophoresis was applied. To produce an Agarose gel matrix, 1x TBE-buffer was mixed with Agarose (final concentration 0.5-2.0%, dependent on the size of the nucleic acid fragments to be separated). The Agarose was dissolved by heating and Ethidium bromide was added (final concentration of 5 µg/ml) just before pouring the gel. Gels were run at 140V for 30-45 min and analyzed by visualization of Ethidium bromide stained nucleic acid fragments in a gel documentation device (peqlab).

6.2.1.3 Purification of DNA from Agarose gels or PCR-reactions

DNA was purified from excised Agarose gel fragments or PCR-reactions using the corresponding clean-up kit purchased from Macherey-Nagel.

6.2.1.4 Restriction digest of DNA-fragments

DNA-fragments or plasmid-vectors for sub-cloning purposes were specifically hydrolysed with the help of restriction endonucleases (Fermentas). 1-4 µg of plasmid DNA or total amounts of purified PCR-products were incubated with 1.5 U of restriction enzymes in the buffers recommended by the manufacturer for 4 h at 37°C. When plasmid-vectors were digested phosphatase was added after 3 h. After digest completion plasmid-vectors were purified by Agarose gel electrophoresis and PCR-products were kit-purified.

6.2.1.5 Dephosphorylation of DNA-fragments

To avoid re-circularization and -ligation of digested plasmid-vectors, 5'- and 3'-phosphate groups were removed with Shrimp Alkaline Phosphatase (SAP; Fermentas). Therefore, 1 µl of SAP was added to a vector restriction digest reaction and incubated for 1 h at 37°C.

6.2.1.6 Ligation of DNA-fragments

To generate recombinant vector-plasmids containing an insert of choice, the digested recipient vector was mixed with a 10x excess of the desired insert. 1U of T4 DNA ligase and T4 DNA ligase buffer (1x final concentration; both Fermentas) was added and the reaction mixture was incubated either over night at 14°C or 3 h at room temperature. The Ligation reaction was subsequently transformed into chemically competent *E. coli* cells.

6.2.1.7 Preparation of competent E. coli strains

E. coli strains of interest (DH5a, BL-21-Rosetta, XL1 Blue) were grown in 50 ml of LB medium without antibiotics (over night; 37°C; 180 rpm). 4 ml of the culture were transferred to 400 ml LB medium and incubated likewise until reaching an OD of 0.375. After incubation on ice for 10 min, cells were collected by centrifugation (7 min; 2°C; 1600 *xg*) and the pellet was re-suspended in 80 ml in $CaCl_2$-buffer (60 mM $CaCl_2$; 15% (v/v) glycerol; 10 mM PIPES, pH 7.0). The cells were again collected by centrifugation and the procedure was repeated. Subsequently the cells were kept on ice for 30 min and again pelleted and re-suspended in 16 ml of $CaCl_2$-buffer. After that aliquots of 250 µl were prepared, snap-frozen and stored at -80°C.

6.2.1.8 Transformation of chemically competent E. coli strains

To introduce recombinant plasmid-vectors into *E. coli* strains, 100 ng of DNA was added to 100 µl of competent bacteria. After gentle mixing, cells were kept on ice for 15-20 min and subsequently transferred to 42°C for 45 sec. After cooling on ice for 2 min, 500 µl of LB medium (without antibiotics) was added and cells were incubated for 1 h at 37°C on a shaker (1000 rpm). Hereafter, 10 or 90% of the cells were plated on selection agar plates containing antibiotics corresponding to the vector-encoded resistance genes.

6.2.1.9 Colony screening (colony-PCR)

To test for positive cloning results, vector-plasmid transformed *E. coli* colonies growing on selection agar plates (containing vector specific antibiotics) were picked

and dipped into a PCR master mix (20µl; Promega) before being re-spotted. The bacteria containing PCR reaction (including insert and vector specific primers) was incubated in a thermo cycler (95°C for 5 min, 25 amplification cycles (95°C for 30 sec; 48°C for 30 sec; amplicon length dependent elongation at 72°C), final elongation 7 min at 72°C. presence of amplified DNA was checked by Agarose gel electrophoresis of the whole PCR-reaction. Amplicon-positive clones were further analyzed by sequencing (GATC; Konstanz).

6.2.1.10 Site-directed mutagenesis

For introduction of mutations or deletions into pre-existing plasmid-vectors, PCR-based site-directed mutagenesis was applied. Therefore, two 50 µl reaction mixtures were prepared:

100ng template-vector
2 µl Pfu DNA polymerase (institute of biochemistry; University of Würzburg)
5 µl 10x Pfu DNA polymerase buffer (Fermentas)
1 µl dNTP mix (10 mM each)
either 25 pmol of *sense* **or** *antisense* mutagenesis primer
add H_2O to 50 µl

The mixtures were incubated in a thermo cycler according to the following program: 10 cycles of 95°C for 30 sec; 55°C for 1min; 68°C dependent on the vector length. Final elongation 68°C for 8 min. Half of the sense and the antisense reactions were mixed and again subjected to the previously described PCR program. Subsequently maternal DNA was digested by addition of 1 µl DpnI (Thermo Scientific) and incubation for 1 h at 37°C. 30 µl of the reaction mixture were transformed into *E. coli* DH5α and plated on adequate selection media. Growing colonies were tested for positive mutants by sequencing.

6.2.1.11 Purification of bacteria amplified plasmid-vectors

Recombinant vector-plasmids were purified from small-scale (5ml) or large-scale (500ml) bacterial cultures using "Nucleospin Plasmid QuickPure" or "Nucleobond PC500" (both Macherey-Nagel), respectively, according to manufacturers instructions.

6.2.1.12 Bacterial cryo-stock preparation

To produce cryo-stocks of transformed E. coli strains, 500 µl of a growing suspension culture were mixed with 750 µl of sterile glycerol (87%; v/v) and stored a -80°C.

6.2.2 Eukaryotic cell culture

6.2.2.1 Culture of adherent growing eukaryotic cell lines

Cells were cultivated in adequate media at 37 °C; 5 % CO_2 and 100% humidity. Cells were splitted (1:10 or to experimentally specified densities) at latest when reaching a confluency of 100 %. Therefore, cells were washed once with 1x PBS and incubated with 0.25 % Trypsin-EDTA (Life technologies) until they detached from the growing surface, diluted in fresh, pre-warmed medium and then passaged to a new cell culture plate/flask.

6.2.2.2 Preperation of cryo-stocks of eukaryotic cell lines

To freeze eukaryotic cells, cells were detached from the growing surface with Trypsin-EDTA (Life technologies), mixed with cell culture medium and collected by centrifugation at room temperature (5 min; 400 *xg*). The pelled was re-suspended in cryo medium, aliquoted into cryo-tubes and kept at -20 °C for 2 h then transferred to -80 °C for at least 4 h and then stored in liquid nitrogen.

For seeding, frozen cryo-stocks were thawed in a water bath (37 °C), mixed with culture medium and collected by centrifugation at room temperature (5 min 400 *xg*). The pellet was re-suspended in cell culture medium and seeded into a cell culture plate/flask.

6.2.2.3 Transient transfection of eukaryotic cells

Apart from thethering assays, transient transfection of plasmid-vector DNA was carried out with Nanofectin (GE Healthcare) according to manufacturers recommendations at a confluency of 40-60 %.

To transfect cells with siRNA, cells were grown to a max. confluency of 40 % in medium free of antibiotics. Transfection was carried out with Lipofectamine RNAiMax Reagent (Life technologies) according to manufacturers recommendations.

6.2.2.4 Generation of Flip-In™ T-REx™ 293 (Flp-In T-Rex) cell lines

To generate stable cell lines, the Flip-In™ T-REx™ Core Kit (Invitrogen) was used. Flp-In T-Rex-cells were grown to 40 % confluency in medium containing 10 µg/ml Blasticidin and 100 µg/ml Zeocin. Subsequently they were co-transfected with vector plasmids pOG44 and pFRT/TO/MCS carrying the gene of interest. After 24 h medium containing 10 µg/ml Blasticidine and 100 µg/ml Hygromycin was added. Selection medium was continuously changed on a daily basis until single colonies became visible. Colonies were picked and transferred to single wells of a 12-well plate and cultivated. Expression of the protein of interest was tested by addition of 0.5 µg/ml Tetracycline and monitored by Western blotting.

6.2.3 Biochemical methods

6.2.3.1 Bradford assay

Concentrations of proteins in solution were measured according to Bradford 1976. Therefore, blank and samples were measured (2 µl sample 798 µl ddH_2O and 200 µl Bradford reagent (Bio-Rad)) against a standard curve, which was generated by measuring BSA-samples of known concentrations 0.5 µg, 1 µg, 2 µg, 3 µg, 4 µg and 5 µg (in 800 µl ddH_2O and 200 µl Bradford reagent (Bio-Rad)) in a spectrometer at a wavelength of 595 nm. The blank contained 800 µl ddH_2O and 200 µl Bradford reagent.

6.2.3.2 Protein precipitation

To precipitate proteins from solutions, they were mixed with 0.1 volumes of 100 % TCA (Trichloric acid) and incubated over night on ice. In case of very low protein contents, 0.5 volumes of 10 µM BSA were added prior to TCA addition to serve as a defined precipitation carrier. After precipitation, proteins were collected by centrifugation (tabletop centrifuge; 13000 rpm; 30 min; 4 °C). The pellet was washed with TCA wash buffer (70 % (v/v) Acetone; 20 % (v/v) Ethanol; 7.5 % (v/v) ddH_2O; 50 mM Tris-HCl pH 8.0) until no pH-mediated color change in the wash buffer was observed. Finally the pellet was once washed with 75 % (v/v) Ethanol and then air dried, resolved in equal volumes of ddH_2O and 8 M Urea (15-30 min; 1500 rpm; 65 °C) and subjected to SDS-PAGE.

Alternatively proteins were precipitated with Acetone. Therefore, protein-containing liqids were mixed with 3x volumes of ice-cold Acetone and incubated over might at -20 °C. Precipitates were collected analogous to TCA-precipitations. Protein pellets were washed 2x with 75 % Ethanol prior to resolving them again analogous to the TCA protocol.

6.2.3.3 SDS-PAGE

For separation of proteins or protein-fragments according to their size, denaturing (SDS) polyacrylamide gel electrophoresis (SDS-PAGE) was utilized. SDS-PAGE was run in Lämmli-buffer, at a constant current of 45 mA (mini-gels) or 75-80 mA (large gels).

Composition of a typical 10% gel was as follows:

Separating gel

Rotiphorese Gel 30	10 ml
(Acrylamide/Bisacrylamide 37:1)	
1.5 M Tris-HCl, pH 8.8	5.5 ml
ddH_2O	14.5 ml
10% APS	0.1 ml

TEMED	0.1 ml

Stacking gel

Rotiphorese Gel 30 (Acrylamide/Bisacrylamide 37:1)	1.65 ml
0.5 M Tris-HCl, pH 6.8	2.45 ml
ddH_2O	5.9 ml
10% APS	0.05 ml
TEMED	0.0125 ml

6.2.3.4 Coomassie staining of SDS-gels

SDS-PAGE separated proteins were unspecifically stained with Coomassie Brilliant Blue. Therefore, SDS-gels were incubated with Coomassie staining solution (20% (v/v) isopropanol; 10% (v/v) acetic acid; 0,15% (w/v) Serva blue R) for 30 min, rinsed with H_2O to remove leftovers of the staining solution and then incubated with 20% (v/v) acetic acid until the background was removed and protein bands became visible.

6.2.3.5 Silver staining of SDS-gels

After fixation in 50% (v/v) methanol, 12% (v/v) acetic acid and 0.5 ml/l formaldehyde (37%) for 1 h, SDS-gels were washed 3x for 20 min with 50% (v/v) ethanol and treated with 0.2 g/l sodium thiosulfate for 1 min. After three washing steps with ddH_2O, the gel was incubated in silver staining solution (2 g/l $AgNO_3$, 0.5 ml/l formaldehyde) and again washed 2x with ddH_2O. Protein bands were then visualized by incubation in developing solution (60 g/l NA_2CO_3, 0.5 ml/l formaldehyde). Staining was stopped with a solution containing 50% (v/v) methanol and 12% (v/v) acetic acid.

6.2.3.6 Cell fractionation and gradient centrifugation

Nuclear and cytoplasmic extracts from HeLa cells were prepared with a Qproteome cell compartment kit (Qiagen) according to manufacturer's instructions.

To purify translation factors, HeLa cell pellets were mixed with a packed cell volume of lysis buffer (10 mM KAc; 20 mM HEPES pH 7.5; 5 mM MgAc plus protease inhibitors (1:1000)). After swelling for 15 min on ice, cells were lysed by douncing (22 strokes; Wheaton B-tight; 40 ml). Lysis was controlled by microscopy. The lysate was clarified by centrifugation (30 min; 23000 *xg*; 4 °C; Beckman JA25.50). The supernatant was next layered onto a 1 M sucrose cushion (lysis buffer conditions) and centrifuged (4 h; 40000 rpm; 4 °C; Beckman 45Ti). Pelleted mRNPs were rinsed 2x with re-suspension buffer (500 mM KAc; 20 mM HEPES pH 7.5; 5 mM MgAc plus protease inhibitors (1:1000)) and then re-suspended over night in 2 ml of re-suspension buffer. Suspension was briefly clarified by centrifugation (5000 rpm; 5 min; 4 °C; tabletop centrifuge) and the supernatant again layered onto a 1 M sucrose cushion (re-suspension buffer conditions) and again centrifuged as described above but in a Beckman 60Ti rotor. The pellet was re-suspended in a buffer containing (100 mM KAc; 20 mM HEPES pH 7.5; 5 mM MgAc plus protease inhibitors (1:1000)). Samples were taken from each centrifugation step (supernatants and pellets), resolved by SDS-PAGE and analyzed by Coomassie staining and Western blotting.

For polysome gradient centrifugations (5-45% sucrose) cells were lysed in a buffer containing 100 mM KCl; 20 mM Tris pH 7.5; 5 mM $MgCl_2$; 0.5 % NP40; 1 mM DTT; 100 µg/ml cycloheximide plus protease inhibitors and extracts clarified (11000 rpm; 10 min; 4 °C) and extracts subjected to centrifugation in a SW60Ti rotor (Beckman) (1:35 h; 34500 rpm; 4 °C). After fractionation and UV profiling ([A254nm]; Biocomp Piston gradient fractionator), fractions were subjected to SDS-PAGE and analyzed by Western blotting.

6.2.3.7 Protein expression and pulldown assays

Plasmids for protein expression were transformed into *E. coli* BL21 Rosetta II. Cells were grown in 500 ml of TB medium supplemented with glucose (20 g/l) and antibiotics at 30 °C to 0.4 OD_{600}. Expression was carried out for 4 h at 18 °C after

induction with 0.5 mM IPTG. Subsequently cells were harvested by centrifugation. Pellets were re-suspended in lysis buffer (20 mM HEPES pH8; 500 mM KCl; 5 mM EDTA; 5 mM β-mecaptoethanol (β-ME) and 10 % glycerin, protease inhibitors 1:1000), sonified and lysates clarified (1 h; 35000 rpm; 4 °C) in a Beckman 45Ti rotor. 200 µl of pre-equilibrated Glutathion-Sepharose (GE-Healthcare) was added to the supernatant, incubated for 2 h at 4 °C and washed with lysis buffer (without EDTA). Bound proteins were eluted with 50 mM Glutathione. 200 µl of Ni^{2+}-NTA (Qiagen) matrix were incubated with the pooled elution fractions (2 h; 4 °C) and washed with lysis buffer (without EDTA) containing 10 mM imidazole. Bound protein was eluted (20 mM HEPES pH8; 100 mM KCl; 5 mM β-ME; 500 mM imidazole and 10 % glycerin). For TDRD3-TOP3β interaction studies, TDRD3 was prepared as described above but released by GST-tag cleavage with PreScission protease (4 U/µl; GE Healthcare) (5 h at 4 °C) prior to the Ni^{2+}-NTA purification step. Immobilized GST-TOP3β-6xHis was incubated with TDRD3-6xHis (1 h; 4 °C) and washed 3x with buffer containing 20 mM HEPES pH 8, 300 mM KCl and 0.5 % NP40, eluted with SDS sample buffer and analyzed by SDS-PAGE and Coomassie staining. For wildtype or mutant GST-TDRD3-6xHis pull-down assays from cell lysates equal amounts of protein were immobilized on Glutathion-Sepharose and incubated with HeLa extracts prepared as described for immunoprecipitations. Precipitated proteins were analyzed via SDS-PAGE and Western blot.

Catalytically active recombinant TOP3β generated by Cornelia Brosi. In brief, GST-TOP3β-6xHis was expressed in Sf21 insect cells. *E. coli* DH10EMBacY was transformed with a pACEBac1 transfer plasmid carrying GST-TOP3β-6xHis (wildtype or active site mutant (Y336F)). Recombinant bacmid DNA was transfected into Sf21 cells using Cellfectin II Reagent (Invitrogen). For virus amplification Sf21 were re-transfected 2x using virus containing cell supernatant. Expression was carried out in 200 ml culture volume ($2x10^6$ cells per ml) for 72 h. Cells were harvested by centrifugation (15 min; 1500 rpm; 4 °C), sonicated in lysis buffer (750 mM KCl, 20 mM Tris-HCl pH 7.5; 10 % glycerin; 1 mM EDTA; 0.05 % NP40; 1 mM DTT and

protease inhibitors 1:500) and lysates clarified by centrifugation (45 min, 25000 rpm, 4 °C). Purification was carried out as described above but without purification via Ni^{2+}-NTA.

6.2.4 Immunobiochemical methods

6.2.4.1 Western blotting of SDS-gels

For antibody-mediated detection of individual proteins separated by SDS-PAGE, the protein content of a gel was transferred to a PVDF-membrane in a semi-dry blotting chamber. Therefore, three layers of 1x Towbin buffer soaked Whatman paper were covered with an identically sized PVDF-membrane, which was previously incubated in 100 % methanol. The gel was layered onto the membrane and again covered with three 1x Towbin buffer soaked Whatman paper. The blotting procedure was carried out at 0.8 mA/cm^2 of gel for 2 h or 2,66 mA/cm^2 of gel for 6 h. Protein transfer was controlled by amido black staining. After de-staining with amido black de-staining solution, the membrane was blocked (5 % milk powder in 1x TBT) for 30-45 min.
After washing the membrane thoroughly, it was incubated with the primary antibody (diluted in 1x NET-gelatin with 1:1000 sodium azide) for 4 h at room temperature or over night at 4 °C. The membrane was subsequently again washed with 1x TBT (3x 5 min) and incubated with the horseradish peroxidase-coupled secondary antibody (1:1000 in 1x TBT) for at least 1 h at room temperature. After washing like described above, the blot was developed with the enhanced chemiluminescence system (ECL). Therefore, 10 ml of ECL I-solution (6.8 mM p-Cumaric acid in DMSO) were mixed with 100 µl of ECL II-solution (1.25 mM Luminol; 100 mM Tris-HCl; pH 8.5) and 10 µl H_2O_2. Chemiluminescence was visualized on X-ray film.

6.2.4.2 Purification of polyclonal antibodies (TDRD3 sera)

To purify polyclonal antibodies form total rabbit sera, 2-4 mg of recombinantly expressed antigen fusion-protein were covalently coupled to Glutathion-Sepharose (GE-Healthcare). Therefore, after antigen binding, the column was washed with 0.2 M Sodium tetra-borate and afterwards crosslinked in presence of 20 mM Di-methyl

pimelimelimidate in 0.2 M Sodium tetra-borate for 30 min. Residual reactive groups were blocked with 0.2 M Ethanolamine pH 8.0 for 1h. To remove non-covalently bound antigen, the column was washed with 10 volumes of 0.1 M Glycine pH 2.7. For antibody purification the column was incubated with serum for 2 h and subsequently washed and eluted in 10 900 µl fractions of 0.1 M Glycine pH 2.7 into 100 µl 10x PBS and 100 µl Tris-HCl pH 8.8.

6.2.4.3 Immunoprecipitation

Immunoprecipitations were performed with 25µl of α-FLAG M2 Agarose (Sigma-Aldrich) or protein-G Sepharose (GE-Healthcare) bound α-GFP-antibodies (Roche, amount of antibodies was used according to manufacturers instructions) per ml cell extract.

After addition of lysis buffer (150 mM NaCl; 50 mM Tris pH 7.5; 2.5 mM $MgCl_2$ and 0.5 % NP40; 0.5 mM DTT; 1:1000 protease inhibitors) cells were kept on ice for 10 min. Extracts were cleared (11000 rpm, 10 min, 4 °C) and subjected to IP for 1 h (4 °C). Beads were washed 3x with lysis buffer, 3x with lysis buffer without protease inhibitors and 2x with 1x PBS. Precipitated complexes were eluted with 1 % (w/v) SDS in 1x PBS (15 min, 70°C) and subsequently subjected to SDS-PAGE. Precipitated proteins were analyzed by staining (Coomassie or silver) and/or Western blotting.

For immunoprecipitation of endogenous TOP3β and TDRD3 from mouse brain lysates, mouse brains (supplied by AG-Szalay; University of Würzburg) were reduced to small pieces with a sterile scalpel and then homogenized on ice with lysis buffer (see above) in a small-scale douncer (5ml; loose pestle; 15 strokes). Subsequently the homogenates were aliquoted and clarified via several rounds of centrifugation 1x at 5000 rpm, 1x at 8000 rpm and finally 2x at 11000 rpm (always at 4 °C for 10 min in a tabletop centrifuge). The supernatants were then subjected to immunoprecipitation with protein-G Sepharose bound α-TDRD3 or α-TOP3β antibodies (amount of antibodies was used according to manufacturers instructions).

6.2.4.4 Immunofluorescence microscopy

Adherent growing cells were cultivated in 6-well plates containing cover-slips. Cells were grown to a max. confluency of 70 % and treated as desired (e.g. transfected with recombinant vector-plasmids or chemically treated). For harvesting, the medium was removed and the cover-slips were fixed with 4 % (v/v) Formaldehyde (37 %) in 1x PBS. Cover-slips were washed with 1x ice-cold PBS and incubated with 0.2 % (v/v) Triton X-100; 1 % (w/v) BSA in 1x PBS for 30 min to permeabilize the cell membrane and block unspecific antigens. After subsequent washing, the cover-slips were incubated with the primary antibody in 1 % (w/v) BSA in 1x PBS (incubation times and temperatures were adjusted individually for each antibody). After washing with 1x PBS, the secondary antibody was added (with 1 % (w/v) BSA in 1x PBS), for 4 h at room temperature. The cover-slips were again washed as described and carefully rinsed with ddH_2O, embedded in Vectashild+DAPI (Vector Labs) and sealed with nail polish. The analysis was carried out with a invers light fluorescence microscope (Axiovert 200M; filters 10, 20 and 49; AxioCam MRm and Axiovision software (v4.8); all Zeiss).

Cell treatment for immunofluorescence microscopy comprised:

Leptomycin B (in DMSO)	50 ng/ml LMB for 3 h
Sodium Arsenite (in H_2O)	500 µM for 45-60 min
Cycloheximide (in H_2O)	50 µg/ml for 45-60 min
Emetine (in Ethanol or H_2O)	20 µg/ml for 45-60 min

6.2.5 RNA specific molecular methods

6.2.5.1 Preparation of DEPC ddH_2O

To generate RNase-free water, diethylpyrocarbonate (DEPC) was mixed with ddH_2O 1:1000. After continuous stirring over night (fume hood), residual DEPC was eliminated by autoclaving.

6.2.5.2 RNA purification/extraction

To directly purify cellular RNAs, cells were treated with Trizol Reagent (1 ml/well (6-well)) for 10 min after washing 1x with 1x PBS. Cell lysis was assisted by repetitive up and down pipetting of the mixture. After lysis, the Trizol solution was snap-frozen and kept at -80 °C for approx. 30 min. Subsequently, after thawing, 150 µl BCP (1-bromo-3-chloropropane; Sigma-Aldrich) was added and the mixture was vortexed for 15 sec and phases were separated by centrifugation (Tabletop centrifuge; 15 min; 13000 rpm; 4 °C). The aqueous phase was transferred to a new reaction tube and 2 µl of precipitation carrier (Molecular Research Center, Inc.) or alternatively 1 µl glycogen were added and subsequently mixed with 0.7 volumes of 2-propanol. After incubation on ice for 10 min, precipitated RNA was collected by centrifugation (tabletop centrifuge; 20 min; 13000 rpm; 4 °C) and the pelleted was 1x washed with 75% (v/v) ethanol (p.A.) and again pelleted. The pellet was air dried, resolved in 10-20 µl of DEPC ddH_2O on a shaker (1100 rpm) for 15 min at 65 °C and the RNA-concentration was determined via Nanodrop.

To purify RNA from solutions (e.g. cellular extracts or IP-eluates), the RNA-containing liquid was mixed with PCI (Phenol-Chloroform-Isoamylalcohol; 25:24:1+ 8-hydroxychinolin) in a 2:1 ratio. After incubation in a shaker (15 min; 1600 rpm; RT), phases were separated by centrifugation as described above and the aqueous phase was transferred to a new 1.5 ml reaction tube, mixed with Chloroform-Isoamylalcohol (25:1) and again centrifuged. After transfer of the supernatant to a new reaction tube and upon addition of 3 volumes of ethanol (p.A.) or 0.7 volumes of 2-propanol, 0.1 volume of 3M NH_4OAc (pH 5.2) and 1 µl of glycogen, RNA was precipitated for a minimum of 30 min at -20 °C. Precipitated RNA was processed and washed as described above.

In vitro transcribed RNAs (e.g. Northern bolt probes), were purified via column based kit systems (e.g. RNeasy mini kit; Quiagen) according to manufacturers recommendations.

6.2.5.3 5'-end labeling of RNA-oligonucleotides

For 5'-end-radiolabeling, RNA oligonucleotides were phosphorylated in presence of γ-[^{32}P]-ATP. A typical reaction contained 2 µl RNA (10 µM), 0.9 µl DEPC ddH_2O and 2.1 µl PEG 6000 (24% (w/v)). The mixture was incubated at 96 °C for 60 sec and then immediately transferred on ice. After addition of 1 µl PNK-buffer A (forward reaction; Thermo Scientific) and 1 µl T4-polynucleotidkinase (PNK; 10 U/µl; Thermo Scientific), the mix was supplemented with 3 µl γ-[^{32}P]-ATP (10 µCi/µl; 6000 mCi/mmol) and incubated for 45 min at 37 °C. Subsequently the reaction was cooled on ice and resolved by denaturing PAGE after addition of 10 µl of RNA-sample buffer.

6.2.5.4 3'-end labeling of RNA-oligonucleotides

To label RNA-oligonucleotides at their 3'-end, the following 20 µl reaction mixture was prepared:

2 µl	10X T4-RNA-Ligase buffer (Life technologies)
50-100 pmol	boiled and snap-cooled RNA
equimolar amount	5'-[^{32}P]-pCp (10 µCi/µl; 6000 mCi/mmol)
add to 18 µl	DEPC ddH_2O
2 µl	T4-RNA-Ligase (10 U/µl)

The reaction was carried out on ice over night at 4 °C and subsequently mixed with RNA-sample buffer. Radiolabeled RNA was purified by denaturing PAGE.

6.2.5.5 In vitro transcription (body-labeling)

To generate Northern blot probes, cRNA was synthesized by *in vitro* transcription. Therefore, transcription template plasmids were linearized by PCR or restriction digest and the following reaction mixture was prepared:

2 µl	transcription buffer (10x Roche)
0.5 µl	0.1 M DTT

1.2 µl	10 mM ATP
1.2 µl	10 mM CTP
1.2 µl	10 mM UTP
0.7 µl	RNase inhibitor (40 U/µl)
1.2 µl	SP6 RNA-polymerase (Institute of Biochemistry; University of Würzburg)
5 µl	α-[^{32}P]-GTP
0.5 µg	linearized plasmid DNA
to 20 µl	DEPC ddH_2O

The transcription reaction was incubated for 40-60 min at 40 °C. Subsequently 1.5 µl DNase I (RNase-free; 1 U/µl) were added and the reaction was incubated for 20 min at 37 °C. After dilution of the reaction mixture with DEPC ddH_2O to a total volume of 50 µl, the RNA was column-purified and stored at -20 °C.

6.2.5.6 Denaturing (urea) polyacrylamide gel electrophoresis

Short (< 250 nt) radiolabeled RNAs were purified by denaturing polyacrylamide gel electrophoresis. Dependent on the size of the purified RNAs, gels of 8-15% were prepared. Gels were run in 0.5-1x TBE at 450 mA. After pre-running the gels for at least 20 min, samples were loaded and separated for 1-4 h again dependent on RNA-size and the desired level of separation.

Composition of a typical 10% gel was as follows:

Rotiphorese Gel 40 (Acrylamide/Bisacrylamide 19:1)	12.5 ml
Urea	24 g
5x TBE	10 ml
ddH_2O	9.2 ml
10% APS	0.3 ml

TEMED	0.03 ml

6.2.5.7 Denaturing Agarose gel electrophoresis

Large RNAs (> 250 nt), were separated by denaturing Agarose gel electrophoresis. To prepare the gel Agarose was first melted in ddH_2O by boiling the solution. Right before casting the gel, 10x MOPS buffer and formaldehyde were added.

Samples were prepared as follows:

Sample premix

10 µl	Formamide (deionized)
3.5 µl	Formaldehyde (pH > 4.0; adjust with NaOH)
2 µl	10x MOPS buffer
2-5 µg	RNA (in 3.5 µl volume)

After heating (15 min; 65 °C) the sample premix is cooled on ice and 1 µl Ethidiumbromide (10 mg/ml) and 2µl RNA loading buffer (50 % (v/v); 1 mM EDTA; 0.25 % Bromphenolblue) are added and then loaded on the gel.

Gels were run over night at 30-40 V.

Composition of a typical 1% gel was as follows:

Agarose	5.25 g
ddH_2O	350 ml
10x MOPS-buffer (0.2 M MOPS; 80 mM NaAc; 10 mM EDTA; pH 7.0)	50 ml
Formaldehyde (37 % (w/v); pH > 4.0)	100 ml

6.2.5.8 Elution of RNA from denaturing polyacrylamide gels

Radioactively labeled RNAs were visualized on X-ray film. Non-labeled RNAs were detected by UV-shadowing with UV-light (260nm) on a DC-PEI-cellulose plate (Merck). After excising the RNA bands, gel slices were mixed with 300 µl RNA

elution buffer (300 mM NaOAc; 2 mM EDTA; 0.1 M SDS) and eluted over night on a shaker at room temperature.

6.2.5.9 Northern blotting

After gel electrophoresis, gels were washed gently in ddH2O (2x 10 min). Subsequently gels were incubated with freshly prepared 50 mM NaOH for 5 min, rinsed with ddH2O and subsequently equilibrated with 20x SSC (3M NaCl; 0.3 M trisodium-citrate; pH 7.0) for at least 40 min. To transfer the RNA to the membrane, a gel-sled (wider than the gel) was turned upside down and put into a baking dish filled with 20x SSC. A Whatman paper was cut long enough to extend into the 20x SSC solution, but as wide as the gel-sled. It was layered onto the gel-sled and soaked with 20x SSC. The gel was placed upside down onto the Whatman paper and air bubbles were removed by pipette-rolling. After surrounding the gel with seran, aNothern blot membrane (Roti-Nylon 0.2; Roth) of exactly the size of the gel was pre-wetted in ddH_2O and then placed onto the gel. Again air bubbles were removed and the membrane was covered with a pre-wetted (ddH_2O), identically sized Whatman paper and topped by a dry Whatman paper. The assembly was rolled with a piped until the dry Whatman paper became wettish. Next the assembly was topped with approx. 10 cm paper towels and a glass plate on which weight was added (e.g. a filled 2 L glass bottle). The transfer was carried out for 4 h. There after the membrane was UV-crosslinked (1200 mJ)

The blot membrane was pre-hybridized with Church buffer (0.5 M Na_2HPO_4; 1m mM EDTA; 7 % SDS; pH 7.2) for 2 h. After discarding the pre-hybridization buffer, 10 ml of pre-warmed Church buffer were added to the membrane, mixed with a radioactively labeled cRNA probe and incubated over night at 65 °C. After washing the membrane twice for 15 min with wash buffer I (2x SSC; 0.1 % SDS) and subsequently twice for 15 min with wash buffer II (0.2x SSC; 0.1 % SDS) it is air dried, wrapped in seran and exposed to a phospho-imager screen or X-ray film (-80 °C).

6.2.5.10 Tethering assay

To analyze factor-dependent RNA stability, HeLa cells were co-transfected with:

2000 ng	215 delta C4 MS2 (β-globin MS2-reporter plasmid)
600 ng	WT300+e3 (β-globin wildtype-reporter plasmid)
400 ng	pVenus
800 ng	pCI-MS2-V5 (inserts: $TDRD3_{WT}$ and mutants, TOP3β, SMG5)

DNA-mixes were transfected to HeLa cells via $CaCl_2$. To do so, DNA was mixed in 90 µl of ddH_2O and 10 µl of 2.5 M $CaCl_2$ were added. After vortexing 100 µl of 2x BBS were added and immediately vortexed for 6 sec and then kept on ice for 15 min. After incubation, the transfection mix was added to freshly changed (approx. 3 h prior to transfection) cell culture medium. Cells were cultivated for 48 h, medium was changed after 24 h and the transfection was controlled by fluorescence microscopic detection of pVenus. Cells were harvested in Trizol Reagent and RNAs were precipitated and analyzed by denaturing Agarose gel electrophoresis and β-globin reporter plasmids were detected by Northern blotting.

6.2.5.11 Reverse transcription

Reverse transcriptions were carried with help of a SuperScriptIII first strand kit (Life technologies) according to manufacturers recommendations.

6.2.5.12 Cleavage assay

RNA or DNA oligomers were 5'- 3'-labeled was carried out using. ~ 40 fmol of radiolabeled oligomers were incubated with recombinant TOP3β wildtype or active site mutant (Y336F) (amounts are indicated in the individual experiment) at 42 °C in a buffer containing 40 mM HEPES pH6.5; 10 % PEG400; 40 % glycerol; 1 mM MgCl2; 1 mM DTT and 10 µg/ml BSA for 2 min. SDS was added to a final concentration of 0.2 % and incubated for 1 min. Reactions were transferred on ice

and RNA sample buffer (5'-labeled oligos) or SDS sample buffer (3'-labeled oligos) was added. Released 5'-fragments were analyzed on a 12 % denaturing PAA-Gel. Covalent 3'-labeled TOP3β-RNA intermediates were analyzed on a 10 % SDS PAA-Gel, transferred to nitrocellulose membrane. Recombinant TOP3β was detected with anti-TOP3β antibodies. RNAs were visualized by exposing the blot membrane to an X-ray film.

6.2.5.13 Oligo(dT)-pulldown

Oligo(dT)-pulldown assays were performed with oligo(dT)-cellulose (Fluka) according to manufacturer's instructions. After extensive washing, oligo(dT)-bound mRNPs were eluted, eluates precipitated with TCA and analyzed by SDS-PAGE and Western blot. RNA of extracts was digested with RNase A (Qiagen).

6.2.5.14 Cross linking and immunoprecipitation (CLIP)

Flp-In T-Rex cells stably expressing TOP3β or HEK293 control cells were grown on 15cm plates to approx. 90 % confluency. 5 h post induction cells were UV-crosslinked [254 nm] (CL-1000 Ultraviolet Crosslinker) harvested and cells incubated with lysis buffer containing protease inhibitors (50 mM HEPES pH 7.5; 150 mM KCl; 2 mM EDTA; 0.5 % NP40; 1 mM DTT) for 10 min on ice. Lysates were clarified (11000 rpm; 10 min; 4 °C), treated with RNase T1 (1:10000; 7 min; 22 °C) (Ambion 1000 U/µl), cooled on ice for 5 min and incubated with pre-equilibrated magnetic FLAG M2 Agarose (SIGMA) (1 h; 4 °C). Precipitated complexes were 3x washed with wash buffer (50 mM HEPES pH 7.5; 300 mM KCl and 0.05 % NP40), treated with different RNase T1-concentrations (1:100000, 1:10000, 1:1000 or 1:100), washed 3x with high salt buffer (50 mM HEPES pH 7.5; 500 mM KCl; 0,05 % NP40) and 3x with phosphatase buffer (10 mM Tris-HCl pH.8; 100 mM KCl; 5 mM $MgCl_2$ and 0.2 % Triton X-100). Co-precipitated RNAs were dephosphorylated (40 min, 37 °C) (Fast AP; Fermentas). Beads were washed 3x with labeling buffer (50 mM Tris-HCl pH7.5; 10 mM $MgCl_2$). RNAs were 5'-labeled using (1 h; 37 °C). After washing 5x with labeling buffer, beads were boiled in SDS sample buffer. The eluates were subjected

to gel electrophoresis (NuPAGE Bis-Tris 4-12 %; Life Technologies) and subsequent Western blotting on nitrocellulose membrane. Precipitated FLAG/HA-TOP3β was detected with α-FLAG antibodies; co-precipitated RNAs were visualized by exposing the blot membrane to an X-ray film.

6.2.5.15 RNA-immunoprecipitation (RIP)

To analyze mRNAs co-precipitated with TDRD3 and mutants thereof, TDRD3 variants were precipitated as described above. IP-eluates and 1 % input of the lysates were adjusted to a volume of 200 µl with ddH_2O. After Phenol/Chloroform extraction proteins (to control the IP via Western blot) and RNAs were precipitated. RNA pellets were resolved in 10 (PCR) or 20 µl (qPCR) DEPC ddH_2O and reversely transcribed with oligo(dT)-primers. After cDNA synthesis, the reaction was adjusted to 120 µl with ddH_2O and cDNA was used for qPCR or standard PCR-amplification with gene-specific primers.

6.2.5.16 Quantitative real time PCR (qPCR)

To analyze TDRD3 co-precipitated mRNAs in a quantitative manner, they were subjected to qPCR. Prior to cDNA synthesis, DNA was hydrolyzed from the resolved RNA pellet with a TURBO DNA-free kit (Life technologies). qPCR was performed with a CFX96 Touch real-time system (Bio-Rad).

A typical reaction was prepared as follows:

6 µl	iTaq Universal SYBR Green Supermix (Bio-Rad)
2 µl	Primer-Mix (5'- and 3'-primer; 1.5 µM, each)
4µl	cDNA (pre-diluted 1:10)

PCR-program (40 cycles):

95 °C for 30 sec; 95 °C 5 sec; 60 °C 30 sec

6.2.6 Statistical methods

6.2.6.1 Comparison of FMRP PAR-CLIP and TDRD3 ChIP data sets

Known protein coding genes that are bound by TDRD3 were inferred from a genome-wide TDRD3 chromatin IP dataset[63]. FMRP targets were inferred from a recent study that used photoactivatable ribonucleoside enhanced crosslinking and IP (PAR-CLIP) as well as ribonucleoprotein immunoprecipitation followed by microarray analysis (RIP-chip) to define human FMRP bound mRNAs[36]. Transcripts were considered FMRP targets when they contained at least one identified binding site and were enriched in the RIP-chip (log fold enrichment > 0.1). Statistical significance of the overlap (i.e. FMRP target transcripts of TDRD3-bound genes) was calculated using a Chi-square test with Yates' correction.

7 Bibliography

1. Richard, P. & Manley, J. L. Transcription termination by nuclear RNA polymerases. *Genes Dev.* 23, 1247–1269 (2009).

2. Shuman, S. Capping enzyme in eukaryotic mRNA synthesis. *Prog. Nucleic Acid Res. Mol. Biol.* 50, 101–129 (1995).

3. Lim, L. & Canellakis, E. S. Adenine-rich polymer associated with rabbit reticulocyte messenger RNA. *Nature* 227, 710–712 (1970).

4. Mitchell, P. & Tollervey, D. mRNA turnover. *Curr. Opin. Cell Biol.* 13, 320–325 (2001).

5. Matera, A. G. & Wang, Z. A day in the life of the spliceosome. *Nat. Rev. Mol. Cell Biol.* 15, 108–121 (2014).

6. Seeburg, P. H. A-to-I Editing: New and Old Sites, Functions and Speculations. *Neuron* 35, 17–20 (2002).

7. Egloff, S., Dienstbier, M. & Murphy, S. Updating the RNA polymerase CTD code: adding gene-specific layers. *Trends Genet.* 28, 333–341 (2012).

8. Lee, K.-M. & Tarn, W.-Y. Coupling pre-mRNA processing to transcription on the RNA factory assembly line. *RNA Biol.* 10, 380–390 (2013).

9. Rodnina, M. V. & Wintermeyer, W. Recent mechanistic insights into eukaryotic ribosomes. *Curr. Opin. Cell Biol.* 21, 435–443 (2009).

10. Parker, R. & Sheth, U. P Bodies and the Control of mRNA Translation and Degradation. *Mol. Cell* 25, 635–646 (2007).

11. Keene, J. D. RNA regulons: coordination of post-transcriptional events. *Nat. Rev. Genet.* 8, 533–543 (2007).

12. Baltz, A. G. *et al.* The mRNA-Bound Proteome and Its Global Occupancy Profile on Protein-Coding Transcripts. *Mol. Cell* 46, 674–690 (2012).

13. Castello, A. *et al.* Insights into RNA Biology from an Atlas of Mammalian mRNA-Binding Proteins. *Cell* 149, 1393–1406 (2012).

14. Barbosa, I. *et al.* Human CWC22 escorts the helicase eIF4AIII to spliceosomes

and promotes exon junction complex assembly. *Nat. Struct. Mol. Biol.* (2012). doi:10.1038/nsmb.2380

15. Steckelberg, A.-L., Boehm, V., Gromadzka, A. M. & Gehring, N. H. CWC22 connects pre-mRNA splicing and exon junction complex assembly. *Cell Rep.* 2, 454–461 (2012).

16. Hir, H. L., Izaurralde, E., Maquat, L. E. & Moore, M. J. The spliceosome deposits multiple proteins 20–24 nucleotides upstream of mRNA exon–exon junctions. *EMBO J.* 19, 6860–6869 (2000).

17. Saulière, J. *et al.* CLIP-seq of eIF4AIII reveals transcriptome-wide mapping of the human exon junction complex. *Nat. Struct. Mol. Biol.* 19, 1124–1131 (2012).

18. Hir, H. L., Gatfield, D., Izaurralde, E. & Moore, M. J. The exon–exon junction complex provides a binding platform for factors involved in mRNA export and nonsense-mediated mRNA decay. *EMBO J.* 20, 4987–4997 (2001).

19. Zhou, Z. *et al.* The protein Aly links pre-messenger-RNA splicing to nuclear export in metazoans. *Nature* 407, 401–405 (2000).

20. Hachet, O. & Ephrussi, A. Splicing of oskar RNA in the nucleus is coupled to its cytoplasmic localization. *Nature* 428, 959–963 (2004).

21. Lee, H. C., Choe, J., Chi, S.-G. & Kim, Y. K. Exon junction complex enhances translation of spliced mRNAs at multiple steps. *Biochem. Biophys. Res. Commun.* 384, 334–340 (2009).

22. Nott, A., Le Hir, H. & Moore, M. J. Splicing enhances translation in mammalian cells: an additional function of the exon junction complex. *Genes Dev.* 18, 210–222 (2004).

23. Gehring, N. H., Lamprinaki, S., Kulozik, A. E. & Hentze, M. W. Disassembly of Exon Junction Complexes by PYM. *Cell* 137, 536–548 (2009).

24. Lejeune, F., Ishigaki, Y., Li, X. & Maquat, L. E. The exon junction complex is detected on CBP80-bound but not eIF4E-bound mRNA in mammalian cells: dynamics of mRNP remodeling. *EMBO J.* 21, 3536–3545 (2002).

25. Sato, H. & Maquat, L. E. Remodeling of the Pioneer Translation Initiation Complex Involves Translation and the Karyopherin Importin β. *Genes Dev.* 23, 2537–2550 (2009).

26. Maquat, L. E., Tarn, W.-Y. & Isken, O. The Pioneer Round of Translation: Features and Functions. *Cell* 142, 368–374 (2010).

27. Buchan, J. R. mRNP granules: Assembly, function, and connections with disease. *RNA Biol.* 11, 0–11 (2014).

28. Castello, A., Fischer, B., Hentze, M. W. & Preiss, T. RNA-binding proteins in Mendelian disease. *Trends Genet.* 29, 318–327 (2013).

29. Ule, J. Ribonucleoprotein complexes in neurologic diseases. *Curr. Opin. Neurobiol.* 18, 516–523 (2008).

30. Colak, D., Ji, S.-J., Porse, B. T. & Jaffrey, S. R. Regulation of Axon Guidance by Compartmentalized Nonsense-Mediated mRNA Decay. *Cell* 153, 1252–1265 (2013).

31. Steward, O. & Schuman, E. M. Protein Synthesis at Synaptic Sites on Dendrites. *Annu. Rev. Neurosci.* 24, 299–325 (2001).

32. Ule, J. & Darnell, R. B. RNA binding proteins and the regulation of neuronal synaptic plasticity. *Curr. Opin. Neurobiol.* 16, 102–110 (2006).

33. Fernandez, E., Rajan, N. & Bagni, C. The FMRP regulon: from targets to disease convergence. *Neurogenomics* 7, 191 (2013).

34. Verkerk, A. J. M. H. *et al.* Identification of a gene (FMR-1) containing a CGG repeat coincident with a breakpoint cluster region exhibiting length variation in fragile X syndrome. *Cell* 65, 905–914 (1991).

35. De Boulle, K. *et al.* A point mutation in the FMR-1 gene associated with fragile X mental retardation. *Nat Genet* 3, 31–35 (1993).

36. Ascano, M. *et al.* FMRP targets distinct mRNA sequence elements to regulate protein expression. *Nature* 492, 382–386 (2012).

37. Darnell, J. C. *et al.* Fragile X Mental Retardation Protein Targets G Quartet mRNAs Important for Neuronal Function. *Cell* 107, 489–499 (2001).

38. Darnell, J. C. *et al.* Kissing complex RNAs mediate interaction between the Fragile-X mental retardation protein KH2 domain and brain polyribosomes. *Genes Dev.* 19, 903–918 (2005).

39. Ting, J. T. & Feng, G. Unfolding neurodevelopmental disorders: Found in translation. *Nat. Med.* 17, 1352–1353 (2011).

40. Darnell, J. C. *et al.* FMRP Stalls Ribosomal Translocation on mRNAs Linked to Synaptic Function and Autism. *Cell* 146, 247–261 (2011).

41. Venter, J. C. *et al.* The Sequence of the Human Genome. *Science* 291, 1304–1351 (2001).

42. Thandapani, P., O'Connor, T. R., Bailey, T. L. & Richard, S. Defining the RGG/RG Motif. *Mol. Cell* 50, 613–623 (2013).

43. Cléry, A. & Allain, F. H.-T. FROM STRUCTURE TO FUNCTION OF RNA BINDING DOMAINS. (2011). at <http://www.ncbi.nlm.nih.gov/books/NBK63528/>

44. Kiledjian, M. & Dreyfuss, G. Primary structure and binding activity of the hnRNP U protein: binding RNA through RGG box. *EMBO J.* 11, 2655–2664 (1992).

45. Glisovic, T., Bachorik, J. L., Yong, J. & Dreyfuss, G. RNA-binding proteins and post-transcriptional gene regulation. *FEBS Lett.* 582, 1977–1986 (2008).

46. Ramos, A., Hollingworth, D. & Pastore, A. G-quartet-dependent recognition between the FMRP RGG box and. *RNA* 9, 1198–1207 (2003).

47. Schaeffer, C. *et al.* The fragile X mental retardation protein binds specifically to its mRNA via a purine quartet motif. *EMBO J.* 20, 4803–4813 (2001).

48. Chen, C., Nott, T. J., Jin, J. & Pawson, T. Deciphering arginine methylation: Tudor tells the tale. *Nat. Rev. Mol. Cell Biol.* 12, 629–642 (2011).

49. Côté, J. & Richard, S. Tudor domains bind symmetrical dimethylated arginines. *J. Biol. Chem.* 280, 28476–83 (2005).

50. Liu, H. *et al.* Structural basis for methylarginine-dependent recognition of Aubergine by Tudor. *Genes Dev.* 24, 1876–1881 (2010).

51. Liu, K. *et al.* Structural basis for recognition of arginine methylated Piwi proteins by the extended Tudor domain. *Proc. Natl. Acad. Sci.* 107, 18398–18403 (2010).

52. Selenko, P. *et al.* SMN Tudor domain structure and its interaction with the Sm proteins. *Nat. Struct. Mol. Biol.* 8, 27–31 (2001).

53. Chari, A. *et al.* An Assembly Chaperone Collaborates with the SMN Complex to Generate Spliceosomal SnRNPs. *Cell* 135, 497–509 (2008).

54. Winkler, C. *et al.* Reduced U snRNP assembly causes motor axon degeneration in an animal model for spinal muscular atrophy. *Genes Dev.* 19, 2320–2330 (2005).

55. Ponting, C. P. Tudor domains in proteins that interact with RNA. *Trends Biochem. Sci.* 22, 51–52 (1997).

56. Friberg, A., Corsini, L., Mourão, A. & Sattler, M. Structure and Ligand Binding of the Extended Tudor Domain of D. melanogaster Tudor-SN. *J. Mol. Biol.* 387, 921–934 (2009).

57. Vagin, V. V. *et al.* Proteomic analysis of murine Piwi proteins reveals a role for arginine methylation in specifying interaction with Tudor family members. *Genes Dev.* 23, 1749–1762 (2009).

58. Linder, B. *et al.* Tdrd3 is a novel stress granule-associated protein interacting with the Fragile-X syndrome protein FMRP. *Hum Mol Genet* 17, 3236–3246 (2008).

59. Goulet, I., Boisvenue, S., Mokas, S., Mazroui, R. & Cote, J. TDRD3, a novel Tudor domain-containing protein, localizes to cytoplasmic stress granules. *Hum Mol Genet* 17, 3055–3074 (2008).

60. Pickart, C. M. Targeting of substrates to the 26S proteasome. *FASEB J.* 11, 1055–1066 (1997).

61. Liu, K. *et al.* Crystal Structure of TDRD3 and Methyl-Arginine Binding Characterization of TDRD3, SMN and SPF30. *PLoS ONE* 7, e30375 (2012).

62. Sikorsky, T. *et al.* Recognition of asymmetrically dimethylated arginine by TDRD3. *Nucleic Acids Res.* 40, 11748–11755 (2012).

63. Yang, Y. *et al.* TDRD3 Is an Effector Molecule for Arginine-Methylated Histone Marks. *Mol. Cell* 40, 1016–1023 (2010).

64. Sims, R. J. *et al.* The C-Terminal Domain of RNA Polymerase II Is Modified by Site-Specific Methylation. *Science* 332, 99 –103 (2011).

65. Kashima, I. *et al.* SMG6 interacts with the exon junction complex via two conserved EJC-binding motifs (EBMs) required for nonsense-mediated mRNA decay. *Genes Dev.* 24, 2440 –2450 (2010).

66. Anderson, P. & Kedersha, N. Stress granules: the Tao of RNA triage. *Trends Biochem. Sci.* 33, 141–150 (2008).

67. Buchan, J. R. & Parker, R. Eukaryotic Stress Granules: The Ins and Outs of Translation. *Mol. Cell* 36, 932–941 (2009).

68. Kedersha, N. *et al.* Stress granules and processing bodies are dynamically linked sites of mRNP remodeling. *J. Cell Biol.* 169, 871–884 (2005).

69. Feng, Y. *et al.* FMRP Associates with Polyribosomes as an mRNP, and the I304N Mutation of Severe Fragile X Syndrome Abolishes This Association. *Mol. Cell* 1, 109–118 (1997).

70. Plöttner, O. SMNrp und TUBA - Isolierung und Charakterisierung zweier neuer Gene mit Homologie zu SMN, dem Krankheitsgen der spinalen Muskelatrophie. at <http://hss.ulb.uni-bonn.de/2002/0068/0068.htm>

71. Champoux, J. J. DNA TOPOISOMERASES: Structure, Function, and Mechanism. *Annu. Rev. Biochem.* 70, 369–413 (2001).

72. Kobayashi, M. & Hanai, R. M Phase-Specific Association of Human Topoisomerase III[beta] with Chromosomes. *Biochem. Biophys. Res. Commun.* 287, 282–287 (2001).

73. Ng, S., Liu, Y., Hasselblatt, K., Mok, S. & Berkowitz, R. A new human topoisomerase III that interacts with SGS1 protein. *Nucl Acids Res* 27, 993–1000 (1999).

74. Shimamoto, A., Nishikawa, K., Kitao, S. & Furuichi, Y. Human RecQ5β, a large isomer of RecQ5 DNA helicase, localizes in the nucleoplasm and interacts with topoisomerases 3α and 3β. *Nucleic Acids Res.* 28, 1647–1655 (2000).

75. Stoll, G. *et al.* Deletion of TOP3β, a component of FMRP-containing mRNPs, contributes to neurodevelopmental disorders. *Nat. Neurosci.* 16, 1228–1237 (2013).

76. Eberhart, D., Malter, H., Feng, Y. & Warren, S. The fragile X mental retardation protein is a ribonucleoprotein containing both nuclear localization and nuclear export signals. *Hum Mol Genet* 5, 1083–1091 (1996).

77. Kim, M., Bellini, M. & Ceman, S. Fragile X Mental Retardation Protein FMRP Binds mRNAs in the Nucleus. *Mol Cell Biol* 29, 214–228 (2009).

78. Tamanini, F. *et al.* Different Targets for the Fragile X-Related Proteins Revealed by Their Distinct Nuclear Localizations. *Hum. Mol. Genet.* 8, 863–869 (1999).

79. Kudo, N. *et al.* Leptomycin B inactivates CRM1/exportin 1 by covalent modification at a cysteine residue in the central conserved region. *Proc. Natl. Acad. Sci. U. S. A.* 96, 9112–9117 (1999).

80. Park, S.-W. *et al.* Regulation of the catalytic function of topoisomerase II alpha through association with RNA. *Nucleic Acids Res.* 36, 6080 –6090 (2008).

81. Wang, Y., Knudsen, B. R., Bjergbæk, L., Westergaard, O. & Andersen, A. H. Stimulated Activity of Human Topoisomerases IIα and IIβ on RNA-Containing Substrates. *J. Biol. Chem.* 274, 22839–22846 (1999).

82. DiGate, R. J. & Marians, K. J. Escherichia coli topoisomerase III-catalyzed cleavage of RNA. *J. Biol. Chem.* 267, 20532 –20535 (1992).

83. Wang, H., Di Gate, R. J. & Seeman, N. C. An RNA topoisomerase. *Proc. Natl. Acad. Sci.* 93, 9477 –9482 (1996).

84. Darnell, R. B. HITS-CLIP: panoramic views of protein–RNA regulation in living cells. *Wiley Interdiscip. Rev. - RNA* 1, 266–286 (2010).

85. Mazroui, R. *et al.* Trapping of messenger RNA by Fragile X Mental Retardation protein into cytoplasmic granules induces translation repression. *Hum Mol Genet* 11, 3007–3017 (2002).

86. Antar, L. N., Dictenberg, J. B., Plociniak, M., Afroz, R. & Bassell, G. J. Localization of FMRP-associated mRNA granules and requirement of microtubules for activity-dependent trafficking in hippocampal neurons. *Genes Brain Behav.* 4, 350–359 (2005).

87. Siomi, M. C., Zhang, Y., Siomi, H. & Dreyfuss, G. Specific sequences in the fragile X syndrome protein FMR1 and the FXR proteins mediate their binding to 60S ribosomal subunits and the interactions among them. *Mol. Cell. Biol.* 16, 3825–3832 (1996).

88. Conti, E. & Izaurralde, E. Nonsense-mediated mRNA decay: molecular insights and mechanistic variations across species. *Curr. Opin. Cell Biol.* 17, 316–325 (2005).

89. Gehring, N. H., Hentze, M. W. & Kulozik, A. E. in *RNA Turnover in Eukaryotes: Nucleases, Pathways and Analysis of mRNA Decay* Volume 448, 467–482 (Academic Press, 2008).

90. Imoto, I. *et al.* Frequent Silencing of the Candidate Tumor Suppressor

PCDH20 by Epigenetic Mechanism in Non–Small-Cell Lung Cancers. *Cancer Res.* 66, 4617–4626 (2006).

91. Yin, J. *et al.* BLAP75, an essential component of Bloom's syndrome protein complexes that maintain genome integrity. *EMBO J.* 24, 1465–1476 (2005).

92. Xu, D. *et al.* Top3β is an RNA topoisomerase that works with fragile X syndrome protein to promote synapse formation. *Nat. Neurosci.* advance online publication, (2013).

93. Behm-Ansmant, I. & Izaurralde, E. Quality control of gene expression: a stepwise assembly pathway for the surveillance complex that triggers nonsense-mediated mRNA decay. *Genes Dev.* 20, 391–398 (2006).

94. Ma, X. M., Yoon, S.-O., Richardson, C. J., Jülich, K. & Blenis, J. SKAR Links Pre-mRNA Splicing to mTOR/S6K1-Mediated Enhanced Translation Efficiency of Spliced mRNAs. *Cell* 133, 303–313 (2008).

95. Christensen, A. K., Kahn, L. E. & Bourne, C. M. Circular polysomes predominate on the rough endoplasmic reticulum of somatotropes and mammotropes in the rat anterior pituitary. *Am. J. Anat.* 178, 1–10 (1987).

96. Wells, S. E., Hillner, P. E., Vale, R. D. & Sachs, A. B. Circularization of mRNA by Eukaryotic Translation Initiation Factors. *Mol. Cell* 2, 135–140 (1998).

97. Myasnikov, A. G. *et al.* The molecular structure of the left-handed supra-molecular helix of eukaryotic polyribosomes. *Nat. Commun.* 5, (2014).

98. Bhakar, A. L., Dölen, G. & Bear, M. F. The Pathophysiology of Fragile X (and What It Teaches Us about Synapses). *Annu. Rev. Neurosci.* 35, 417–443 (2012).

99. Santoro, M. R., Bray, S. M. & Warren, S. T. Molecular Mechanisms of Fragile X Syndrome: A Twenty-Year Perspective. *Annu. Rev. Pathol. Mech. Dis.* 7, 219–245 (2012).

100. Narayanan, U. *et al.* S6K1 Phosphorylates and Regulates Fragile X Mental Retardation Protein (FMRP) with the Neuronal Protein Synthesis-dependent Mammalian Target of Rapamycin (mTOR) Signaling Cascade. *J Biol Chem* 283, 18478–18482 (2008).

101. Liu, G. *et al.* Netrin requires focal adhesion kinase and Src family kinases for axon outgrowth and attraction. *Nat. Neurosci.* 7, 1222–1232 (2004).

102. Rico, B. *et al.* Control of axonal branching and synapse formation by focal adhesion kinase. *Nat. Neurosci.* 7, 1059–1069 (2004).

103. Walsh, T. *et al.* Rare Structural Variants Disrupt Multiple Genes in Neurodevelopmental Pathways in Schizophrenia. *Science* 320, 539–543 (2008).

104. Bühler, D., Raker, V., Lührmann, R. & Fischer, U. Essential Role for the Tudor Domain of SMN in Spliceosomal U snRNP Assembly: Implications for Spinal Muscular Atrophy. *Hum. Mol. Genet.* 8, 2351–2357 (1999).

105. Yang, Y. *et al.* Arginine Methylation Facilitates the Recruitment of TOP3B to Chromatin to Prevent R Loop Accumulation. *Mol. Cell* 53, 484–497 (2014).

106. Alpatov, R. *et al.* A Chromatin-Dependent Role of the Fragile X Mental Retardation Protein FMRP in the DNA Damage Response. *Cell* 157, 869–881 (2014).

8 Table of figures

9 Publications

Parts of this work have been published in the following article:

Stoll, G. *et al.* Deletion of TOP3β, a component of FMRP-containing mRNPs, contributes to neurodevelopmental disorders. *Nat. Neurosci.* **16,** 1228–1237 (2013).

10 Acknowledgements

I would like to express my thanks to all people who helped me and thus contributed to preparing this PhD-thesis:

- Prof. Utz Fisher for supervision and funding throughout the course of this work.
- Prof. Alexander Buchberger for helpful discussions and for being the second examiner of the dissertation.
- PD Dr. Sibylle Jablonka for being the third member of the oral defence commission.
- Dr. Bastian Linder for supervision and support throughout the years.
- Lab 119: Anja, Lissy and especially Conny for all the help and contribution.
- The male fraction ;-) Jürgen "die Katze aus Knetzgau" Ohmer, Clemens "Mr. Tricky" Englbrecht, Christopher "Hammer" Stapf, Thomas "Goatthroat" Ziegenhals, Michael "The bee whisperer" Grimm and Stefan "The autumn tree" aka. "The door frame" Juranek.
- All members of the department of biochemistry.
- Last but certainly not least my family and Nadine.

11 Declaration

By this I declare on oath that I have written the dissertation *"IDENTIFICATION OF THE mRNA-ASSOCIATED TOP3β-TDRD3-FMRP (TTF) -COMPLEX AND ITS IMPLICATION FOR NEUROLOGICAL DISORDERS"* by myself and that no other means than those mentioned were used.

Furthermore I assert not having submitted this dissertation in identical or other form to another examination board.

I did neither acquire nor tried to acquire any other academic degrees than those provided in the admission application.

Würzburg, 19 January 2015

……

Georg Stoll